A NOVEL *FR 13* RISK ASSESSMENT OF CORROSION OF PIPELINE STEEL IN DE-AERATED WATER

by

Mr Samuel COLLINS

School of Chemical Engineering
The University of Adelaide

A thesis submitted for examination for the degree of
Master of Philosophy (Chemical Engineering)
April 2018

STATEMENT OF DECLARATION

I, Samuel Collins, certify that this work contains no material which has been accepted for the award of any other degree or diploma in any university or other tertiary institution and, to the best of my knowledge and belief, contains no material previously published or written by another person, except where due reference has been made in the text.

I give consent to this copy of my thesis when deposited in the University Library, being made available for loan and photocopying, subject to the provisions of the Copyright Act 1968.

The author acknowledges that copyright of published works contained within this thesis [1] resides with the copyright holders of those works.

I also give permission for the digital version of my thesis to be made available on the web, via University's digital research repository, the Library catalogue and also through web search engines, unless permission has been granted by the University to restrict access for a period of time.

Lastly, I acknowledge the support I have received for my research through the provision of an Australian Government Research Training Program Scholarship.

Signature:

Date:

---

[1] Collins, S.D., Davey, K.R., Chu, J.Y.G., O'Neill, B.K., 2016. A new quantitative risk assessment of Microbiologically Influenced Corrosion (MIC) of carbon steel pipes used in chemical engineering. In: CHEMECA 2016: Chemical Engineering – Regeneration, Recovery and Reinvention, Sept. 25-28, Adelaide, Australia, paper 3386601. ISBN: 9781922107831

Collins, S.D., Davey, K.R., 2018. A novel *Fr 13* risk assessment of corrosion of carbon-steel pipe in de-aerated water. Chemical Engineering Science – *submitted* CES-D-18-00449, Feb.

EXECUTIVE SUMMARY

Steady-state operations are used globally in chemical engineering. Advantages include ease of control and a more uniform product quality (Ghasem and Henda, 2008; McCabe et al, 2001). Importantly however, there will be naturally occurring, random (stochastic) fluctuations in parameter values about the 'set' mean when process control is inadequate. These are not addressed explicitly in traditional chemical engineering because they are not sufficient on their own to be considered transient (unsteady) and because, generally, fluctuations in one parameter are off-set by changes in others with plant output behaviour seeming to remain steady (Amundson et al., 1980; Sinnott, 2005; Zou and Davey, 2016).

Davey and co-workers, however, have demonstrated these fluctuations can unexpectedly accumulate in one direction and leverage significant (sudden and surprise) change in output behaviour with failure in product or plant (e.g. Abdul-Halim and Davey, 2016; Zou and Davey, 2016; Chandrakash and Davey, 2017). To underscore the unexpected element of the failure event they titled their risk framework *Fr 13* [2] (*Friday 13th Syndrome*). Case studies of their probabilistic risk framework to 1-step operations include loss of thermal efficiency in a coal-fired boiler (Davey, 2015 a) and failure to remove whey deposits in Clean-In-Place (CIP) milk processing (Davey et al., 2015). More recently, to advance their risk framework for progressively, multi-step and complex (in the sense of 'integrated', not 'complicated') processes they demonstrated its usefulness to 2-step membrane fouling with combined ultrafiltration-osmotic distillation (UF-OD) (Zou and Davey, 2016), and; a 3-step microbiological raw milk pasteurization (Chandrakash and Davey, 2017). Findings overall revealed no methodological complications in application - and it was concluded the risk framework was generalizable (Zou and Davey, 2016; Chandrakash and Davey, 2017). A significant advantage of the framework is it can be used in 'second-tier studies' to reduce risk through simulations of intervention strategies and re-design of physical plant or operating practice. It can be applied at both *synthesis* and *analysis* stages.

---

[2] *see* Appendix A for a definition of some important terms used in this research.

Although the risk framework has been successfully applied to corrosive pitting of AISI 316L metal widely used in off-shore oil and gas structures (Davey et al., 2016) [3] it was not known if it could provide new insight into corrosion of metal, more specifically microbiologically influenced corrosion (MIC), a major problem globally that accounts for ~ 20 % of overall corrosion (Flemming, 1996). It is estimated to cost AUD$7 billion to Australia annually (Javaherdashti and Raman-Singh, 2001).

A review of the literature showed that a thorough understanding of MIC has been slow to emerge, both because of the role of micro-organisms in corrosion and because of a lack of methodology to determine any impact of natural fluctuations in the internal pipe environment. Importantly, the insidious nature of MIC was known to pose a practical risk of failure of pipes used to transport wet-fluids. However, because modelling of direct MIC would be uniquely complex it was planned that a general model for corrosion should be synthesized and understood that could be extended.

A limited research program was therefore undertaken with the aim to advance the *Fr 13* framework and to gain unique insight into how naturally occurring fluctuations in fluid temperature (*T*) and pH of the internal pipe environment can be transmitted and impact corrosion.

A logical and stepwise approach was implemented as a research strategy.

The initial model of Smith et al. (2011) was modified to simulate MIC causing micro-organisms such as sulphate-reducing bacteria (SRB) on widely used ASTM A105 carbon-steel pipe that is corroded under steady-state, abiotic and synthetic conditions. This was solved using traditional, deterministic simulations to give a predicted, underlying corrosion rate (*CR*) of 0.5 mm yr^{-1} as impacted by internal pipe-fluid *T* and pH.

Importantly, findings underscored the controlling importance of low pH on *CR*.

This initial model was then simulated, for the first time, using the probabilistic *Fr 13* framework (Collins et al., 2016) [4] in which distributions to mimic fluctuations in *T* (K) and

---

[3] This research was a Finalist, IChemE Global Awards 2016, *Innovative Product*, Manchester, UK, Nov.

[4] Collins, S.D., Davey, K.R., Chu, J.Y.G., O'Neill, B.K., 2016. A new quantitative risk assessment of Microbiologically Influenced Corrosion (MIC) of carbon steel pipes used in chemical engineering. In:

pH in the pipe were (reasonably) assumed as truncated Normal, and; a new corrosion risk factor (p) was synthesized such that all $p > 0$ characterized a *CR* failure i.e. a corrosion rate greater than 0.5 mm yr^{-1}. Normal distributions that were truncated were used because these permitted *T* and pH to fluctuate randomly during process operations but limited these to values that could occur only practically.

Predictions showed that 28.1 % of all corrosion of ASTM A105 pipe, averaged over the long term for a range of fluctuations $290.15 \leq T \leq 298.15$ K, and $4.64 \leq \text{pH} \leq 5.67$, would in fact be greater than the underlying value despite a design margin of safety (*tolerance*) of 50 % *CR*, and were therefore process failures ($p > 0$). Findings highlighted that corrosion was a combination of 'successful' and 'failed' operations. This insight is not available from traditional risk approaches, with or without sensitivity analyses.

It was concluded that the *Fr 13* framework was an advance over the traditional, deterministic methods because all corrosion scenarios that can practically exist are simulated.

It was concluded also that if each simulation was (reasonably) thought of as one operational day, there would be (28.1/100 days × 365.25 days / year) ~103 corrosion failures in ASTM A105 pipe per year.

However it was acknowledged that to enhance corrosion simulation, the free corrosion potential (E_{corr}, V vs SCE), a key parameter in this initial model formulation, should more realistically be considered a combined function of the internal pipe-fluid *T* and pH, and; that this assumption should be tested, and, that this would necessitate a trial-and-error simulation for corrosion rate (*CR*). It was also determined that the truncations that were used for *T* and pH were too restrictive for off-shore oil processing (Arnold and Stewart, 1999; J. Y. G. Chu, Upstream Production Services Pty Ltd., Australia, *pers. comm.*).

To address this, the initial model was extended mathematically for the first time, and; *Fr 13* risk simulations carried out using spread-sheeting techniques utilizing the *Solver*

CHEMECA 2016: Chemical Engineering – Regeneration, Recovery and Reinvention, Sept. 25-28, Adelaide, Australia, paper 3386601. ISBN: 9781922107831

function (Microsoft Excel™). A significant advantage was that the distributions defining the naturally occurring fluctuations in T and pH could be entered, viewed, copied, pasted and manipulated as Excel formulae.

Predictions showed (Collins and Davey, 2018) [5] an underlying corrosion rate CR = 0.45 mm yr^{-1} – a change of approximately 10 % when the design margin of safety (tolerance) was reduced from 50 % to a more realistic 20 % for the improved model. This is significant because the tolerance of a model should be as low as can be accepted, as higher tolerances can infer that the process is safer than it actually is.

Fr 13 simulations showed that 43.6 % of all corrosion of internal ASTM A105 pipe, averaged over the long term for a range of realistic fluctuations $282.55 \leq T \leq 423.75$ K, and $4.12 \leq \text{pH} \leq 6.18$ would be deemed to be process pipe-failures ($p > 0$). This translates to a corrosion failure in ASTM A105 pipe every 160 days, averaged over the long term. It is not expected that these would be equally spaced however.

Findings were used in investigative 'second-tier' studies to explore possible intervention strategies to reduce vulnerability to corrosion and to improve plant design and safety. For example, repeat *Fr 13* simulations revealed that, for a fixed mean-value of T = 353.15 K a decrease in pH from 5.15 to 4.5 resulted in an increase in carbon-steel pipe corrosion of ~1.55 mm yr^{-1} i.e. ~347 % increase. This implied that the pipe vulnerability to *Fr 13* corrosion failure could be practically minimised by adding bases, such as potassium hydroxide or sodium carbonate (Kemmer, 1988). However, if the pH is too high, anions in the pipe-fluid could precipitate and form insoluble mineral scales, leading to fouling (Pichtel, 2016).

It is acknowledged that the present research is limited to an abiotic system i.e. one without micro-organism kinetics. A justification is that the models presented in this research should be seen as a 'starting point', which could be expanded in later iterations to include: biotic model components such as the simple bacterial kinetics in the predictive MIC model of Maxwell and Campbell (2006); other species that are involved in MIC such

---

[5] Collins, S.D., Davey, K.R., 2018. A novel *Fr 13* risk assessment of corrosion of carbon-steel pipe in de-aerated water. Chemical Engineering Science – *submitted* CES-D-18-00449, Feb.

as sulphates, chlorides and hydrogen sulphide (H_2S); different metals/alloys that are used in pipe equipment where MIC can be found e.g. copper or zinc (Roberge, 2000), or; a 'global' model i.e. two or more connected unit-operations (Chandrakash and Davey, 2017). (A global model however, might not be applicable because MIC can be initiated in localized sites (Roberge, 2000)).

It is concluded that these thesis findings nevertheless significantly enhance understanding of factors that lead to excessive corrosion rates in ASTM A105 pipes. It is concluded also that the *Fr 13* risk framework appears generalizable to a range of micro-organism-metal systems and is an advancement over current existing risk and hazard assessments. If properly developed, it is thought that this risk technique could be adopted as a new design tool for steady-state unit-operations in both the *design* and *synthesis* stages and to increase understanding of MIC behaviour and outcomes.

This research is original and not incremental work.

Results and findings will be of immediate benefit and interest to a range of risk analysts, and to a broad range of practical operations involving carbon-steel pipe flows.

ACKNOWLEDGEMENTS

I would like to express my sincere gratitude to Dr K R (Ken) Davey, FIChemE, FAIFST, CEng, CSci, my principal supervisor from the School of Chemical Engineering, The University of Adelaide, for giving me an opportunity to do my Masters of Philosophy (Research) and for his help and guidance throughout my candidature. I would also like to thank A/Prof. Brian O'Neill, FIChemE, CEng, from the School of Chemical Engineering, The University of Adelaide, for being co-supervisor for my research.

Also, I wish to thank Prof. Peter Ashman, FIChemE, Head of School, and staff members in the School of Chemical Engineering, for helping me complete my studies.

I am indebted to Dr James Chu, FIChemE, for his help and guidance and my colleagues in the *Risk Research Group* including: Dr Saravanan Chandrakash, Dr Nadiya Abdul-Halim, Mr Connor Skoss and Dr Olivier Lavigne.

I trust that the results of my research work justify the expectations and confidence of all the people involved, and the interest and encouragement of all my family, friends and colleagues.

TABLE OF CONTENTS **PAGE**

LIST OF FIGURES **PAGE**

LIST OF TABLES **PAGE**

CHAPTER ONE

INTRODUCTION

Steady-state unit-operations are used globally in chemical engineering. Advantages include ease of control and a uniform product quality (Ghasem and Henda, 2008; McCabe et al., 2001).

Davey and co-workers (e.g. Abdul-Halim and Davey, 2016; Zou and Davey, 2016; Chandrakash and Davey, 2017) have demonstrated that naturally occurring, random fluctuations about apparent 'set' values can result in process and product failures. These fluctuations are not addressed explicitly in traditional chemical engineering where they are seen as being problematic. This is because they are not sufficient on their own to be considered transient i.e. unsteady-state (Amundson et al., 1980; Sinnott, 2005; Zou and Davey, 2016). Their underlying hypothesis is that random fluctuations in the value of process parameters can unexpectedly accumulate in one direction in amounts sufficient to leverage significant change and thereby make seemingly well-operating processes vulnerable to random (surprise) failure. To quantitatively explain these surprise failures in process or product, they titled their framework *Fr 13* (*Friday 13th Syndrome*). Performing a *Fr 13* risk assessment requires a unit-operations model, a carefully defined unique risk factor and a refined Monte Carlo (r-MC) (*Latin Hypercube*) sampling. Distributions are carefully selected to ensure that the naturally occurring fluctuations in input process parameters are realistically simulated.

Published studies of their probabilistic risk framework to one-step (1-step) unit-operations include a sudden shift from: sterile to non-sterile milk contaminated with *Bacillus stearothermophilus* and *B. thermodurans* in raw milk pasteurization (Davey and Cerf, 2003); 'safe' to 'unsafe' in cleaning whey deposits in Clean-In-Place (CIP) milk processing (Chandrakesh, 2012; Davey et al., 2013, 2015); and potable to non-potable water contaminated with *Escherichia coli* using ultraviolet (UV) irradiation (Abdul-Halim and Davey, 2016). Other examples include the loss of thermal efficiency in a coal-fired boiler (Davey, 2015 a) and the initiation of pitting (corrosion) of metals used in off-shore oil and gas equipment (Davey et al., 2016).

More recently, to test and develop the *Fr 13* risk framework for progressively, multi-step and complex (in the sense of 'integrated', not 'complicated') processes Davey and co-workers demonstrated its utility to 2-step membrane fouling with combined ultrafiltration-osmotic distillation (UF-OD) (Zou and Davey, 2016), and; a 3-step microbiological raw milk pasteurization (Chandrakash and Davey, 2017). Findings revealed no methodological complications in applying the risk framework to simulations of increasingly integrated

processes – and it was concluded the risk framework was generalizable (Zou and Davey, 2016; Chandrakash and Davey, 2017).

Whilst the *Fr 13* framework has been successfully applied to pitting (corrosion) of AISI 316L metal used in off-shore oil and gas structures (Davey et al., 2016), it was not known if it could be adapted to other forms of corrosion, for example microbiologically influenced corrosion (MIC).

MIC is a major problem globally that can impact a wide range of materials such as metals, alloys, polymers and concrete (Roberge, 2000; Zhao, 2008; Javaherdashti, 2013), and accounts for ~ 20 % of overall corrosion (Flemming, 1996) (estimations are in the region of AUD$7 billion to Australia annually (Javaherdashti and Raman-Singh, 2001)).

A review of the literature showed that MIC modelling can be imperfect, both because of the wide variety of micro-organisms and range of conditions in which they can survive, and because of a lack of methodology to uncover any impact of natural fluctuations in the pipe environment. Importantly, MIC poses a practical risk due to its ability to cause unexpected and potentially catastrophic failure in pipes used to transport wet-fluids.

Because modelling of direct MIC would be uniquely complex it was planned that a general model for corrosion should be synthesized and understood that could be extended.

A limited research program was therefore undertaken to advance the *Fr 13* framework and to gain unique insight into how naturally occurring fluctuations in fluid temperature (T) and pH of the pipe environment can be transmitted and impact corrosion.

The initial model of Smith et al. (2011) was selected as a timely and stringent test of development of the *Fr 13* framework. It was adapted to simulate MIC causing micro-organisms such as sulphur-reducing bacteria (SRB) on widely used carbon-steel pipe (ASTM A105) that is corroded under pseudo steady-state, abiotic and synthetic conditions. Failure was defined by an off-specification from a tolerable corrosion rate, plus a practical tolerance as a design safety.

The principle aim of the research is to gain new insights into processes that could lead to unexpected corrosion and potential metals failure due to corrosion, and to stringently test the *Fr 13* framework as a useful design tool for corrosion modelling and to simulate intervention strategies.

A justification of this research is that the acquisition of an improved and realistic model will help increase the understanding of MIC and therefore permit more reliable and safer designs that might optimise MIC mitigation in a range of chemical engineering process applications.

A logical and stepwise approach was implemented as a research strategy.

Relevant literature is covered in Chapter 2 which reviews the *Fr 13* framework with recent examples, applications and limitations. As MIC was selected as the focus of this research, a general background is first covered, and MIC unit-operations models are identified and reviewed.

In Chapter 3 an initial unit-operations model of corrosion under abiotic conditions, based on the work of Smith et al. (2011), is synthesized, and then refined in Chapter 4 through the use of *Solver* spread-sheeting techniques. Second-tier studies are undertaken to evaluate re-design of the unit-operation for improved process safety.

In Chapter 5, limitations of the model are discussed, along with possible future developments of the research; the thesis concludes with a summary and conclusions in Chapter 6.

A definition of important terms used in this research is listed and carefully defined at end of the thesis. All symbols used are defined in the relevant Nomenclature.

Refereed publications resulting from this research are given in Appendix C.

CHAPTER TWO

LITERATURE REVIEW

2.1 Introduction

Friday 13th (*Fr 13*) is a concept that has long persisted in the industrial West (Suddath, 2009) whereby unexpected (surprise) mishaps or failures occur seemingly out of nowhere. It is defined as 'one of those days when just about all the bad in everything seems to combine' in order to induce failure. The concept of these unexpected, surprise failures is anecdotally widely acknowledged to occur in steady-state industrial (chemical) manufacturing and processing unit-operations. These failures are usually attributed to 'human error' or 'faulty fittings' and can occur no matter how 'good' the design and maintenance of the unit-operation (Davey and Cerf, 2003; Davey, 2010, 2011, 2015 a).

Davey and co-workers however (e.g. Davey et al., 2013; Chandrakash et al., 2015; Davey et al., 2015; Abdul-Halim and Davey, 2016; Zou and Davey, 2016; Chandrakash and Davey, 2017) have developed a novel quantitative *Fr 13* risk framework to show that the accumulation of random (stochastic), naturally occurring fluctuations in key process parameters can be the cause of the unexpected process failures. This framework has been used successfully in a number of steady-state unit-operations (e.g. Chandrakash et al., 2015; Davey et al., 2015; Abdul-Halim and Davey, 2016; Davey et al., 2016; Hathurusingha and Davey, 2016; Zou and Davey, 2016; Chandrakash and Davey, 2017).

In this chapter a detailed review of the *Fr 13* risk methodology, recent applications, benefits and limitations are presented, and a comparison made with traditional unit-operations assessments and alternative risk methods.

Microbiologically influenced corrosion (MIC) of metals was chosen to test and advance the framework as it can cause significant economic and physical devastation if not properly understood and controlled. A description of MIC, and the micro-organisms commonly associated with MIC (in particular, sulphate-reducing bacteria, SRB), is reviewed in this chapter and MIC unit-operations models are identified and evaluated.

To conclude this chapter, a steady-state corrosion model based on the work of Smith et al. (2011) is selected for *Fr 13* investigation as a first step, with a view to extend it to include MIC in future research.

2.2 Traditional single value assessment (SVA) deterministic solution

The traditional method of simulating chemical engineering unit-operations is a single point, deterministic approach, with or without a sensitivity analysis (Sinnott, 2005; Davey,

2015 a; Chandrakash and Davey, 2017). Davey and Cerf (2003) called this methodology a deterministic, Single Value Assessment (SVA).

This method involves using a single or 'best guess' (mean) value for each process parameter used in the model (e.g. temperature, pH, pressure, etc.) to solve for a single 'best estimate' outcome. A small variation (± 1 to 5 % tolerance) is usually used around these single, mean process input values to test for *uncertainty* (Davey et al., 2015).

In the SVA, model input parameters are linked with each other and output values via normal mathematical expressions such as addition, subtraction, multiplication, division and exponentiation. The equations can be solved through mathematical software such as Microsoft Excel™ spread-sheeting software. This SVA method is used to solve many unit-operations in chemical engineering (e.g. Foust et al., 1980; McCabe et al., 2001).

However, the potential impact of stochastic (random) uncertainties with naturally occurring fluctuations in the value of inputs and possible impact on unit-operation outcomes are not accounted for implicitly with this traditional method.

2.3 Development of the probabilistic *Fr 13* framework

The term *Fr 13* (*Friday the 13th Syndrome*) was coined by Davey and co-workers to quantitatively explain surprise failure in a well-operated and well-designed UHT (ultra-high-temperature) pasteurizer with unexpected survival of *Bacillus stearothermophilus* and *B. thermodurans* in raw milk pasteurization (Davey and Cerf, 2003).

Their underlying hypothesis was that naturally occurring, random fluctuations in the value of key process parameters can accumulate in one direction in amounts sufficient to leverage significant change in plant output behaviour - and thereby make seemingly well-operating processes vulnerable to random (surprise) failure. This can lead to a process or product becoming inefficient, unstable, or, more generally, 'unsafe' (Davey, 2015 a; Abdul-Halim and Davey, 2015; 2016; Zou and Davey, 2016; Chandrakash and Davey, 2017).

2.3.1 A typical *Fr 13* assessment

The structure of a *Fr 13* risk assessment is similar to the traditional SVA in that all mathematical operations (additions, subtractions, multiplications, divisions,

exponentiations, etc.) that link the model parameters are the same, except that a probability distribution is used for the key input parameters in place of the single 'best guess' mean value (Davey, 2010; Davey et al., 2013; Abdul-Halim and Davey, 2015; Hathurusingha and Davey, 2016; Zou and Davey, 2016; Chandrakash and Davey, 2017).

There are five steps in a *Fr 13* probabilistic risk assessment of a steady-state unit-operations process:

1. Unit-operation model synthesis

A unit-operations model must first be formed. This is usually done through synthesis and validation of key process parameters into a new or existing computational model and testing for stability

2. Probability distribution selection

A probability distribution is a range of probable values an input process parameter may take, together with the likelihood that parameter will take a unique (single) value. These can be taken from experimental data, or based off expert knowledge, or opinion. Generally, there are some 40 theoretical distribution types that could be selected (Vose, 2008) such as: *normal*, *triangle*, *beta subjective* or *tnormal* (Abdul-Halim and Davey, 2015). Truncation is a measure to ensure that only values that could physically occur in the system are used (Zou and Davey, 2016; Chandrakash and Davey, 2017)

3. Establishing an unambiguous definition of process failure

A definition of process (or product) failure must be carefully synthesized that is both unambiguous and practical to use. Depending on the type of process this could be unwanted survival of contaminant spores in milk pasteurization (Chandrakash and Davey, 2017), loss of thermal efficiency in a coal-fired boiler (Davey, 2015 a), chemical taste taint in farmed barramundi fish (Hathurusingha and Davey, 2016), or excessive pitting corrosion of stainless steel AISI 316L in the Bass Strait (Davey et al., 2016)

4. Sampling using refined (*Latin Hypercube*) Monte-Carlo (r-MC)

A Monte-Carlo simulation is a statistical technique that involves the random sampling of each probability distribution within a process input parameter to produce 1000's (up to 100,000's) of scenarios, or iterations. Each probability distribution is sampled in a manner

that reproduces the shape of the distribution. Two major components of Monte Carlo simulations are uncertainty and *variability* (Vose, 2008).

A refined Monte Carlo (r-MC) with *Latin Hypercube* refinement is used in *Fr 13* risk modelling however because 'pure' Monte Carlo can over- or under-sample values from various parts of the distribution (Davey, 2015 a; Abdul-Halim, 2017; Chandrakash and Davey, 2017). When the sample size is large enough (some 1,000 to 50,000 iterations (Abdul-Halim and Davey, 2015; Davey et al., 2015)), the output distribution will approximate the *normal* distribution (Vose, 2008; Davey, 2015 a).

With a sufficiently large number of r-MC samples in the *Fr 13* simulation, it can be reasonably assumed that all possible combinations of input parameters and resultant outputs, including scenarios that are considered failures, will have been simulated

5. Interpretation of steady-state unit-operation process simulation behaviour with 'second-tier' studies

The output of a probabilistic *Fr 13* risk simulation is a distribution of all possible process outputs, including failures.

A significant advantage claimed for the *Fr 13* assessment is that it can be used to reduce risk through repeat simulations in order to investigate intervention strategies and the potential re-design of the physical plant or unit-operation.

These are defined as 'second-tier studies' and can be applied at both the *synthesis* and *analysis* stages (Chandrakash and Davey, 2017).

2.3.2 The 5-step *Fr 13* risk algorithm

Davey (2010) proposed a generalized 5-step algorithm for a *Fr 13* risk assessment - that has subsequently been successfully applied by Davey and co-workers (Abdul-Halim and Davey, 2015; 2016; Zou and Davey, 2016; Chandrakash and Davey, 2017). This algorithm is thought to be applicable to any steady-state unit-operation.

The 5-steps of the algorithm are:

1. Select an identifiable unit-operation and process
    a. Synthesize and validate key process parameters in a computational model and software for particular plant outputs
    b. Establish a clear definition (or definitions) of process (or product) failure

2. Identify key process input parameters on process (or product) failure using traditional engineering SVA approaches
3. Define, investigate and test plausible probability distributions for the identified key process parameters
4. Simulate the unit-operation process using *Fr 13* with r-MC (*Latin Hypercube*) sampling
5. Distil insights from *Fr 13* framework to improve unit-operation process design with minimised venerability to failure
    a. Identify and rank the significance of key process input parameters on failure through sensitivity analysis
    b. Investigate effects of 'what if' scenarios and consequences of proposed intervention strategies. Evaluate risks and potential opportunities

2.3.3 *Fr 13* applications

Table 2-1 presents a chronological summary of five applications of *Fr 13* that have been published in the refereed literature.

The genesis of the *Fr 13* risk framework was to quantitatively explain the vulnerability to failure of a 'well-operated' UHT milk pasteurizer (Davey and Cerf, 2003). In this, failure was defined as a 1 L pack of UHT milk that had an unacceptable level of unwanted viable *Bacillus stearothermophilus* and *B. thermodurans* (plus a tolerance) - pathogens that can cause serious public health problems.

The key UHT process operating parameters identified and simulated using r-MC were the decimal reduction time at reference temperature (D_r), the temperature change for a ten-fold change in decimal reduction time (z), heating temperature (T), residence time (t), and the spore concentration (C_0). The *Fr 13* assessment showed that, for 100,000 iterations, there were 16 non-sterile milk packs (packs whose level of surviving contaminants spores were unacceptably high), i.e. a risk value of 1.6×10^{-4}. This value was 1.6×10^{5} greater than the SVA risk value of 1×10^{-9}, and importantly 16 times greater than the industry accepted value of 1×10^{-5} for the non-sterility of UHT milk packs. The authors concluded that a higher proportion of non-sterile milk packs could occur due to the unexpected, random fluctuations of unit-operation parameters within the UHT sterilization process.

Davey (2015 a) performed a *Fr 13* risk assessment of fuel-to-steam fuel efficiency of a coal-fired boiler (CFB) to quantitatively determine the risk to reduced CFB efficiency due

to naturally occurring random (stochastic) changes in key parameters. Simulation of 20 key input parameters (including coal feed and quality) revealed an underlying risk of 73 failures per 10,000 operations, equating to on average three failures each year over a prolonged period. This represented approximately \$7,560 year^{-1} in additional coal costs due to these instantaneous and random losses of efficiency. However, a benefit of the *Fr 13* simulation was through the use of 'second-tier' studies, which showed that if the feed coal was pre-mixed and pre-sized to a consistent blend before being fed to the boiler, then the standardized feed would minimise the unwanted impact of fluctuations on CFB efficiency and therefore minimise costs.

Davey et al. (2016) applied the *Fr 13* risk framework to metals pitting (stainless steel AISI 316L) in the Bass Strait. Pitting (i.e. failure) was defined as a pitting potential (E_{PIT}) lower than the open circuit potential of the steel (E_{OCP}), plus a tolerance. Simulation of key input parameters sea surface temperature (T) and salinity (Cl^-) revealed that 463 out of 5,000 samples (i.e. 9.26 %) were deemed to be failures, i.e. pitting has occurred. The model was then used to create a new atlas for metals pitting at sea. Termed 'isorisque', this map was defined as contours of equal probability of risk of metal pitting due to naturally occurring, random fluctuations in sea surface temperature and salinity. It was envisioned that the map could be made real-time and 'zoom-able', in order to determine the change in pitting risk after a sudden shift in sea surface temperature or salinity due to circumstances such as a major storm or ice (salt-free) melt, or to simulate the impact of (slow) climate change.

Davey (2016) used *Fr 13* to analyse the use of ice slurry cooling of fish (Southern Bluefin Tuna – *Thunnus maccoyii*) to determine the risk of not meeting regulatory guidelines to cool to a particular temperature in a given time. Failure was determined as the inability to cool to the centreline of the fish (the slowest cooling point) to a regulatory 5 °C in under 12 h, plus a tolerance. Simulation of key input parameters ice slurry (convection environment) bulk temperature (T_s), initial (conduction environment) uniform temperature (T_i) and mean mass of the fish at harvest (m_f) revealed that 693 out of 10,000 random samples (i.e. 6.93 %) were deemed to have failed, i.e. the temperature had not cooled to below 5 °C in under 12 h.

Table 2-1: Summary and chronological listing of published *Fr 13* risk studies for steady-state, unit-operation processing

	Unit-operation	*Fr 13* model	Reference(s)
1	UHT milk sterilization	First use of *Fr 13* risk framework. Failure defined as 1 L pack of UHT milk with unacceptable level of unwanted micro-organisms. UHT parameters (D_r, z, T, t and C_0) described by probability distributions. 16 out of 100,000 simulations (i.e. 0.016 %) were deemed to be failures i.e. non-sterile milk. Risk was shown to be 16 times greater than industry accepted value of 1×10^{-5}.	Davey and Cerf (2003)
2	Coal-fired boiler (CFB)	*Fr 13* analysis of thermal efficiency of coal-fired boiler (CFB). Failure defined as efficiency η' < SVA efficiency η = 77.82 %. 20 CFB parameters chosen including coal feed and quality. 73 out of 10,000 simulations (i.e. 0.73 %) deemed to be failures, requiring additional coal costs of ~ \$7,650 year^{-1}. Second-tier studies showed that feed coal could be pre-mixed and pre-sized to standardize blend and minimize impact of fluctuations on efficiency and therefore minimize cost.	Davey et al. (2015 a)
3	Metals pitting at sea	*Fr 13* was used to investigate metals pitting (stainless steel AISI 316L) in Bass Strait. Failure defined as pitting potential E_{PIT} lower than open circuit steel potential E_{OCP}. Pitting parameters sea surface temperature (T) and salinity (Cl^-) chosen. 463 out of 5,000 samples (i.e. 9.26 %) deemed to be failures i.e. pitting has occurred. Simulation used to create 'isorisque', an atlas defined as contours of equal probability of risk of metal pitting.	Davey et al. (2016)
4	Ice slurry cooling of fish (Southern Bluefin Tuna – *Thunnus maccoyii*)	*Fr 13* was applied on the use of ice slurry cooling of fish (Southern Bluefin Tuna – *Thunnus maccoyii*). Failure defined as inability to cool to fish centerline to regulatory 5 °C in under 12 hours. Cooling parameters included ice slurry bulk temperature (T_s), initial uniform temperature (T_i) and mean mass of the fish at harvest (m_f). 693 out of 10,000 samples (i.e. 6.93 %) deemed to be failures i.e. insufficient cooling. Simulation required use of *Solver* function to iterate to a sensible output. Second-tier studies showed cooling risk could be mitigated if slurry temperature was maintained as close as possible to theoretical 0 °C, could be achieved by observation of visible ice pieces in slurry.	Davey (2016)

5	3-step pasteurization of raw milk containing *Mycobacterium avium* subsp. *Paratuberculosis* (*MAP*)	*Fr 13* analysis of integrated 3-step microbiological failure synthesis of pasteurization of raw milk containing *Mycobacterium avium* subsp. *Paratuberculosis* (*MAP*). Failure defined as unwanted survival of *MAP* during holding (regulatory design reduction of >99.999 % in viable *MAP* on heat-up to 72 °C with 15 s holding. Pasteurization parameters included inlet temperature (T_i), mass flow rate (m) and specific heat (C_P) of raw milk, heat-up water and cool-down brine. 5.75 % deemed to be failures, ~21 failures with unwanted *MAP* survival each year. Insights included that failure in one unit-operation did not necessarily lead to failure in the following unit, or even in the final pasteurized milk. Second-tier studies showed that vulnerability to microbiological failure could be mitigated by installation of precise mass flow controllers on raw milk inlet, as well as establishment of strict system to maintain design required holding time of heated raw milk in holding tube.	Chandrakash and Davey (2017)

The model required the use of *Solver* spread-sheeting tools to iterate to a sensible output value. Quantitative evidence showed that variance around the mean fish mass had the most impact on cooling failure, and that risk could be mitigated if the slurry temperature was maintained as close to the theoretical minimum of 0 °C (notwithstanding the acceptable use of brine slurries). This could be achieved by ensuring that visible pieces of ice were observed and maintained in the slurry mixture.

The latest development in application of the *Fr 13* risk framework is the analysis of an integrated 3-step microbiological failure synthesis of pasteurization of raw milk containing *Mycobacterium avium* subsp. *Paratuberculosis* (*MAP*) by Chandrakash and Davey (2017). The aim was to study how naturally occurring, random fluctuations in processing parameters can be transmitted and impact multi-step unit-operations. The three steps included in the pasteurizer (and model) were: the heat-up of the raw milk, holding for thermal inactivation of the *MAP* contaminant, and the cool-down of the heat-treated milk. The overall pasteurizer failure was defined as the unwanted survival of *MAP* following holding. A (regulatory) design reduction of $\log_{10} = 5.5$ (>99.999 %) in viable *MAP* on heat-up to 72 °C with 15 s holding (with a design safety margin of 2 %) was chosen as the success / failure margin. Simulation of key input parameters inlet temperature (T_i), mass flow rate (m) and specific heat (C_p) of the raw milk, heat-up water and cool-down brine showed failure in 5.75 % of cases, equating to ~21 failures with unwanted *MAP* survival each year, average over an extended period of daily batch-continuous operations. Important insights gained from the simulation were: a) failure in one unit-operation did not

necessarily lead to failure in the following unit, or even in the final pasteurized milk, and b) (batch) continuous pasteurization were seen to be a mix of successful operations together with unsuccessful ones. Second-tier studies showed that the pasteurizer vulnerability to microbiological failure could be mitigated by 1) installing precise mass flow control on the raw milk inlet, and 2) establishing stringent methods to maintain the design required holding time of the heated raw milk in the holding tube apparatus.

Table 2-1 shows that the concept of *Fr 13* is being widely accepted in the risk assessment literature.

2.3.4 Benefits and limitations of *Fr 13*

The *Fr 13* risk framework has a number of benefits over similar probabilistic methodologies such as those of Aven (2010), Haimes (2009) and Milazzo and Aven (2012). It is based on established unit-operations principles in chemical engineering (Foust et al., 1980; Ozilgen, 1998; McCabe et al., 2001), and because of the probabilistic element, it provides a quantitative picture of all mathematically practically possible process scenarios, including carefully defined failures (Davey, 2015 a; Zou and Davey, 2016; Chandrakash and Davey, 2017).

It is mathematically more correct than alternative risk assessment methods such as Hazard and Operability Studies (HAZOP) or Hazard Analysis Critical Control Point (HACCP) because it separates the effect of chance (variability) from knowledge about the process (uncertainty) (Davey and Cerf, 2003; Chandrakash, 2012; Chandrakash and Davey, 2017).

Additionally, it can be used in ‘second-tier’ studies to reduce risk by making physical changes to either the process or operating procedure. The framework can be applied at either the *design* or *synthesis* stages. For example, Zou and Davey (2016) suggested that the addition of (regulatory acceptable) enzymes as an additional step before treatment of concentrated juice through combined ultrafiltration-osmotic distillation (UF-OD) could reduce the number of macromolecules which are more likely to cause fouling on the membrane.

A limitation of the *Fr 13* risk framework is that, to date, experimental validation of the published research has been lacking. One possible reason for this is that obtaining experimental data (and therefore running validation studies) can be problematic in the sense that unexplained and non-equipment failure data are usually not disclosed publicly.

This means that the true impact of these failures can be hidden (Zou and Davey, 2016). However, there is published *Fr 13* research that has relied on historical/independent data e.g. Davey et al., 2016; Zou and Davey, 2016; Chandrakash and Davey, 2017.

2.3.5 *Fr 13* and other risk approaches

The impact of random, naturally occurring fluctuations in physical parameters in a unit-operation process around an expected steady-state 'set' mean has also been the subject of the recent risk assessment approaches of Aven (2010), Haimes (2009) and others including Milazzo and Aven (2012). For example, Milazzo and Aven (2012) performed a quantitative risk assessment (QRA) on accidental events related to the rupture of pipes in a chemical plant. They advocated that while a probabilistic approach was useful in evaluating risk, it should be extended to place a stronger emphasis on uncertainties i.e. whether or not data used in a risk assessment is applicable to the specific process/scenario currently being modelled.

To account for this perceived drawback, they proposed two methods. The first was to use probability distributions (e.g. *beta* distribution, *triangular* distribution or *uniform* distribution), along with an event-tree model, to reflect the uncertainties in process parameters for a particular risk. The use of probability distributions is similar to the *Fr 13* risk framework. However, for the process uncertainties, they adopted a 'score system' of Low, Medium and High. The authors acknowledged that this approach meant that the risk technique was still largely qualitative, and that it still restricted scenarios to the most credible outcomes.

Because the *Fr 13* framework is based on established unit-operations principles (Foust et al., 1980; Ozilgen, 1998; McCabe et al., 2001), it is openly quantitative, generalizable (in principle), and provides a quantitative picture of all practically possible process scenarios, including carefully defined failures (Davey, 2015 a; Zou and Davey, 2016; Chandrakash and Davey, 2017; Davey, 2018). It should be noted however that both methods share the same goal of placing a 'stronger emphasis (on the impact of) …uncertainties' (Milazzo and Aven, 2012; Zou and Davey, 2016).

It is important to note that the insights gained from both the *Fr 13* and Milazzo and Aven (2012) probabilistic methods are not available from risk assessment alternatives such as Hazard and Operability Studies (HAZOP), Hazard Analysis Critical Control Point (HACCP) or Reliability Engineering. This is because the random element is not explicit.

2.3.6 *Fr 13* as terminology

Although *Fr 13* is usually considered a day in which everything 'bad' can happen to bring about unexpected failure, Davey and co-workers (Abdul-Halim and Davey, 2015; 2016; Zou and Davey, 2016; Chandrakash and Davey, 2017) have carefully defined it as a 'particular outcome behaviour that is a measurable failure'.

An alternative terminology suggested for the *Fr 13* risk framework (Zou and Davey, 2016; Chandrakash and Davey, 2017) was *Iterative Random-impacts Assessment* (IRA), where it was thought it might be used to predict (and fix) probable events before they occur.

More generally, however, unexplained and non-equipment failure is problematic as these are not disclosed (publicly at least). Compare this situation with for example with the vast equipment failure contained in data bases such as OREDA (2015).

However, *Fr 13* clearly conveys the unexpected (surprise) nature of a failure in plant outcome behaviour despite apparent good design and maintenance.

2.4 Microbiologically Influenced Corrosion (MIC)

Microbiologically influenced corrosion (MIC) is a general term used to describe insidious and unwanted corrosion caused directly or indirectly by micro-organisms (Zhao, 2008; Javaherdashti, 2013). It occurs when these attach themselves to a surface through either physical adhesion or through the use of a 'biofilm' (secretions that help microbial colonies adhere to and thrive on a metal or concrete surface), and then release metabolic products that change the electrochemical conditions at the surface/fluid interface. These changes can lead to initiation of corrosion (Moura et al., 2013).

MIC can be found on both above- and below-ground processing equipment, and in internal pipe-fluid environments (Jacobson, 2007) that transport water-based fluids such as 'water-oil-chemical' cuts. Typically, MIC occurs at low points in pipe internals due to the water and water-soluble nutrients being relatively denser than the oil, causing them to settle.

The particular micro-organisms of interest are bacteria, but also fungi, algae and protozoa (Pope et al., 1989; Zhao, 2008).

MIC impacts globally in off-shore and on-shore chemical engineering gas and oil industries.

In particular, in Australia in the Bass Strait with 23 off-shore oil and gas platforms and thousands of kilometres of pipe (Exxon Mobil Australia, 2015; Davey et al., 2016; J. Y. G. Chu, Upstream Production Services Pty Ltd., Australia, *pers. comm.*), also; more widely, in water treatment plants, and nuclear power plants with stainless and carbon-steel tanks and piping, and aluminium and bronze cooling tubes (Jack, 2002; Zhao, 2008).

2.4.1 Problems associated with MIC

MIC can lead to the corrosion and ultimate failure of a wide range of materials used in process engineering, including metals and alloys, some polymers, and hessian and concrete (Roberge, 2000; Zhao, 2008; Javaherdashti, 2013).

Micro-organisms can accelerate various types of corrosion, such as: uniform corrosion, crevice corrosion, galvanic corrosion, intergranular corrosion, and stress corrosion cracking (Rawat et al, 2014). Of particular concern is rapid pitting corrosion. This is a localized form of corrosion where ‘cavities’ are formed in the material (Szklarska-Smialowska, 1986). It is considered to be more serious than uniform corrosion, as it can cause equipment to fail quickly (Dillion, 1982; Zhao, 2008).

MIC can also cause a loss of structural and technical integrity in process equipment, that can lead to structural failures and loss of containment. It can lead to the rapid destruction of concrete sewer mains and reinforced concrete (Roberge, 2000). It can also be a cause of major accident events (MAEs) and potential multiple fatalities in widely used steady-state processes in chemical engineering. The corrosion of storage tanks and pipelines used in oil transportation by MIC can lead to leaks which cause environmental contamination and environmental problems. In the Gulf of Guinea, pitting corrosion reduced the life of oil sub-sea pipe lines to one year (Crolet, 1993), and; in some European countries, replacement of steel piling in quays, harbours and jetties with 60-year design lives was required after only 10 to 20 years, due to micro-organisms causing accelerated low-water corrosion (Gubner and Beech, 1999; Breakell et al., 2005).

MIC can also increase the friction factor inside pipes by increasing the surface roughness of the pipe. This occurs as the micro-organism colonies can have irregular surfaces and ‘spongy’ behaviour that can exaggerate fluid-flow drag (Roberge, 2000). This leads to reduced flow capacity, as well as a reduction in the capacity for heat transfer of the pipe surface in, for example, heat exchangers (Holman, 2010).

2.4.2 Economics of MIC

Costs associated with MIC are wide ranging as it is difficult to determine what damage is classified as MIC and what is classified as other forms of corrosion. The World Corrosion Organisation puts the annual cost of corrosion as greater than 3 % of global GDP (Hays, 2012). Enning (2014) states the (inferred) cost of metal corrosion to be an estimated 2 to 3 % of GDP in developed countries, whilst Geesey et al. (2000) estimated it to be approximately 4 % of GNP.

MIC is believed to account for 10 to 20 % of the damage caused by corrosion (Flemming, 1996; Geesey et al., 2000; Moura et al., 2013). Other sources (Rajasekar et al., 2007) state it is responsible for 40 % of pipe corrosion in the oil industry, 15 to 30 % of corrosion in the oil and gas industry (Beech and Sunner, 2007), and; 10 % of corrosion cases in the United Kingdom (de Romero et al., 2000). A staff report in World Oil (Anon., 1972) claimed that 10 % of the world's crude oil has been destroyed and another 10 % significantly reduced in value due to activity of micro-organisms.

In monetary terms, Hansson (2010) estimated that costs related to corrosion were equivalent to US$500 billion in the United States, whilst Koch et al. (2001) estimated all forms of corrosion costs $13.4 billion per year, with $2 billion being attributed to MIC. In the US oil and gas industry, it is estimated to be in the range US $100 million annually (Beech and Sunner, 2007). In Australian industries, MIC-related losses are estimated to be more than AUD $7 billion per year (Javaherdashti and Raman-Singh, 2001).

2.4.3 Classification of micro-organisms commonly associated with MIC

There are numerous types of micro-organisms that are involved in microbiologically influenced corrosion (MIC). The five major groups are: bacteria, fungi, algae, protozoa and viruses (Chilingar, 2008).

Bacteria are typically under 10 μm, simple prokaryotic micro-organisms (Chilingar, 2008; Moura et al., 2013) that can exist under a wide range of temperature, pH, pressure, nutrient availability, and other environmental or operating conditions. They possess the ability to maintain exponential growth when supplied with essential nutrients. Some can tolerate harsh environments of high temperature and high pressure and salinity. There is a wide variety of bacteria that are commonly associated with MIC. Some of the most common include: sulphate-reducing bacteria (SRB), sulphur-sulphide-oxidizing bacteria

(SOB), metal-reducing bacteria (such as iron-reducing bacteria), iron/manganese-oxidizing bacteria, aerobic slime formers, methane producers, and; organic acid-producing bacteria (Roberge, 2000; Zhao, 2008; Javaherdashti, 2013).

Fungi are eukaryotic organisms that grow by decomposing and absorbing organic material (Alberts et al., 2002; Moore et al., 2017). They can be broadly separated into yeasts and moulds. Fungi cause degradation of materials through the production of corrosive by-products as a result of their metabolism. They also accelerate corrosion by trapping other organic or non-organic materials, which can lead to fouling.

Algae are mainly aquatic, eukaryotic uni- or multi-cellular organisms that contain chlorophyll but differ from plants due to their lack of true roots, stems and leaves (Alberts et al., 2002; Lewin and Andersen, 2017). They can survive under a wide range of environmental conditions and usually have simple nutritional requirements (Roberge, 2000). Algae can cause corrosion through the formation of organic acids, and unmitigated growth can lead to fouling or blockages in pipes and equipment (Chilingar, 2008).

Protozoa are organisms that eat bacteria and algae, and in some circumstances, can reduce potential for MIC in a system (Roberge, 2000).

Micro-organisms can also be classified by the following criteria: oxygen tolerance, temperature tolerance, shape, metabolism, and whether they are gram-negative or gram positive (Roberge, 2000; Chilingar, 2008; Javaherdashti, 2013) (note that this list of classification is not exhaustive).

Oxygen tolerance divides micro-organisms into how well they can live and grow in the presence of oxygen. Groups include:

- Strict anaerobes (will not function if oxygen is present)
- Aerobes (require oxygen to function)
- Facultative anaerobes (can function in either the absence or presence of oxygen)
- Microaerophiles (use low levels of oxygen)
- Aerotolerants (anaerobes that are not affected the presence of oxygen)

Another way to classify micro-organisms is by temperature tolerance. Examples of classifications by temperature include (note that these temperature ranges are approximate):

- Psychrophiles (-20 - 16°C)
- Mesophiles (5 - 44°C)
- Thermophiles (44 - 100°C)

Micro-organisms can also be divided by their metabolism:

- The nutrients from which they obtain carbon for growth and reproduction
- The chemical means by which they obtain energy or recharge the oxidative capacity of the cell (fermentation or respiration)
- The by-products as a result of their metabolism (metal ions, organic acids, etc.)

A fourth way of classifying micro-organisms is by cell shape. Examples include:

- *Bacillus* – rod shape
- *Coccus* – round shape
- *Vibrio* – comma-shape

It should be noted that while the shape of a particular micro-organism is predictable under laboratory conditions, in a natural environment, their shape will often be determined by growth conditions (Roberge, 2000).

Overall, micro-organisms can be divided by whether they are gram-negative or gram-positive (Chilingar, 2008). These classifications are used when the micro-organism (primarily bacteria) is subjected to a common microbiological identification and characterization technique called Gram staining (Madigan et al., 2003) (*see* Appendix A).

2.4.4 Identification and enumeration of MIC-causing micro-organisms

Determining a system's susceptibility to MIC requires accurate identification of both the type and number of micro-organisms found in the system (Roberge, 2000).

The simplest method of identifying micro-organisms is by direct inspection. This is best suited to planktonic (free-floating) cells in relatively clear water, as water with densities > 10^7 cells cm^{-3} can appear turbid. However, this method is usually only seen as a starting point as it is both very rudimentary and non-quantitative.

To perform more accurate analyses, some form of water or fluid sampling must be performed. Depending on the system, this could be as simple as scraping surfaces and collecting samples in an open system. For closed systems, using coupons (which must be made of the same material as the pipe or equipment and flush mounted in the wall so that they don't disturb fluid flow (Videla and Herrera 2005)) or inspection ports are sufficient for low pressure systems. For high pressure systems, there are devices that allow the implantation of coupons directly into pipes or equipment (sidestream systems). However,

they are expensive, technically difficult to install and remove, and have location restrictions such as those required from pressure vessel codes. Sidestream sub-systems can also be installed to collect samples without mostly disturbing the process fluid flow.

Samples collected from the field must be carefully handled to avoid contamination with foreign matter. The introduction of any oxygen can also be significant, depending on whether the micro-organism being sampled is aerobic or anaerobic. Commercial kits are available that can analyse process fluid samples on the spot, reducing the potential for sample contamination. If samples are to be analysed in a laboratory (either on- or off-site), it must be done as quickly as possible, as micro-organisms can either grow or die due to such effects as temperature and nutrient availability changes, and oxygen exposure. This would affect the accuracy of the sampling results (Jack, 1999).

The most common way to assess the type and number of micro-organisms in a field sample is through growth assays using commercially available growth media. These are tailored for micro-organisms that are normally found in industrial settings. The samples are diluted and grown on substrates like solid agar or in liquid broths. The micro-organisms grow on the substrate and an estimate of the cell counts can be made using microscopy techniques (Costerton and Colwell, 1977). The process can be enhanced by the addition of fluorescent dyes that cause the cells to light up under UV radiation, such as acridine orange, fluorescein diacetate and *p*-idonitrotetrazolium. The main downside to this technique is that only a small fraction of micro-organisms found in nature will grow in artificial media, and therefore many important micro-organisms might be missed in an analysis.

Assays can also be used to assess the activity of micro-organisms. One method uses radioisotopically labelled substrates that change depending on what micro-organisms are present in the sample. The technique requires the substrate to be carefully selected but offers numerous advantages such as: field samples can be used directly, the technique is very sensitive, micro-organisms don’t need to be separated beforehand, and samples can be compared against other supplemented test samples under various conditions (Roberge, 2000). Radioisotope techniques are not usually used by field operators, but have a number of applications including biocide selection, nutrient source identification and micro-organism metabolic studies (Jack, 1999).

Another micro-organism activity technique is the use of commercial kits to analyse the enzymes associated with particular micro-organisms. For example, there are kits available that can detect the sulphate reductase enzyme required for some SRB strains to function

(Odom et al., 1991). A downside to this technique is that it generally has a narrower range of application compared to a growth media-based method.

Micro-organism activity can also be determined by measuring the chemical adenosine triphosphate (ATP). This metabolic molecule drives many cellular reactions. Instruments that use this technique measure the release of light from a firefly enzyme (luciferase) binding with ATP and correlate it with a measure of micro-organism activity. The method is best suited with clean, aerobic aqueous samples, as particulate matter can affect the results.

A major drawback with growth and activity assays is that they focus mainly on planktonic micro-organisms. This is problematic because these analyses do not reflect the types and numbers of micro-organisms that live within the biofilm matrix (i.e. sessile (immobile) cells). A micro-organism's susceptibility to biocides is also different depending on whether it is in a planktonic or sessile state.

More recent monitoring techniques involve the use of molecular methods incorporating the DNA and RNA of a micro-organism. This method involves the use of a DNA probe, which is a small piece of DNA that is designed to bind to a specific part of DNA (e.g. an enzyme) in a target micro-organism. For example, a DNA probe was developed to detect the hydrogenase enzyme that can occur in SRB from genus *Desulfovibrio* in an oil field that had signs of iron sulphide-related corrosion (Voordouw et al., 1995). It is thought that this monitoring technique have the potential to: a) identify the dominant micro-organism in a system without the limitations of cell counting techniques; b) calculate the proportion of MIC-contributing micro-organisms in the total microbial population; c) identify the micro-organisms that are susceptible or resistant to biocide treatments; d) assess changes in the microbial population due to either the use of biocides or changes in nutrient availability; and e) achieve a more accurate and reliable sampling procedure that is less vulnerable to errors due to time delays or transport issues between sampling and analysis (Videla and Herrera, 2005).

However, a downside to these molecular methods is that they are still very specific in what micro-organism is being enumerated.

2.4.5 Types of bacteria commonly associated with MIC

2.4.5.1 Sulphate-Reducing Bacteria (SRB)

Sulphate-reducing bacteria (SRB) are a group of organisms that, generally, reduce sulphur compounds (sulphate, thiosulphate, sulphite, polythionates, polysulphides and even elemental sulphur) to sulphide (Le Faou et al., 1990; Roberge, 2000; Zhao, 2008). Mohanty et al. (2000) narrowed the description to all uni-cellular bacteria that are capable of reducing sulphate to sulphide. They gain their energy for growth through the reduction of these compounds to hydrogen sulphide (H_2S) (or black ferrous sulphide FeS if iron is present), with the required electrons usually derived from the degradation of organic matter (such as volatile fatty acids (e.g. acetate), alcohols, aromatic compounds or sugars), CO_2, or from molecular hydrogen (H_2) through the use of an enzyme called hydrogenase (Roberge, 2000; Ollivier et al., 2007; Enning, 2014).

SRB mostly require a complete lack of oxygen (anaerobic) and a highly reduced environment to function properly, with some strains being able to handle low levels of oxygen (Roberge, 2000; Beech and Sunner, 2007; Moura et al., 2013). They can grow across a wide range of environmental conditions (Ollivier et al., 2007): temperatures of 25 to 35, °C (most common strains), although some can grow over 60 °C or even over 100 °C (at high pressures) (Roberge, 2000); pH of around 4 to 10 (Zhao, 2008); and pressures of up to 500 atmosphere (Javaherdashti, 2013).

SRB was first isolated in 1895 (Beijerinck, 1895). The first report of the bacteria in an oil reservoir came in 1926 (Bastin, 1926). They are found in a variety of environments including: canals, harbours, estuaries, stagnant water from industry, sand, soils (clay) (Roberge, 2000; Ollivier et al., 2007; Javaherdashti, 2013), and can live on the surfaces of particles, minerals, or within biofilms (Characklis and Marshall, 1990). They can also be the first micro-organisms that are found to be colonising a new environment. This is particularly true of oil-field environments (Ollivier et al., 2007).

SRB are one of the most investigated groups of micro-organisms that are implicated in MIC damage (Beech and Sunner, 2007). They have been linked to MIC of cast iron and steel, ferritic stainless steels, 300 series stainless steels, copper-nickel alloys, and high nickel molybdenum alloys (Roberge, 2000). SRB have been reported in the corrosion of drilling and pumping machinery and storage tanks and can lead to the acidification and

contamination of crude oil and gas through the production of H_2S, a substance that is toxic to humans (Magot et al., 2000; Chilingar, 2008; Javaherdashti, 2013; Moura et al., 2013).

There are some 40 genera of SRB that have been reported, with the most studied genus being *Desulfovibrio* (Ollivier et al., 2007). Examples of strains include: *Desulfovibrio desulfuricans* (one of the most important strains as it metabolizes sulphate ions in the system to form H_2S), *Clostridium nigrificans* (thermophilic strain), and *Clostridium tetani* (Jones, 1988).

2.4.5.2 Sulphur-sulphide-oxidizing bacteria (SOB)

Sulphur-sulphide-oxidising bacteria (SOB) are aerobic and facultative anaerobic bacteria that derive energy for growth from the oxidation of inorganic sulphur compounds such as sulphide, sulphite, thiosulphate or elemental sulphur to sulphate (Roberge, 2000). Some strains (e.g. *Beggiatoa* or *Thiobacillus*) can oxidise sulphur to sulphuric acid, lowering the pH of the system to as low as one. These are usually found in mineral deposits and are largely responsible for acid mine damage. In situations where corrosion has occurred, *Thiobacillus* is almost always found together with SRB, as both bacteria are able to draw energy in a synergistic cycle (Moura et al., 2013; Javaherdashti, 2013).

2.4.5.3 Other types of bacteria

The list of bacteria associated with MIC is numerous. Other types include:

- Iron/manganese-oxidizing bacteria - aerobes that get their energy from the oxidation of iron and manganese (Chilingar, 2008). When they oxidise iron, they can form iron hydroxides like ferric hydroxide ($Fe(OH)_3$), usually forming insoluble precipitates which can create tubercles (hemispherical mounds) over pits in the metal surface (Roberge, 2000). This can lead to oxygen gradients (allowing anaerobic bacteria such as SRB to initiate and grow) and blockages in oil pipelines. They are widely found in water from rivers, lakes and oil production (Moura et al., 2013). Examples include *Gallionella*, *Crenothrix*, and *Sphaerotilus* (Jones, 1988)
- Methane producers – methanogens that consume hydrogen (like SRB) and carbon dioxide to produce methane. In low-nutrient conditions, they can become

fermenters and consume acetate instead. In natural systems, methanogens and SRB are often found in a synergistic relationship: SRB produce hydrogen, carbon dioxide and acetate by fermentation, which are then consumed by the methanogens (Roberge, 2000)

- Organic acid-producing bacteria – aerobes that can produce short-chain organic acids such as formic (methanoic), acetic (ethanoic), propionic and butyric (butanoic) acids as a result of their metabolism from the fermentation of organic materials. They are one of the initial colonizers in a system due to their aerobic nature and are found in many environments including gas and oil tanks. These bacteria can also be found working synergistically with SRB: the organic acid products can act as substrates for the SRB, which accelerates the corrosion process and lowers the pH of the system (Roberge, 2000; Moura et al., 2013).

2.5 Biofilms

A biofilm is a consortium of microbial cells that attach themselves to solid surfaces through the production of sticky secretions called extracellular biopolymer substances (EPS) (e.g. macro-molecules like polysaccharides, proteins, nucleic acids and lipids), which allows them to form a thin slimy film matrix which keeps them in one spot in the system (Beech and Sunner, 2007). They are the predominant form of bacterial growth in almost all aquatic systems, with about 98 % of the micro-organisms in the biofilm being bacteria (Donlan and Costerson, 2002). A biofilm is made up of 5 to 25, % (by volume) micro-organisms, with the remaining water. The dry weight consists mainly of the acidic EPS produced by micro-organisms. As surface roughness and material composition play a major role in biofilm formation, they tend to colonize at locations like welding zones, grain boundaries, and crevices.

The formation of a biofilm in a system occurs through a series of steps (Roberge, 2000; Zhao, 2008; Moura et al., 2013):

1. Organic and inorganic molecules will adsorb onto a completely clean surface to create a conditioning film
2. Planktonic bacteria attach to this thin film and form EPS that envelop the bacterial cells. This allows the cells to replicate without being sloughed off by fluid flow and allows them to become sessile

3. Over time (a few days to several weeks depending on the operating conditions or micro-organisms present), other planktonic micro-organisms (and abiotic particles) become entrained with the biofilm, causing micro-colonies to develop due to the establishment of beneficial relationships. This, along with the sessile cells producing greater quantities of EPS, cause the biofilm to increase in thickness. As the biofilm matures, enzymes and proteins accumulate and react to form more complex biopolymers, increasing the stability of the biofilm matrix
4. As the biofilm increases in thickness, the diffusion of gases and nutrients from the bulk fluid environment to biofilm matrix becomes retarded. Therefore, conditions at the base of the biofilm start to become intolerable and micro-organisms start to die off. This causes the foundation of the biofilm to weaken and then eventually break off due to the velocity of the fluid. This exposes the bare surface to the bulk fluid
5. These exposed areas are quickly recolonized and interwoven with the existing biofilm. This flux occurs even when the physical conditions of the pipe are constant.

Almost all micro-organisms form biofilms because it provides them numerous advantages. One is that it provides a consistent environment that traps nutrients flowing through the system and allows the enzymes in the micro-organism to use them for initiation and growth. This can lead to different groups working synergistically by using the metabolic by-products of each other for energy and growth and is a reason why MIC is seldom linked to a single type of micro-organism when it occurs in a system (Valencia-Cantero et al., 2003). Another advantage is that the bridging and cross-linking of the EPS helps stabilize the biofilm and makes it more resistant to shear due to fluid flow. Biofilms can also protect from external attacks like protozoa (which eat bacteria) (Roberge, 2000) and the use of biocides (which can also be affected by the corrosion products in the biofilm).

Biofilms contribute to MIC in numerous ways. Firstly, they can reduce the oxygen levels in the system, creating oxygen gradients that allows anaerobic micro-organisms to function and grow (Beech and Sunner, 2007). This allows for the accumulation of usually acidic metabolic products near the metal surface, accelerating corrosion. Secondly, the ‘patchy’ nature of biofilms generates differential aeration (oxygen) or ionic species cells. This leads to the creation of anodic and cathodic sites on the surface, which can start and

sustain the corrosion process. Thirdly, biofilms can trap and bind metal ions from the fluid into the organic matrix, which can increase the electronic and ionic conductivities of the biofilm and allow the ions to participate in the electron transfer process (Harrison et al., 2005). Fourthly, the EPS can act as a nutrient source for the micro-organisms in times of lean nutrient availability (Moura et al., 2013). Other undesirable elements of biofilms are: they can retain potentially harmful pathogens within their matrix, they can reduce the heat transfer if found within equipment such as heat exchangers, and they can increase the friction factor and the chance of blockages within the system (Roberge, 2000; Zhao, 2008; Javaherdashti, 2013).

2.6 Factors influencing MIC

Problems due to MIC most often occur in a new system when it is first 'wetted' (when equipment is exposed to fluids), or in an old system when operating conditions are changed such as new/different fluid quality, operating conditions, or materials of construction (Geesey, 1993). Operating parameters known to have, or suspected of having, an effect on MIC are temperature, pH, oxygen levels, pressure, flow velocity, water quality (cleanliness), and salt concentration (Roberge, 2000; Chilingar, 2008; Zhao, 2008, Moura et al., 2013):

Temperature – All micro-organisms have an optimal temperature range for initiation and growth. The rate of reaction of growth increases with increasing temperature, but only up to a certain point (after which the micro-organism will begin to die). Therefore, it is expected that that increasing temperature increases corrosion problems, but this is not always the case with MIC. The temperature of the system is also affected by conditions like the weather, equipment location (inside or outside) and the water source

pH – The pH of the water in the system can have an important effect on the function of micro-organisms. For example, some strains of SRB slow their growth at pH 11, while stopping completely at pH 12.5. This could be because too much of a pH change to a system can affect enzymes within certain bacteria types

Oxygen level – Depending on whether a micro-organism is aerobic, anaerobic, or facultative, the oxygen level can have a significant effect on its growth. Some microbiologically corrosion problems could be alleviated if the system is kept anaerobic. However, if facultative aerobes were present, they could just switch to an anaerobic

metabolism. This means that removing oxygen from a system could affect the rate of MIC, but will probably not eliminate a severe problem

Pressure – Micro-organisms can be found at a variety of pressures (up to 1400 bar) and can modify their function depending on the pressure change. For example, Bubela (1983) found that an increase in pressure increased the optimum metabolic temperature and rate of growth of rod-shaped bacteria, and that the shape of the bacteria also transformed from rod-shaped to coccoidal (spherical). High pressure can affect bacterial growth and therefore could be used to control micro-organisms, but maintaining such an environment is usually cost-prohibitive and/or impractical

Flow velocity – The ability of microbial cells to attach directly to a surface has little long-term effect due to flow velocity. However, once attachment is made, flow velocity affects the nature of the biofilm that forms. If the system is run at low velocity, biofilms will tend to be bulky and easily disturbed. If it is run at high velocity, the biofilm will be much more dense, thicker and harder to remove.

As a general rule, velocities of above 1.5 m s^{-1} should be maintained to minimize the settling out of solids as stagnant conditions will usually lead to problems. This rule is not foolproof however, as equipment material can be damaged if the flow velocity is too high (for example, copper can erode at 20°C if the flow velocity is above 1.5 m s^{-1})

Water quality (cleanliness) – Water quality usually refers to the turbidity of the water. Solids settling in the system usually enhances corrosion by creating surfaces that micro-organisms can establish and grow on. Monitoring the organic and dissolved solids content of the water is important in MIC control as ‘cleaning up the water’ can help reduce its effects. This is not necessarily a solution though because, as a rule, if micro-organisms are able to grow in the water, the potential for MIC to occur is present. It should be noted that the cleanliness of the equipment surface is usually the more important consideration

Salt concentration – Salt concentration refers to the levels of sodium chloride (NaCl) and calcium chloride ($CaCl_2$) in the water. A difference in the salt concentration of the surroundings versus the inside of the cell causes a large osmotic pressure differential which can lead to cell dehydration, inhibiting its growth or even killing the cell outright. Some micro-organisms, however, can tolerate low concentrations of salt within their cell walls and some (called halophiles) may actually require high salt concentrations for growth.

Other factors influencing MIC include time of equipment usage.

2.7 MIC control

Controlling MIC can potentially be difficult and expensive (Zhao, 2008). Micro-organisms can exist in several metabolic states, have the ability to grow spores when conditions are unfavourable (e.g. when treatment of equipment is occurring), and; can regrow when conditions become favourable again (Roberge, 2000).

An important method in controlling MIC is the strict and careful monitoring of pipes and equipment. It must be: 1) done over the whole system and not just at a single point, and; 2) done over a period of time and not just one point in time.

Monitoring the system to determine susceptibility to MIC and choosing an effective control method can be performed in a stepwise manner (Nalco/Exxon Energy Chemicals, 1997):

1. Flow Diagram – Drawing a flow diagram with all relevant information (e.g. pipe distances and configurations, operating conditions, chemical treatment injection sites etc.) can help increase understanding of the system and can be used in the later stages to guide treatment options
2. List of Historical Problems – Creating a record of problems that have occurred in the system, including: dates, locations in the system where the issue occurred, type of problem (e.g. corrosion, fouling, or leak), suspected micro-organism causing said problem, method used to rectify issue, and outcomes (positive and negative)
3. Visual inspection – Where possible, visual inspection of the system can indicate fouling and scaling materials such as biofilms, algae, fungi or rust. Discoloured water can also indicate microbial activity (e.g. black water can indicate SRB activity, and red water can indicate iron-oxidising bacteria)
4. Water analysis – The chemical analysis of water samples taken across the system can help locate problems areas and develop cost-effective treatment programs. Comparing samples across different parts of the system is also important, as changes in parameters can infer problems in certain locations
5. Microbial analysis – Identifying and counting bacteria by laboratory analysis, as some micro-organisms can only be identified in a laboratory setting through culturing in some growth medium. Various methods include: pour plate (to detect aerobic bacteria), deep agar tube (SRB), serial dilution (SRB), Epi-fluorescence and ATP monitoring.

One of the classical concepts of maintaining a system free of the effects of MIC is to 'keep the system clean' (Videla, 2002). This can be done by any number of methods, each having application depending on where the corrosion is found, and under what operating conditions the system is running at. These methods can be broadly classified into two principal approaches; *physical* or *chemical* (or a combination of the two).

Physical approaches can be defined as a catch-all term for all techniques that do not involve the use of chemicals. This includes, for example, mechanical objects such as sponge balls or brushes, fluids such as water (flushing or backwashing) or steam, or even physical techniques such as UV radiation or ultrasound (along with flushing or backwashing).

Chemical approaches usually involve the use of biocides, which are some of the most commonly used and effective options in controlling MIC (Moura et al., 2013). They can be either oxidising (e.g. chlorine, ozone, bromine), or non-oxidising, and are usually used in combination with another biocide(s) to optimise effectiveness.

There are, however, some disadvantages to using biocides:

- They can lose efficacy from prolonged use due to the development of resistance in the microbiological population
- Biofilms created by the micro-organisms can prevent the biocide from reaching them at/near the surface (Javaherdashti, 2013)
- There is increasing concerns about their use on the environment.

Physical and chemical techniques are generally used in tandem to limit the disadvantages of using just one method. For example, a mechanical device called a PIG (Pipeline Inspection Gadget) can be sent down a pipeline to disturb the biofilm on the surface, whereby a chemical 'pig' is sent afterwards to kill or inactivate the remaining micro-organisms (Moura et al., 2013).

Table 2-2 presents some of the physical and chemical means of treatment of MIC growth, together with advantages and disadvantages. These tabulated data however, are not exhaustive.

Micro-organisms themselves can also directly (or indirectly) control MIC. The formation of biofilms by some bacteria slow down the anodic and/or cathodic reactions required for corrosion to occur. The biofilm can also increase the resistance of the

electrochemical corrosion circuit, thereby decreasing corrosion (Chilingar, 2008). An example of micro-organisms purposely being used to control MIC is through the addition of nutrients (in this case, nitrates and nitrites) to control SRB. The increased level of nitrogen-based molecules can adjust the pH of the system and stimulate growth of competing bacterial populations (namely nitrate-reducing bacteria (NRB)). This has the effect of displacing the more harmful SRB from the microbial community, thus reducing corrosion. Other less aggressive micro-organisms can grow as well (such as fungi), also reducing corrosion (Videla and Herrara, 2005; Zhao, 2008). In fact, the use of nitrate to control SRB and H_2S production is a proven biotechnology (Eckford and Fedorak, 2004; Vance and Trasher, 2005).

Professional knowledge is also an important factor in controlling MIC, as failure to understand the system can lead to ineffective cleaning and monitoring strategies. This can result in consumables wastage and increased downtime or corrosion loss (Moura et al., 2013).

MIC can be limited or mitigated by the judicious selection of materials, or modifying operating conditions within practical ranges (Roberge, 2000; Moura et al., 2013). For example, it has been quoted (Malard et al., 2008) that steel with a higher alloying content slows growth of sessile SRB.

2.8 Critical analyses of MIC models

The first reports of MIC date back to the start of the twentieth century (Gaines, 1910). However, models attempting to explain and predict it were not rigorously developed until the 1960s (e.g. Iverson, 1966). An exception is the work of von Wolgozen Kuhr and van der Flugt (1934), who developed what they called the ‘cathodic depolarization theory’, which was the first attempt to understand MIC from an electrochemical standpoint (Videla and Herrera, 2005).

MIC models developed to date use a combination of biological, chemical or physical parameters, along with experimental data, in order to attempt to explain the complex interplay between biotic and abiotic processes in either a qualitative, or quantitative manner (Maxwell and Campbell, 2006).

Table 2-3 presents a chronological summary of 16 models in the literature for MIC, and; contributions made by the various researchers are critically reviewed in what follows:

Recent MIC models include the work of Maxwell and Campbell (2006), who expanded the model of Pots et al. (2002) - which was itself an extension of the work by De Waard et al. (1991). They added first-order bacterial kinetics to the Pots model to describe the development of a sulphur-based biofilm as the first stage of MIC. The aim was to synthesize a model that could use commonly gathered field-data such as viable bacterial numbers, sulphide concentrations and water chemistry to predict performance of biocide treatments. The model gave results similar to those of Pots et al. (2002), however, the addition of the bacterial kinetics allowed a time-scale for MIC risk and biocide efficacy to be computed.

An acknowledged drawback was that the predicted corrosion rate was not sufficiently accurate and that rates calculated were only a guide to MIC in pipelines.

Smith et al. (2011) attempted to improve on this by studying the effect of corrosive species identified in 'synthetic water' analyses of oil-field samples using parameters that could be readily measured. The authors expressed corrosion rate as a function of these species of sulphate, chloride and hydrogen sulphide. Their model was based on electrochemical processes that describe both the charge and mass transfer at the interface of a carbon-steel pipe. Results showed a reasonable qualitative match with experimental data near the corrosion (equilibrium) potential, but deviations occurred when the overpotentials of the system became large.

Although the work of Smith et al. (2011) simulated abiotic parameters and not biotic ones, it was assumed that the synthetic water used adequately simulated microbial activity and was therefore suitable for modelling MIC.

Sorensen et al. (2012) and Skovhus et al. (2012) developed an 'MIC risk-assessment tool' for pitting corrosion. They divided the calculation into 2-steps: the first computed an Integrated MIC Risk Factor (IMRF) - that estimated the time taken to initiate MIC below a biofilm - whilst the second computed a Potential Pit Generation Rate - a measure of the pitting corrosion rate on a metal surface after a sufficient time calculating the IMRF had been reached. There were no physical or chemical parameters in the model, and the 2-steps were calculated using the rate of iron dissolution (oxidation) due to microbial activity as:

$$Rate\ of\ iron\ dissolution = 4 \times N_{SRB} \times S_{SRB} + 4 \times N_{SRA} \times S_{SRA} + 4 \times N_{MET} \times S_{MET} \quad (2.1)$$

Table 2-2: Types of MIC control techniques together with advantages and disadvantages of each (Roberge, 2000; Videla and Herrara, 2005; Maxwell and Campbell, 2006; Abdul-Halim and Davey, 2015)

	Advantages	**Disadvantages**
Physical		
Flushing	Simple, low cost	Limited efficacy
Backwashing	Effective in tubes	Limited in ion exchangers
Sponge balls (abrasive or non-abrasive)	Extensively used in industry	Issues with thick biofilms and smearing organics (non-abrasive) Can damage protective passive films (abrasive)
Brushing	Very effective	Limited applicability, expensive, can lead to selection of firmly adhering films
Hot water (steam)	Good in high-purity water systems No need for dangerous chemicals	May not treat thermophilic microbes in hot-water systems
UV Radiation	'Nothing added' to fluid Inactivates bacterial, viral contaminants No harmful by-products Increasingly cost-effective	Very low effectiveness against biofilms Entrapped particles may shield bacteria
Ultrasound	Promising for soft biofilms	Limited to non-sensitive material Ineffective on extremely stable biofilms
Chemical		
Chlorine (Cl_2)	Broad spectrum of activity Can be generated on site Active in low concentrations Destroys biofilm, supports detachment	Toxic by-products Can promote microbe resistance Corrosive Low penetration into biofilms Affected by pH
Hypochlorite (ClO^-)	Cheap and effective Easy to handle Destabilizes and detaches biofilm matrix	Poor stability Oxidizing Rapid after-growth can occur Corrosive Toxic by-products
Hydrogen peroxide (H_2O_2)	Decomposes to water and oxygen Relatively non-toxic Can be generated on site Weakens biofilm, supports detachment	High concentrations needed Frequent resistance Corrosive
Ozone (O_3)	Oxidizes many organic and inorganic substances Breaks down to oxygen Can be generated on site	Breakdown of material can lead to higher microbial activity downstream Power intensive process Can be cost-ineffective

Peracetic acid (CH_3CO_3H)	Very effective in small concentrations Broad spectrum Kills spores No toxic by-products Penetrates biofilm	Corrosive Not very stable Increases dissolved oxygen content (DOC)
Glutaraldehyde ($CH_2(CH_2CHO)_2$)	Effective in low concentrations Cheap Non-oxidising and non-corrosive	Does not penetrate biofilm well Degrades to formic acid Increases DOC
Tetrakis-hydroximethyl phosphonium sulphate (THPS)	Wide-spectrum efficiency on bacteria, fungi and algae Specific action against SRB Low environmental toxicity	Limited activity in heavily fouled systems

where, N is the number of micro-organisms per cm^2, and S is the average cell-specific activity. The subscripts denote that the model focussed on sulphate-reducing bacteria (*SRB*), sulphate-reducing *Archaea* (*SRA*), and methanogens (*MET*).

The model was applied to several off-shore pipeline locations in the North Sea, and; areas that were at high risk of MIC were successfully identified with good estimation of the pitting rates at the sites. However, the IMRFs and pitting rates calculated by this model were considered to be 'worst-case' scenarios.

Xu et al. (2016) presented a pitting corrosion model based on the biocatalytic cathodic sulphate reduction (BCSR) MIC mechanism theory of Gu et al. (2009). The theory assumes that MIC occurs due to electrons being released by iron dissolution (oxidation) at the anode, which are then utilized by the reduction of sulphate at the cathode, with the overall reaction:

$$SO_4{}^{2-} + 9H^+ + 8e^- \rightarrow HS^- + 4H_2O \qquad (2.2)$$

The model is based on electrochemical processes describing both charge and mass transfer in a similar method to the Smith et al. (2011) model. However, this model also included a mechanism to describe acid producing bacteria (APB) attack based on the local pH at the pit bottom. Results showed that the pitting rate decreased over time as the pit became deeper. The authors hypothesized – but did not test - that this was due to the nutrients required by the bacteria at the bottom of the pit becoming limited. The model was developed into pitting prediction software (MICORP) which could predict long-term pitting rates and worst-case scenarios using SRB short-term pit depth experimental data.

Javaherdashti (2017) presented a qualitative model of microbial and non-microbial carbon-steel in post-cracked reinforced concrete, which was solved using 'fuzzy logic'. This method of modelling MIC is similar to *Fr 13* in that the author acknowledged that, with most MIC models, the parameters have 'static', not 'dynamic' values, and therefore MIC should be modelled using mathematics that can account for the 'grey' i.e. transient nature of MIC processes. The model used open circuit potential patterns to define the rate of corrosion.

The author considered that whether or not corrosion happened depended on two scenarios: 1) a suitable environment, and a 2) susceptible material. If both were present, the probability of MIC was *relatively high*. If either scenario was present, the probability was *relatively low*. If neither was present, the probability was *too low*.

An example given by Javaherdashti (2017) showed that a biotic environment containing SRB had the same effect on carbon-steel corrosion as an abiotic environment that contained chlorides.

A downside, however, was that the author did not specify all the parameters that went into the development of the model.

Skovhus et al. (2017) synthesized a MIC risk-based inspection ranking model, similar in methodology to the CHECworks, Union Electric Callaway and Lutey/Stein MIC Index models. They considered that risk was equal to the Probability of Failure (*PoF*) in a system, multiplied by the Consequence of Failure (*CoF*):

$$Risk = PoF \times CoF \tag{2.3}$$

The aim was to establish a new procedure for calculating the PoF of MIC in a system. They divided the procedure into 2-parts: 1) a screening assessment and 2) a PoF ranking. The screening assessment was used with established data to identify if the system was at a high risk of MIC. If so, the second part of the procedure (the PoF ranking tool) was required. The PoF ranking tool focused on the following qualitative parameters and assigned them a ranking based on the operating conditions found in the system:

- Settlement potential (potential for material in the system to settle in low-flow areas), assigned rankings *High*, *Medium* or *Low*
- Availability of nutrients or expected (metal) dissolution rate (performed using microbial sampling at several locations along the system), *High* or *Low* ranking

Table 2-3: A general overview of MIC models

Author(s)	Proposal	Parameters	Result	Comment
Iverson (1966)	Simple corrosion model using polarization data of mild steel in SRB culture	Biological, chemical	Quantitative	
De Waard et al. (1991)	De-Waard-Milliams CO_2 model for wet natural gas lines	Chemical, physical	Quantitative	Does not consider MIC
Chexal et al. (1997)	Union Electric Callaway MIC Index - MIC susceptibility model based on historical data	Biological, physical	Qualitative	Susceptibility ranking of 0 (low potential/low degree of severity) to 100 (very high potential/ very high degree of severity Emphasises input data collected from the field
Electric Power Research Institute (1999)	CHECworks MIC susceptibility model	Chemical, physical	Qualitative	Susceptibility ranking between 0 (none or very low) to 10 (highest)
Lutey and Stein (1999)	Lutey/Stein MIC index – 'fault-tree' risk model	Biological, physical	Qualitative	Places significant emphasis on presence of bacteria related to corrosion Susceptibility ranking of <75 (low) to >150 (highly likely or severe)
Picioreanu and van Loosdrecht (2002)	Three-dimensional model study on biofilm development and initiation of micro-organisms to cause localized corrosion	Biological, chemical, physical	Quantitative	Does not require *a priori* specification of where the anodic and cathodic regions exist
Pots et al. (2002)	Extension of De-Waard-Milliams (1991) model	Biological, chemical, physical,	Quantitative	Incorporated into HYDROCOR computer program

Maxwell and Campbell (2006)	Extension of Pots et al. (2002) model using simple bacterial kinetic models	Biological, chemical, physical	Quantitative	Addition of bacterial kinetics allowed a timescale for MIC risk and biocide efficacy to be computed
Sooknah et al. (2007); (2008)	Internal MIC (biotic) + pitting (abiotic) susceptibility model	Chemical, physical	Qualitative	Susceptibility ranking of 0-1.4 (very low risk) to 8.1-10 (highly likely)
Allison et al. (2008)	3-step model	Biological, chemical	Qualitative	Uses microbiological analysis of planktonic cells, not sessile
Melchers (2009)	Corrosion of steel in seawater and marine environments	Biological, chemical, physical	Quantitative, qualitative	
Smith et al. (2011)	Abiotic, electrochemical model based on charge and mass transfer	Chemical, physical	Quantitative	Simulated bacterial activity using synthetic produced water (containing sulphate, chloride and hydrogen sulphide)
Sorensen et al. (2012); Skovhus et al. (2012)	2-step, microbial-focused 'MIC risk-assessment tool'	Biological	Quantitative	Implemented in North Sea pipeline operations by Maersk Oil
Xu et al. (2016)	Electrochemical model based on biocatalytic cathodic sulphate reduction (BCSR) theory of Gu et al. (2009)	Biological, chemical, physical	Quantitative	Incorporated into MICORP computer program
Javaherdashti (2017)	Fuzzy logic MIC model	Biological, chemical, physical	Qualitative	
Skovhus et al. (2017)	Risk-based inspection model	Biological, chemical, physical	Qualitative	Susceptibility ranking of very high to very low

- MIC mitigation effectiveness (assessed on a case-by-case basis), *Ineffective* or *Effective* ranking
- Oxygen ingress (identified by assessment of the pipe-fluid), *Yes* (present) or *No* (not present) ranking.

Based on the combination of the four parameters, the PoF caused by MIC was ranked into five groups: *Very high*, *high*, *medium*, *low* or *very low*. This PoF ranking was combined with a previously evaluated CoF to determine the overall risk of the system to MIC. A field case was then used to illustrate the practicality of the procedure.

However, a major drawback with this model is that it is qualitative.

Overall, it is concluded that with the exception of the work of Javaherdashti (2017), published MIC models do not involve stochastic elements that could be used to investigate the cumulative impact of natural fluctuations in the fluid materials environment.

Of particular interest, however, is the impact that these stochastic and natural fluctuations might have on initiating the insidious nature of MIC in widely used internal metal pipe flows in off-shore oil and gas structures – especially ASTM A105 carbon-steel. This is very widely used in the oil and gas industry globally and, importantly, in Australia.

The model of Smith et al. (2011) was selected with the aim to test the *Fr 13* framework and to gain unique insight into how naturally occurring fluctuations in pipe-fluid temperature (T) and pH can impact corrosion. It is acknowledged that this model is actually abiotic and only models corrosion, but it is seen to be a 'first-step' model, which can be extended to MIC in future research. The Smith et al. (2011) model is also advantageous because it can be synthesized based on widely used and quantitative unit-operations approaches in chemical engineering (Foust et al., 1980; McCabe et al., 2001).

A logical and stepwise research strategy was therefore planned and implemented to advance the *Fr 13* risk framework.

2.9 *Fr 13* framework for corrosion

Following a review of both the *Fr 13* risk framework and MIC, a logical and stepwise research strategy to advance the *Fr 13* risk framework for corrosion of ASTM A105 carbon-steel pipe was planned to include:

1. Develop corrosion of an ASTM A105 carbon-steel pipe as a steady-state unit-operation and establish a clear definition of pipe failure
2. Identify key corrosion parameters (*T* and pH) on pipe failure using a traditional deterministic chemical engineering approaches
3. Simulate the corrosion unit-operation model for failure using the probabilistic *Fr 13* risk framework with r-MC (*Latin Hypercube* refinement)
4. Apply new insights via second-tier simulation studies to highlight the impact of mitigation strategies of corrosion in carbon-steel pipe, with a view to extend it to MIC in future research .

2.10 Chapter summary and conclusions

Based on the literature review of *Fr 13* and MIC, the important features that are relevant to this research are:

1. The *Fr 13* risk assessment methodology is being successfully developed and utilized in steady-state chemical engineering unit-operations to show how naturally occurring, random (stochastic) fluctuations within process parameters can unexpectedly accumulate in one direction and lead to significant (sudden and surprise) change in output behaviour, with failure in product or plant

2. The *Fr 13* risk framework has a number of benefits over similar probabilistic methodologies as it is based on well-established unit-operations principles and, because of the probabilistic element, it provides a quantitative picture of all mathematically practically possible scenarios, including well-defined failures. Additionally, the framework can be used to reduce risk through repeat simulations (i.e. second-tier studies) in order to investigate intervention strategies and the potential re-design of the physical plant or unit-operation. This can be applied at both the *synthesis* and *analysis* stages

3. MIC is an insidious and unwanted degradation of materials used in process engineering that is directly or indirectly caused by micro- and macro-organisms. It can occur in above- or below-ground process equipment and in internal pipe-fluid environments that transport water-based fluids. MIC poses a practical risk because it can initiate unexpectedly and, eventually it can cause sudden and unexpected failure of pipes. This can lead to loss of containment (with subsequent environmental damage), personnel or product

4. The *Fr 13* risk framework appears to be applicable to a novel risk assessment of steady-state corrosion model of ASTM A105 carbon-steel pipe

5. The independent, abiotic experimental work of Smith et al. (2011) was selected as suitable for *Fr 13* risk assessment of corrosion of widely-used ASTM A105 carbon-steel pipe. Failure is defined as a higher than acceptable corrosion rate.

In the following chapter, Chapter 3, an initial corrosion unit-operations model of ASTM A105 carbon-steel pipe under abiotic, synthetic conditions is synthesized and solved using traditional deterministic approaches for pipe that is corroded under steady-state conditions. The model is then simulated, for the first time, using the probabilistic *Fr 13* risk framework in which distributions are used to mimic natural fluctuations in pipe-fluid internal temperature and pH. Results are quantitatively compared.

CHAPTER THREE

AN INITIAL *FR 13* RISK MODEL FOR CORROSION OF WIDELY-USED ASTM A105 CARBON-STEEL PIPE

Parts of this chapter have been published as:

Collins, S.D., Davey, K.R., Chu, J.Y.G., O'Neill, B.K., 2016. A new quantitative risk assessment of Microbiologically Influenced Corrosion (MIC) of carbon steel pipes used in chemical engineering. In: CHEMECA 2016: Chemical Engineering – Regeneration, Recovery and Reinvention, Sept. 25-28, Adelaide, Australia, paper 3386601. ISBN: 9781922107831

3.1 Introduction

The review of literature showed that *Fr 13* risk framework has been successfully applied to a number of unit-operations.

In this chapter, *Fr 13* is applied for the first time to an initial steady-state corrosion model of ASTM A105 carbon-steel pipe under abiotic, synthetic conditions to simulate MIC bacterial activity.

The aim was to gain quantitative, new insights and knowledge into both corrosion, and the impact of random, naturally occurring fluctuations that could lead to unexpected (surprise) corrosion.

An unambiguous definition of corrosion failure is developed - based on the introduction of a risk factor p such that for all $p > 0$. If the observed corrosion rate is greater than a tolerable design-corrosion rate it is deemed a pipe metals failure.

3.2 Initial corrosion model

In the following synthesis, all symbols used for parameters are carefully defined in the relevant Nomenclature at the end of this thesis.

3.2.1 Synthesis of an initial unit-operations corrosion model

The conventional three-electrode corrosion cell and potentiostat model of Smith et al. (2011) provides a realistic basis for synthesis of an initial unit-operations model of corrosion, both in terms of responding to changes in input parameter values and the prediction of the corrosion rate for each system within experimental variability (Fig. 3-1). The model is a simplified version of carbon-steel pipe corrosion subjected to synthetic water to simulate MIC activity.

A rotating-disk-electrode was used as the working-electrode (WE) with the tip containing a sample of carbon-steel pipe, for example ASTM A105. A counter-electrode (CE), made from platinised titanium, was used as the electron sink/source, and a saturated calomel electrode (SCE) reference-electrode (RE) used for potential measurement. Synthetic produced water was used to simulate MIC bacterial activity. This contained sulphate, chloride and hydrogen sulphide.

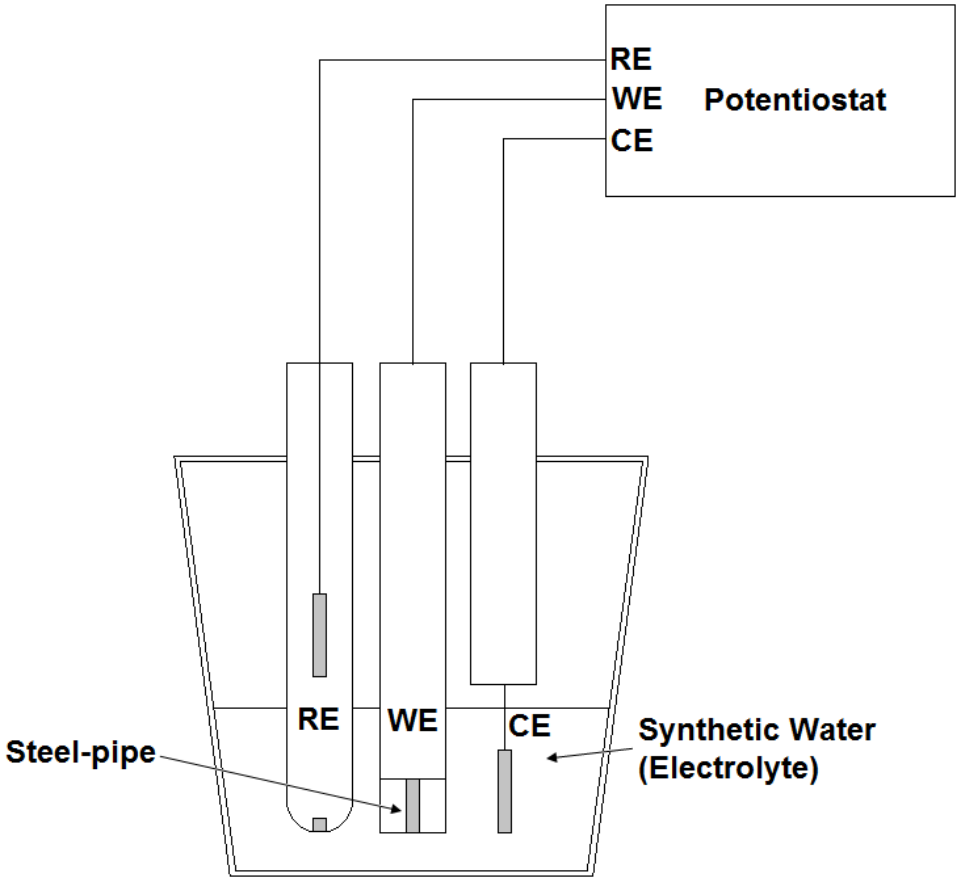

Fig. 3-1: Schematic of experimental three-electrode corrosion cell and potentiostat with synthetic-water (electrolyte) containing sulphate, chloride and hydrogen sulphide to mimic MIC bacterial activity (adapted from Smith et al., 2011)

In the initial model, the process of corrosion takes place in two steps:

1. Oxidation of the metal at the surface
2. Reduction of species in the bulk electrolyte

It is assumed that the electrons formed by the oxidation of iron in the carbon-steel pipe (Eq. 3.1) are consumed by the reduction of protons (Eq. 3.2):

$$Fe \rightarrow Fe^{2+} + 2e^{-} \tag{3.1}$$

$$H^{+} + e^{-} \rightarrow \tfrac{1}{2}H_2 \tag{3.2}$$

The transfer of charge (electrons) occurs only at the carbon-steel pipe surface between the steel pipe and the water (electrolyte) because of the nature of electron transport. This is shown schematically in Fig. 3-2.

The overall corrosion reaction is:

$$Fe + 2H^+ \rightarrow Fe^{2+} + H_2 \tag{3.3}$$

The charge transfer at the carbon-steel pipe surface (j_{ct}) can be predicted by the established Butler-Volmer equation (Gu, 2009) for each of the electrical species due to charge transfer (Roberge, 2000):

$$j_{ct,i} = j_{0,i}\left(exp\left(\frac{\alpha_{a,i}\cdot n_i\cdot F}{R\cdot T}\cdot \eta_i\right) - exp\left(\frac{-\alpha_{c,i}\cdot n_i\cdot F}{R\cdot T}\cdot \eta_i\right)\right) \tag{3.4}$$

where j_0 = exchange current density, α_a = anodic transfer symmetry function, α_c = cathodic transfer symmetry function, n = number of electrons transferred in the redox process, F = Faraday constant, R = universal gas constant, T = temperature, and η = overpotential. The subscript i denotes the reacting species such as Fe or H^+. Note that for the initial corrosion model, the current densities due to both charge and mass transfer are written in terms of reduction of protons (cathodic process). Eq. (3.4) then becomes:

$$j_{ct,H^+} = j_{0,H^+}\left(exp\left(\frac{\alpha_{a,H^+}\cdot n_{H^+}\cdot F}{R\cdot T}\cdot \eta_{H^+}\right) - exp\left(\frac{-\alpha_{c,H^+}\cdot n_{H^+}\cdot F}{R\cdot T}\cdot \eta_{H^+}\right)\right) \tag{3.5}$$

where the exchange current density (which is the current density at equilibrium conditions) (Nesic et al, 1996) is:

$$j_{0,H^+} = j_{0,H^+}^{ref}\exp\left(-\Delta H_{H^+}/R\left(1/T - 1/T_R\right)\right) \tag{3.6}$$

and j_{0,H^+}^{ref} = reference exchange current density, ΔH = enthalpy of activation, and T_R = reference temperature.

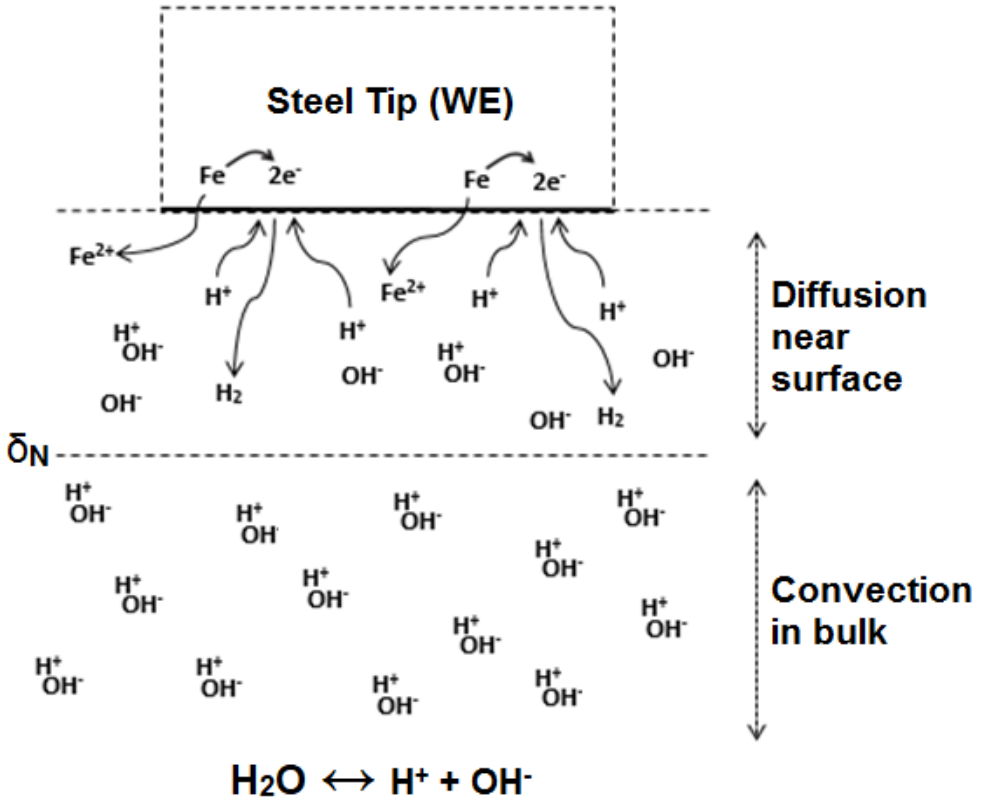

Fig. 3-2: Corrosion of surface interactions of steel pipe with deaerated, low conductivity synthetic-water containing sulphate, chloride and hydrogen sulphide (adapted from Smith et al., 2011)

The reversible (equilibrium) potential (E_{rev}) is calculated using the Nernst equation (Roberge, 2000), where the activity of each species (in this case, only the reduction (proton) process) is represented as the surface concentration of that species. This is a valid assumption for the pipe surface because: 1) the concentration profile for each species is formed from the surface out to the bulk of the solution, and; 2) the electrolyte solution is dilute. Therefore:

$$E_{rev,H^+} = E^{\circ}{}_{H^+} + \frac{2.3 \cdot R \cdot T}{n_{H^+} \cdot F} \cdot \log\left(c_{s,H^+}\right) \tag{3.7}$$

where $E°$ = standard (equilibrium) potential and C_S = concentration at the carbon-steel pipe surface.

When equilibrium is achieved in the system between the oxidation of iron and reduction of protons, a balance in the transfer of charge is created, giving a measured current density

of zero. The potential at which this happens is defined as the free corrosion potential (E_{corr}). The overpotential (η) is given by:

$$\eta_{H^+} = E_{corr} - E_{rev,H^+} \tag{3.8}$$

and is defined as the difference between the potential of the system and each half-reaction's equilibrium potential (for this initial model, only the reduction (proton) process is considered).

The mass transfer at the carbon-steel pipe surface (j_{mt}) is described by a flux balance arising from the dependency on diffusion and charge consumption (Smith et al., 2011):

$$\frac{j_{mt,H^+}}{n_{H^+} \cdot F} = -D_{H^+}\left(\frac{c_{b,H^+} - c_{s,H^+}}{\delta_{N,H^+}}\right) \tag{3.9}$$

where D = diffusion coefficient, C_b = concentration in bulk pipe-fluid (electrolyte), and δ_N = Nernst diffusion layer thickness.

Eq. (3.9) can be rearranged to isolate the current density due to mass transfer to give:

$$j_{mt,H^+} = (n_{H^+} \cdot F) \cdot \left(-D_{H^+}\left(\frac{c_{b,H^+} - c_{s,H^+}}{\delta_{N,H^+}}\right)\right) \tag{3.10}$$

Because the number of electrons produced in the oxidation of iron is balanced by the reduction of protons (shown by Eq. 3.3), the total current density in the system (j_T) i.e. the sum of the current densities due to oxidation and reduction, must be zero. The overall current density for the proton reduction component (j_{H^+}) is the sum of the current densities for proton reduction due to both charge transfer (j_{ct,H^+}) and mass transfer (j_{mt,H^+}). Therefore, j_T can be written as:

$$j_T = j_{Fe} + \left(j_{ct,H^+} + j_{mt,H^+}\right) = j_{Fe} + j_{H^+} = 0 \tag{3.11}$$

where j_{Fe} = current density due to the oxidation (iron) process, and j_{H^+} = current density due to the reduction (proton) process.

Eq. (3.11) can be rearranged to give:

$$j_{Fe} = -j_{H^+} \tag{3.12}$$

The current density due to iron oxidation can be converted to corrosion rate (CR) using molecular weight (M_{Fe}) and density (ρ_{Fe}) (Gu, 2009) to yield:

$$CR = \frac{M_{Fe}}{2F \cdot \rho_{Fe}} \cdot j_{Fe} \tag{3.13}$$

which can be simplified for a wide range of temperature to:

$$CR = 1.155 j_{Fe} \tag{3.14}$$

Eqs. (3.4) through (3.14) compose the mathematical equations of the initial corrosion model of ASTM A105 carbon-steel pipe.

The solution to the model is as follow: solve Eq. (3.6) for the exchange current density, Eq. (3.7) for the reversible potential, and Eq. (3.8) for the overpotential. The exchange current density, overpotential and reversible potential are then used to solve Eq. (3.5) for the current density due to charge transfer. Eq. (3.10) is then solved for the current density due to mass transfer. The current densities due to charge and mass transfer are then summed to solve for Eq. (3.11), which is rearranged to solve for Eq. (3.12). Eq. (3.14) is then solved to obtain the corrosion rate in mm yr^{-1}.

3.3 Traditional single value assessment (SVA)

The method traditionally used in chemical engineering for solution of a unit-operations model is the 'deterministic' or single value assessment (SVA) (Sinnott, 2005; Davey, 2015 a; Davey et al., 2015). This can be done with or without a sensitivity analysis (Sinnott, 2005).

Using this method, the initial unit-operations model for corrosion of can be solved using the data of Smith et al. (2011) for water at a temperature T = 293.15 K, pH = 5.15 (which is equivalent to $C_{b,H^+} = 10^{-pH} \times 10^3 = 7.08 \times 10^{-3}$ mol m^{-3}), and an assumed E_{corr} = -0.616 V vs SCE (Smith et al., 2008). Substitution and simplification yields: j_{0,H^+} = 0.050 A m^{-2} from Eq. (3.6); E_{rev,H^+} = -0.590 V vs SCE from Eq. (3.7) and η_{H^+} = -0.0264 V vs SCE from Eq. (3.8). Substitution of these values into Eq. (3.5) gives j_{ct,H^+} = -0.0493 A m^{-2}, and from Eq. (3.10), j_{mt,H^+} = -0.387 A m^{-2}.

From Eq. (3.11), the addition of j_{ct,H^+} and j_{mt,H^+} gives j_{H^+} = -0.437 A m^{-2}. Therefore, from Eq. (3.12), j_{Fe} = 0.437 A m^{-2}.

From Eq. (3.14), converting iron oxidation corrosion current density to corrosion rate gives CR = 0.504 mm yr^{-1}. That is, using typical values for the experimental corrosion cell

of Fig. 3-1, a corrosion rate of 0.504 mm per year of ASTM A105 carbon-steel pipe pipeline would be expected.

3.4 *Fr 13* risk assessment

The probabilistic *Fr 13* risk assessment of Davey and co-workers (Davey, 2015 a; Davey et al., 2015; Abdul-Halim and Davey, 2015) replaces the single value of the process input parameters with probability distributions of values, the mean of which usually agree with the SVA values. A refined Monte Carlo (r-MC) with *Latin Hypercube* refinement is used to ensure that sampling covers the entire range of the distribution and not only certain parts, as what could happen with pure Monte Carlo sampling (Vose, 2008). The method uses a random number generator.

3.4.1 Defining corrosion rate failure (risk factor)

An essential step in *Fr 13* risk framework is the derivation of a practical and unambiguous definition of failure.

For the initial unit-operations model for corrosion, a corrosion risk factor (P) can be defined by an off-specification from a tolerable corrosion rate:

$$P = CR' - CR \tag{3.15}$$

where *CR'* = instantaneous rate of corrosion (or mathematically more strictly, the *CR* obtained in a particular probabilistic scenario).

However, a mathematically more convenient form (Abdul-Halim and Davey, 2015; Davey, 2015 a; Davey et al., 2015) is:

$$p = 100\left(\frac{CR'}{CR} - 1\right) \tag{3.16}$$

Generally, the design specification includes some measure of tolerance i.e. design safety. The corrosion risk factor of Eq. (3.16) can therefore be written as:

$$p = 100\left(\frac{CR'}{CR} - 1\right) - \%tolerance \tag{3.17}$$

In the absence of hard (unconditional) data it is assumed that a practical tolerance = 50 %, so Eq. (3.17) gives:

$$p = 100\left(\frac{CR'}{CR} - 1\right) - 50 \tag{3.18}$$

The practical upshot of Eq. (3.18) is that for corrosion rates greater than acceptable plus the tolerance, the rate of corrosion is seen to be a failure. This equation is also computationally convenient because it is dimensionless and corrosion rates greater than tolerable, that is failures, can be readily identified for all values $p > 0$. These values can also be easily isolated using standard spread-sheeting tools (Abdul-Halim and Davey, 2016).

Eqs. (3.4) through (3.14) plus (3.18) defines the probabilistic *Fr 13* initial unit-operations corrosion model of ASTM A105 carbon-steel pipe.

3.4.2 *Fr 13* simulation

The *Fr 13* risk simulation is used to identify every possible practical scenario that could produce an unacceptable rate of corrosion of the carbon-steel pipe. To ensure that the output mean is normally distributed, a sufficiently large number of r-MC samples (1,000 to 50,000) is required (The number of samples is sufficient when, on a plot of number of failures (values for $p > 0$) versus the number of samples, the percentage of failures plateaus to a constant) (Abdul-Halim and Davey, 2015; Davey et al., 2013, 2015).

3.5 Results

The simulations were carried out using Microsoft Excel™ spread-sheeting with a commercially available add-on *@Risk* (version 7.5 Palisade Corporation). Excel is chosen as it is widely available and is generally readily understood - thereby streamlining communication. Further, the distributions defining naturally occurring fluctuations in the parameters can be entered, viewed, copied, pasted and manipulated as Excel formulae (Abdul-Halim and Davey, 2016).

For the initial unit-operations model for corrosion of the carbon-steel pipe, a comparative summary of results from both the traditional SVA and new *Fr 13* simulation are presented in Table 3-1. Ten thousand (10,000) r-MC samples were found to be sufficient. Key parameters are given in column 2 of Table 3-1. The traditional SVA is read down column 3 where the corrosion rate 0.5042 mm yr^{-1} is shown. The *Fr 13* simulation is

summarized in columns 4 and 5. Column 4 also shows the distributions used for the key input parameters *T* and pH, defined as: **RiskNormal** (mean, stdev, **RiskTruncate** (minimum, maximum)). In the absence of conditional data, an initial, general estimate of a standard deviation about the mean value was assumed at stdev = 10 %. Column 4 shows that for T = 297.92 K and pH = 4.93, the corrosion rate CR' = 0.7906 mm yr^{-1}, the risk factor p = 6.80 (> 0), showing a corrosion rate failure, plus a tolerance = 50 %.

It is important to note, however, that the data shown in column 4 is for only one of the 10,000 scenarios. A graphical summary of all 10,000 simulations are presented in Fig. 3-3.

It can be seen from Fig. 3-3 that a total of 2,810 (28.1 %) of all corrosion rate scenarios resulted in $p > 0$ i.e. $CR' > CR$ (with a 50 % tolerance), that is, a failure, over an extended period of time.

3.6 Discussion

3.6.1 Corrosion rate failures

If every scenario is thought of as one day there would be (2,810 / (10,000 days) × 365.25 days / year ≈) 103 unacceptable rates of corrosion per year plus a tolerance = 50 %, over a prolonged period of time. There is no reason to expect these events to be equally spaced in time however. This insight is not available from traditional solutions such as the SVA.

The actual combination of *T* and pH that gave rise to an unacceptable rate of corrosion in ten (10) widespread failure values in the 2,810 with a 50 % tolerance is presented in Table 3-2. A significant advantage of the table and the *Fr 13* risk framework is that each and every scenario can be identified (Davey, 2015 a; Zou and Davey, 2016). For example, row 9 of Table 3-2 shows a combination of T = 297.92 K and pH = 4.93 gives a CR' = 0.79 mm yr^{-1} with resulting p = 6.80, indicating corrosion rate failure. This is the scenario shown in Table 3-1.

Table 3-1: Comparative summary of the deterministic SVA with the initial probabilistic *Fr 13* simulations for corrosion of ASTM A105 carbon-steel pipe with a tolerance of 50 %. Column 3 is the SVA value. Column 4 is for one only of 10,000 simulated *Fr 13* scenarios. *CR* failure is defined for all $p > 0$

Row	Parameter	SVA[a]		*Fr 13* model[b]
1	**Inputs**			
2	T (K)	293.15	297.92[c]	**RiskNormal**(293.15,29.3, **RiskTruncate**(290.15,298.15))
3	*pH*	5.15	4.93[c]	**RiskNormal**(5.15,0.515, **RiskTruncate**(4.64,5.67))
4	**Constants**			
5	E_{corr} (V vs SCE)	-0.616	-0.616	constant
6	$\alpha_{a,H+}$ (dimensionless)	0.6	0.6	constant
7	$\alpha_{c,H+}$ (dimensionless)	0.4	0.4	constant
8	n_{H+} (dimensionless)	1	1	constant
9	$j^{ref}_{0,H+}$ (A m^{-2})	0.05	0.05	constant
10	ΔH_{H+} (J mol^{-1})	30000	30000	constant
11	T_R (K)	293.15	293.15	constant
12	$E°_{H+}$ (V vs SCE)	-0.241	-0.241	constant
13	$C_{s,H+}$ (mol m^{-3})	0.000001	0.000001	constant
14	D_{H+} (m^2 s^{-1})	9.47E-09	9.47E-09	constant
15	$\delta_{N,H+}$ (m)	0.0000167	0.0000167	constant
16	F (C mol^{-1})	96485	96485	constant
17	R (J mol^{-1} K^{-1})	8.314	8.314	constant
18	*%tolerance* (%)	-	50	
19	**Calculations**			
20	$C_{b,H+}$ (mol m^{-3})	0.0071	0.0117	Conversion from pH
21	$j_{0,H+}$ (A m^{-2})	0.0500	0.0609	Eq. (3.6)
22	$E_{rev,H+}$ (V vs SCE)	-0.5896	-0.5953	Eq. (3.8)
23	η_{H+} (V vs SCE)	-0.0264	-0.0207	Eq. (3.7)
24	$j_{ct,H+}$ (A m^{-2})	-0.0493	-0.0466	Eq. (3.5)
25	$j_{mt,H+}$ (A m^{-2})	-0.3873	-0.6379	Eq. (3.10)
26	j_{H+} (A m^{-2})	-0.4365	-0.6845	Eq. (3.11)
27	j_{Fe} (A m^{-2})	0.4365	0.6845	Eq. (3.12)
28	**Output**			
29	*CR'* (mm yr^{-1})	0.5042	0.7906[c]	Eq. (3.14)
30	p	-	**6.80**[c]	Eq. (3.18)

[a] Traditional deterministic single point, or, single value assessment.
[b] One only of 10,000 scenarios.
[c] Values are reproduced from the r-MC sampling; it is not implied they are measured to this significance.

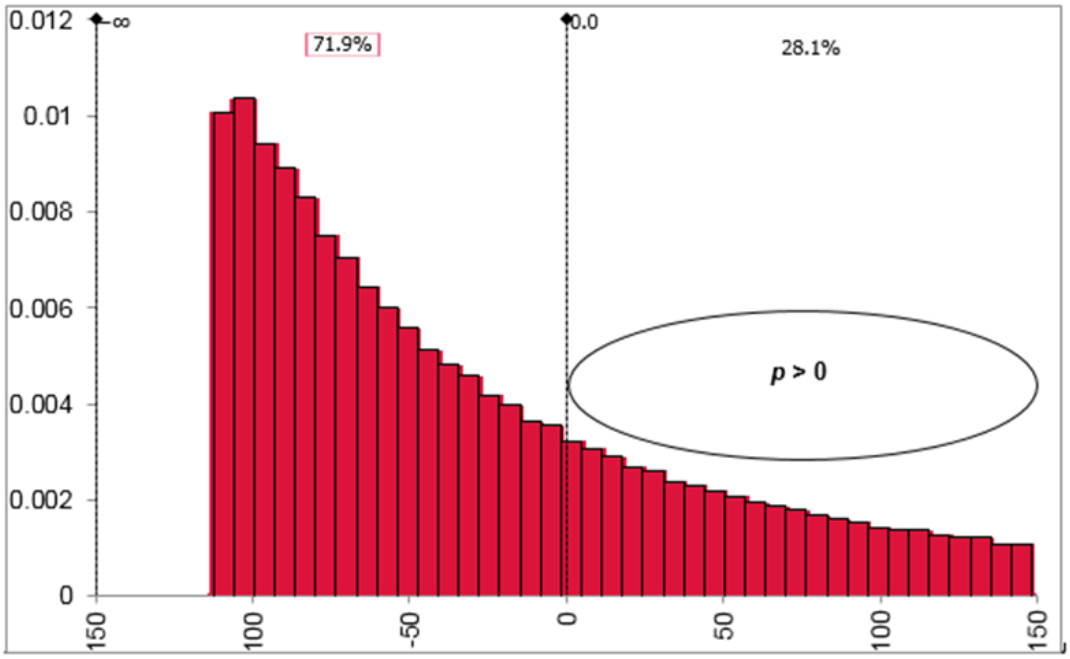

Fig. 3-3: *Fr 13* simulation of the corrosion rate risk factor, *p*, for corrosion with 10,000 scenarios and 50 % tolerance. The *x*-axis is the value of the risk factor and *y*-axis the probability of that value. To the R of the figure shows the 28.1 % failure scenarios with unwanted corrosion > to the right of the figure i.e. $p > 0.5042$ mm yr^{-1} with $p > 0$

Table 3-2: Ten (10) selected *Fr 13* failures in the 10,000 scenarios with 50 % tolerance

Failure	***T*** [b] **(K)**	**pH** [b] **(dimensionless)**	***CR'*** **(mm yr^{-1})**	***p*** **(dimensionless)**
1	297.83	4.64	1.50	147.21
2	297.17	4.66	1.44	135.84
3	297.34	4.67	1.39	126.66
4	296.92	4.69	1.34	115.42
5	294.49	4.70	1.31	109.07
6	291.20	4.80	1.06	60.86
7	294.71	4.85	0.94	37.39
8	296.00	4.90	0.86	19.93
9[a]	**297.92**	**4.93**	**0.79**	**6.80**
10	294.14	4.96	0.76	0.01

[a] Particular scenario of Table 3-1.

[b] Values are reproduced from the r-MC sampling; it is not implied they are measured to this significance.

It can be seen that for each of the ten scenarios, corrosion rate calculated (*CR'*) is found to be greater than corrosion rate expected (*CR*) plus a 50 % tolerance, as evidenced by all $p > 0$. Also of note for this assessment is that a maximum corrosion rate of $CR_{max} = 1.504$ mm yr^{-1} was found at $T = 291.73$ and pH = 4.64 with a corresponding maximum value of the corrosion rate risk factor of $p_{max} = 148.36$. The table also shows that the corrosion rate overall increases with lower pH. A potential application of this insight could be that steps should be taken to increase the pH of the system wherever practical.

3.6.2 Visualizing *Fr 13* risk failures

A concern in risk analysis is how to present data obtained from risk simulations in a manner that is both easy to understand and can be interpreted easily in order to make informed decisions about said risk and ways in which it can be mitigated. This difficulty has been acknowledged in previous *Fr 13* analyses (Abdul-Halim and Davey, 2016; Zou and Davey, 2016; Chandrakash and Davey, 2017).

An advantage of using tabulated data (e.g. Table 3-1 and Table 3-2) is that the value of each input parameter that could lead to corrosion rate failures can be easily identified, isolated and studied. This information can also be used in second-tier studies to provide insights for changes that can be made to the physical system to help mitigate corrosion rate failures. This is important because vulnerability to failure cannot be reduced through further study or knowledge of the system (Davey, 2011).

A drawback of tabled results, however, is that models with increased input parameters result in the table size becoming increasingly complex.

3.6.3 Probability distributions to define key input parameters

The value of the *CR* risk factor *p* will be determined directly by the probability distributions used to define the key corrosion parameters *T* and pH. In the absence of unconditional data, the distributions selected to simulate the naturally occurring fluctuations of *T* and pH in MIC were **TruncatedNormal**. To establish better distributions some experimenting is needed or expert knowledge drawn upon (Davey et al., 2013).

It might be that distributions can be 'tailored' for particular metal-bacterial systems or geographical locations. Regardless, distributions need to be carefully considered so that the model outcomes are those that could be observed in practical situations.

3.6.4 Limitations of the *Fr 13* model

A shortcoming of the model is that there is no biotic component, but it is acknowledged that the model can be seen as a 'starting point' which can be expanded in later iterations to include:

1. Biotic model components, for example, the work of Maxwell and Campbell (2006) who incorporated simple bacterial kinetics into their predictive model for MIC risk

2. Other corrosion species such as sulphate (sodium sulphate), chloride (sodium chloride) and hydrogen sulphide (H_2S) to (cathodic) reduction to better simulate the corrosion rate of iron oxidation

3. Different metals that are used where MIC is found such as copper and zinc (Roberge, 2000)

4. A 'global' model approach, defined by Davey and co-workers (Chandrakash et al., 2015) as two (2) or more connected unit-operations, that could be applied to a series of pipes over a section, or the entire plant. (However, this may not be applicable since MIC can be initiated in localized sites (Roberge, 2000)).

Another key limitation of the model is that the free corrosion potential (E_{corr}), a key parameter, was taken to be a single value when in fact it is a multi-parameter function of T and pH.

3.7 Chapter summary and conclusions

1. An initial *Fr 13* model for corrosion of ASTM A105 carbon-steel pipe was synthesized and developed based on the three-electrode corrosion cell and potentiostat model of Smith et al. (2011). A drawback with this model is that it is simulating an abiotic system without any bacterial kinetics, but it is acknowledged that the model can be seen as a 'starting point' which can be expanded in later iterations. Another drawback to the model was that a key parameter E_{corr} (free corrosion potential) was taken to be a single value when in fact it is a multivariable function of T and pH.

2. Results show that with a temperature of 293.15 K and pH of 5.15 and a practical tolerance of 50 % as a design margin of safety, an unacceptable corrosion of carbon-steel pipe can occur in 28.1 % of all scenarios. If every scenario is thought of as one day, there would be approximately 103 unacceptable rates of corrosion each year averaged over the long term.

3. The model form appears generalizable to a range of micro-organism-metal systems. A refined model could be used to quantitatively investigate MIC preventative intervention strategies.

In the following chapter, Chapter 4, this initial *Fr 13* risk model is extended to more realistically simulate corrosion through the use of solver function implementation and a more practical T and pH range.

CHAPTER FOUR

A NOVEL *FR 13* MODEL FOR CORROSION OF WIDELY-USED ASTM A105 CARBON-STEEL PIPE

Parts of this chapter have been published as:

Collins, S.D., Davey, K.R., 2018. A novel *Fr 13* risk assessment of corrosion of carbon-steel pipe in de-aerated water. Chemical Engineering Science – *submitted* CES-D18-00449, Feb.

4.1 Introduction

In Chapter 3, an initial *Fr 13* risk assessment was successfully applied to the three-electrode corrosion cell and potentiostat model of Smith et al. (2011) and simplified as a 1-step unit-operations model of corrosion of ASTM A105 carbon-steel pipe. A significant drawback of the model, however, was that the free corrosion potential (E_{corr}), a key parameter, was taken to be a single, constant value when in fact it is a multi-parameter function of T and pH. However, familiarization with the *Fr 13* risk assessment method and technique was acquired.

In this chapter, the initial unit-operations model of corrosion is refined using spread-sheeting techniques to introduce a solver function that employs a convergence criterion to calculate a unique E_{corr} for each input of T and pH, which is then used to calculate the corrosion rate for each *Fr 13* simulation. The aim for this extended work is to obtain an improved corrosion unit-operations model that will lead to more accurate and realistic simulations, as well as enhanced system designs and safety through the exploration of intervention strategies.

A risk factor (p) is defined as a corrosion rate higher than a tolerable corrosion rate.

4.2 A novel corrosion model

All symbols used for parameters are carefully defined in the relevant Nomenclature at the end of this thesis.

4.2.1 Synthesis of a novel unit-operations corrosion model

The synthesis for the novel unit-operations corrosion model is similar in form to the initial corrosion model as shown in Chapter 3, but as a solver function is introduced, this requires the current densities of both species (Fe and H^+) to be considered. The model was based on the experimental work of Smith et al. (2011), whereby a three-electrode cell in which a rotating-disk-electrode was used as the working-electrode (WE) together with a sample of steel pipe embedded in the tip. A counter-electrode (CE), made from platinised titanium, was used as the electron sink/source, and a saturated calomel electrode (SCE) reference-electrode (RE) was used for measurement of potential. ‘Synthetic-water’ (Smith et al.,

2011) containing sulphate, chloride and hydrogen sulphide was used to simulate MIC (*see* Fig. 3-1).

As in the initial corrosion model, it was assumed that the electrons formed by the oxidation of iron in the carbon-steel pipe (Eq. 4.1) were consumed by the reduction of protons (Eq. 4.2) in the following half-reactions:

$$Fe \rightarrow Fe^{2+} + 2e^{-} \tag{4.1}$$

$$H^{+} + e^{-} \rightarrow \tfrac{1}{2}H_2 \tag{4.2}$$

The transfer of charge (electrons) occurs only at the surface between the carbon-steel pipe and the synthetic water (electrolyte) because of the nature of electron transport (see Fig. 3-2).

The overall corrosion reaction was:

$$Fe + 2H^{+} \rightarrow Fe^{2+} + H_2 \tag{4.3}$$

The charge transfer at the carbon-steel pipe surface can be predicted by the Butler-Volmer equation (Gu, 2009) for each of the electrical species due to charge transfer (Roberge, 2000):

$$j_{ct,Fe} = j_{0,Fe}\left(exp\left(\frac{\alpha_{a,Fe}\cdot n_{Fe}\cdot F}{R\cdot T}\cdot \eta_{Fe}\right) - exp\left(\frac{-\alpha_{c,Fe}\cdot n_{Fe}\cdot F}{R\cdot T}\cdot \eta_{Fe}\right)\right) \tag{4.4a}$$

$$j_{ct,H^+} = j_{0,H^+}\left(exp\left(\frac{\alpha_{a,H^+}\cdot n_{H^+}\cdot F}{R\cdot T}\cdot \eta_{H^+}\right) - exp\left(\frac{-\alpha_{c,H^+}\cdot n_{H^+}\cdot F}{R\cdot T}\cdot \eta_{H^+}\right)\right) \tag{4.4b}$$

The exchange current density (the current density at equilibrium) for each species, respectively, was given by (Newman and Thomas-Alyea, 2004):

$$j_{0,Fe} = \frac{e_{0,Fe}}{A_E}\cdot\left(\frac{c_{s,Fe}}{c_{b,Fe}}\right)^{\gamma_{Fe}} \tag{4.5a}$$

$$j_{0,H^+} = \frac{e_{0,H^+}}{A_E}\cdot\left(\frac{c_{s,H^+}}{c_{b,H^+}}\right)^{\gamma_{H^+}} \tag{4.5b}$$

where e_0 = experimental value for the exchange current, A_E = area of the working-electrode, and γ = concentration sensitivity parameter (which is determined by examining the change in concentration of ions at the surface).

The reversible (equilibrium) potential was calculated using the Nernst equation (Roberge, 2000), where the activity for each species is represented by the surface concentration. This is a reasonable assumption for the pipe surface because: 1) the concentration profile for each species is formed from the surface out to the bulk of the solution, and; 2) the electrolyte solution is dilute. Therefore:

$$E_{rev,Fe} = E^{\circ}{}_{Fe} + \frac{2.3 \cdot R \cdot T}{n_{Fe} \cdot F} \cdot \log\left(c_{s,Fe}\right) \tag{4.6a}$$

$$E_{rev,H^+} = E^{\circ}{}_{H^+} + \frac{2.3 \cdot R \cdot T}{n_{H^+} \cdot F} \cdot \log\left(c_{s,H^+}\right) \tag{4.6b}$$

When equilibrium is achieved between oxidation and reduction, a balance in the transfer of charge is created. The potential at which this happens is the free corrosion potential (E_{corr}). The overpotential for each species then was:

$$\eta_{Fe} = E_{corr} - E_{rev,Fe} \tag{4.7a}$$

$$\eta_{H^+} = E_{corr} - E_{rev,H^+} \tag{4.7b}$$

The mass transfer at the carbon-steel pipe surface for each species can be described by:

$$\frac{j_{mt,Fe}}{n_{Fe} \cdot F} = -D_{Fe}\left(\frac{c_{b,Fe} - c_{s,Fe}}{\delta_{N,Fe}}\right) \tag{4.8a}$$

$$\frac{j_{mt,H^+}}{n_{H^+} \cdot F} = -D_{H^+}\left(\frac{c_{b,H^+} - c_{s,H^+}}{\delta_{N,H^+}}\right) \tag{4.8b}$$

Eqs. (4.8a) and (4.8b) can be rearranged to isolate the current density due to mass transfer for each species to give:

$$j_{mt,Fe} = (n_{Fe} \cdot F) \cdot \left(-D_{Fe}\left(\frac{C_{b,Fe} - C_{s,Fe}}{\delta_{N,Fe}}\right)\right) \tag{4.9a}$$

$$j_{mt,H^+} = (n_{H^+} \cdot F) \cdot \left(-D_{H^+}\left(\frac{c_{b,H^+} - c_{s,H^+}}{\delta_{N,H^+}}\right)\right) \tag{4.9b}$$

However, a drawback with Eqs. (4.8a) and (4.8b) resulting from adaption of the synthesis of Smith et al. (2011) is that there is no explicit term to predict that as temperature increases, D_{Fe} and D_{H^+} must increase, and therefore CR must increase also.

A mathematically convenient, and robust, way to deal with this necessary addition to the model is to use a temperature-correction suggested by Nesic et al. (1996) such that Eqs. (4.8a) and (4.8b) become, respectively:

$$j_{mt,Fe} = (n_{Fe} \cdot F) \cdot \left(-D_{Fe} \left(\frac{T}{T_{ref}} \right) \left(\frac{C_{b,Fe} - C_{s,Fe}}{\delta_{N,Fe}} \right) \right) \tag{4.9c}$$

$$j_{mt,H^+} = (n_{H^+} \cdot F) \cdot \left(-D_{H^+} \left(\frac{T}{T_{ref}} \right) \left(\frac{C_{b,H^+} - C_{s,H^+}}{\delta_{N,H^+}} \right) \right) \tag{4.9d}$$

where T_{ref} is the value of the SVA mean = 80 °C (353.15 K).

Because the number of electrons produced in the oxidation of iron is balanced by the reduction of protons (seen in Eq. (4.3)), the total current density must be zero:

$$j_T = j_{Fe} + j_{H^+} = \left(j_{ct,Fe} + j_{mt,Fe} \right) + \left(j_{ct,H^+} + j_{mt,H^+} \right) = 0 \tag{4.10}$$

The current density for iron oxidation can be computed by the addition of the current density for iron oxidation due to charge transfer, and the current density for iron oxidation due to mass transfer:

$$j_{Fe} = j_{ct,Fe} + j_{mt,Fe} = 0 \tag{4.11}$$

The current density due to iron oxidation was used by Collins et al. (2016) to determine a corrosion rate (CR) (Gu et al., 2009) using molecular weight and density such that:

$$CR = \frac{M_{Fe}}{2F \cdot \rho_{Fe}} \cdot j_{Fe} \tag{4.12}$$

which can be simplified for a wide range of temperature to:

$$CR = 1.155 j_{Fe} \tag{4.13}$$

Eqs. (4.4a) through (4.13) define the novel corrosion model of ASTM A105 carbon-steel pipe.

To realistically solve the model for ASTM A105 carbon-steel pipe however, E_{corr} must be treated as a multi-parameter function of pipe-fluid T and pH.

4.2.2 The *Solver* SVA solution

The model was set up to seek the free corrosion potential E_{corr} of the system at a given pipe-fluid T and pH through the calculation of surface concentrations for iron and protons and by employing convergence criteria.

Solution of the novel corrosion model with E_{corr} as a function of pipe-fluid T and pH was carried out as follows (Davey, 2015 b):

1. Each of T (K) and pH must be specified
2. $j_{0,Fe}$ and j_{0,H^+} (A m^{-2}) are obtained from, respectively, Eqs. (4.5a) and (4.5b) and substituted, respectively, into Eqs. (4.4a) and (4.4b)
3. $E_{rev,Fe}$ and E_{rev,H^+} (V vs SCE) are computed from, respectively, Eqs. (4.6a) and (4.6b) and substituted, respectively, into Eqs. (4.7a) and (4.7b)
4. η_{Fe} and η_{H^+} (V vs SCE) are obtained from, respectively, Eqs. (4.7a) and (4.7b) and substituted, respectively, into Eqs. (4.4a) and (4.4b)
5. $j_{mt,Fe}$ and j_{mt,H^+} (A m^{-2}) are computed from, respectively, Eqs. (4.9c) and (4.9d)
6. $j_{ct,Fe}$ and j_{ct,H^+} (A m^{-2}) are computed from, respectively, Eqs. (4.4a) and (4.4b) and are, together with $j_{mt,Fe}$ and j_{mt,H^+}, substituted into Eq. (4.10)
7. E_{corr} (V vs SCE) is computed by employing a convergence criterion on Eq. (4.10) such that $j_T = 0$
8. E_{corr} is substituted into Eq. (4.7a) to obtain η_{Fe}
9. η_{Fe} is substituted into Eq. (4.4a) to obtain $j_{ct,Fe}$
10. $j_{ct,Fe}$ is substituted into Eq. (4.11) to obtain j_{Fe}
11. j_{Fe} (A m^{-2}) is substituted into Eq. (4.13) to obtain CR (mm yr^{-1}).

The computations can be readily performed in Microsoft Excel™ with, for example, the *Solver* function used for step-7 such that a target cell is set to $j_T = 0$ – with an absolute value for practical convergence of 0.001 V vs SCE. Excel is convenient as it is widely available and is generally readily understood, thereby streamlining communication.

4.3 Deterministic single value assessment (SVA)

For the refined unit-operations model for corrosion, the SVA is computed as follows: for example, for water at a temperature of T = 353.15 K, pH = 5.15 (which is equivalent to $C_{b,H^+} = 10^{-pH} \times 10^3 = 10^{-5.5} \times 10^3 = 7.08 \times 10^{-3}$ mol m^{-3}, an initial 'guess' (Smith et al., 2011) of the values $C_{s,Fe} = 1 \times 10^{-4}$ mol m^{-3}, $C_{b,Fe} = 1 \times 10^{-6}$ mol m^{-3} and E_{corr} = -0.556 V vs SCE is made to give $j_{0,Fe}$ (Eq. (4.5a)), j_{0,H^+} (Eq. (4.5b)), $E_{rev,Fe}$ (Eq. (4.6a)), E_{rev,H^+} (Eq. (4.6b)), η_{Fe} (Eq. (4.7a)), η_{H^+} (Eq. (4.7b)), $j_{mt,Fe}$ (Eq. (4.9c)), and; j_{mt,H^+} (Eq. (4.9d)). Values for $j_{0,Fe}$, $E_{rev,Fe}$, and η_{Fe} are used to give $j_{ct,Fe}$ (Eq. (4.4a)). Values for j_{0,H^+}, E_{rev,H^+}, and η_{H^+} are substituted into j_{ct,H^+} (Eq. (4.4b)) and $j_{ct,Fe}$, j_{ct,H^+}, $j_{mt,Fe}$ and j_{mt,H^+} are substituted into Eq. (4.10).

The *Solver* loop converges to give E_{corr} = -0.54 V vs SCE, from Eq. (4.5a), $j_{0,Fe} = 3.57 \times 10^{-5}$ A m^{-2}, from Eq. (4.5b), $j_{0,H^+} = 4.63 \times 10^{-8}$ A m^{-2}, from Eq. (4.6a), $E_{rev,Fe}$ = -0.89 V vs SCE, from Eq. (4.6b), E_{rev,H^+} = -0.66 V vs SCE, from Eq. (4.7a), η_{Fe} = 0.35 V vs SCE, and from Eq. (4.7b), η_{H^+} = 0.12 V vs SCE. Substitution of values of $j_{0,Fe}$, $E_{rev,Fe}$, and η_{Fe} into Eq. (4.4a) is used to give $j_{ct,Fe} = 0.39$ A m^{-2}, whilst substitution of values of j_{0,H^+}, E_{rev,H^+}, and η_{H^+} into Eq. (4.4b) give $j_{ct,H^+} = 5.18 \times 10^{-7}$ A m^{-2}.

From Eq. (4.9c), $j_{mt,Fe} = -5.86 \times 10^{-20}$ A m^{-2}, and from Eq. (4.9d), $j_{mt,H^+} = -0.39$ A m^{-2} is computed. From Eq. (4.11), addition of $j_{ct,Fe}$ and $j_{mt,Fe}$ is used to give $j_{Fe} = 0.39$ A m^{-2}.

The predicted iron corrosion rate is then CR = 0.45 mm yr^{-1} (Eq. (4.13)).

4.4 *Fr 13* risk assessment

4.4.1 Risk factor and failure

The *Fr 13* risk assessment for the novel unit-operations corrosion model is performed in a similar manner as for the initial corrosion model discussed in Chapter 3.

For the novel unit-operations model for corrosion, a corrosion risk factor P is defined in terms of CR' and CR, such that $P = CR' - CR$. However, a mathematically more convenient, dimensionless corrosion rate risk factor (Abdul-Halim and Davey, 2016; Chandrakash and Davey, 2017) is:

$$p = 100\left(\frac{CR'}{CR} - 1\right) \tag{4.14}$$

Generally, the design specification would include some measure of tolerance i.e. design margin of safety. The corrosion rate risk factor of Eq. (4.14) can therefore be written as:

$$p = 100\left(\frac{CR'}{CR} - 1\right) - \%tolerance \tag{4.15}$$

In the absence of hard (unconditional) data it is assumed that a practical tolerance = 20 %, so that:

$$p = 100\left(\frac{CR'}{CR} - 1\right) - 20 \tag{4.16}$$

In practical terms, if the actual corrosion rate is 1.2 times greater than the acceptable corrosion rate i.e. $CR' > 1.2 \times CR$, the rate of corrosion is seen to be a failure. The 20 % practical tolerance is seen as a starting point - this can be delimited in more refined models.

Eq. (4.16) is convenient because it is dimensionless and all values $p > 0$ are readily identified as failures. Standard spread-sheeting tools can be used to easily isolate these values.

Eqs. (4.4a) through (4.13) plus (4.16) defines the probabilistic *Fr 13* novel unit-operations corrosion model of ASTM A105 carbon-steel pipe.

4.4.2 *Fr 13* simulation

In contrast to the traditional deterministic SVA, the probabilistic *Fr 13* risk simulation defines input parameters as distributions of values to mimic naturally occurring fluctuations, together with the probability of a particular value actually physically occurring. This means that the output behaviour will be a distribution of probabilities of particular outcomes. A refined Monte Carlo (r-MC) with *Latin Hypercube* sampling of the distributions ensures sampling covers the entire range of the distributions. ('Pure' MC cannot be relied on because it can over- and under-estimate from parts of the distribution (Vose, 2008)).

The probability distributions for the pipe-fluid parameters *T* and pH, in the absence of conditional data, for a large enough sample size are assumed normal and truncated, namely **RiskNormal** (mean, stdev, **RiskTruncate** (minimum, maximum)) (Vose, 2008). A standard deviation around the mean value in the distribution is assumed at stdev = 10 %, with the distributions truncated with a 2 x stdev about the mean to limit the minimum and

maximum values of the system parameters to that that could occur practically i.e. **RiskNormal** (mean, stdev, **RiskTruncate** (minimum = mean – 2 x stdev, maximum = mean + 2 x stdev)). This means that nearly all r-MC samples (95.45 %) will fall within these intervals (Sullivan, 2004).

For example, for pipe-fluid temperature, *T* = **RiskNormal** (353.15, 35.3, **RiskTruncate** (282.55, 423.75)), which sets a mean = 353.15, stdev = 35.3, and minimum = 282.55 and maximum = 423.75, K. This is a practical way to say that in operation the temperature of the pipe-fluid does vary randomly but not outside this range. To recognize the natural variability in sensitivity to pH, it is assumed pH = **RiskNormal** (5.15, 0.515, **RiskTruncate** (4.12, 6.18)).

A schematic for the novel *Fr 13* corrosion model of ASTM A105 carbon-steel pipe is shown as Fig. 4-1, showing the carbon-steel pipe unit-operation and the truncated probability distributions used to define naturally occurring fluctuations in key input parameters, *T* and pH.

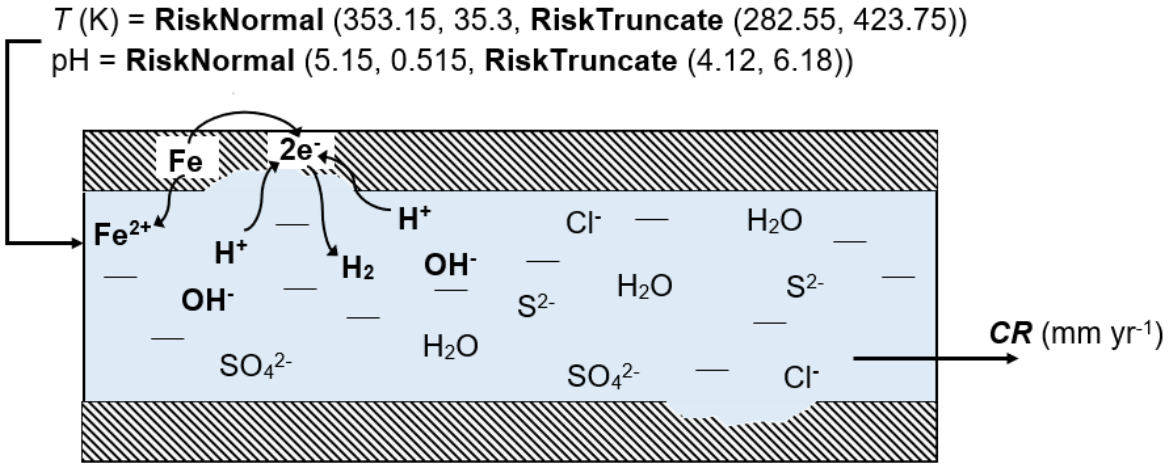

Fig. 4-1: Novel *Fr 13* corrosion model of ASTM A105 carbon-steel pipe

An alternative schematic of the novel *Fr 13* corrosion model of ASTM A105 carbon-steel pipe can be shown as a flow sheet using a fish bone (Ishikawa) diagram Fig. B-1 (Appendix B) in which the figure is read from left to right.

From the figure, the bones represent input parameters that lead to the model output. This identifies the relationship between the output and possible related causes. A clear benefit of this style of presentation is that the combination of key input parameters that lead to a possible output are highlighted. The diagram layout is simple to read and can easily be adapted to increasing levels of model sophistication.

To ensure that the output distribution of the mean is sufficiently normal, a minimum number of samples is needed (Vose, 2008) - this is usually some 1,000 to 50,000 (e.g. Zou and Davey, 2016; Chandrakash and Davey, 2017). This number can be determined when a plot of percentage of *Fr 13* failures versus number of simulations plateaus to a constant. (This can also be established by visual inspection of the output distribution).

Importantly, with a sufficient number of simulations it means that all possible practical combinations of scenarios that could occur with corrosion will have been reproduced, including unwanted corrosion rates of the steel pipe as failures.

The simulations were carried out using standard Microsoft Excel spread-sheeting with a commercially available add-on @Risk version 7.5 (Palisade Corporation™).

4.5 Results

A comparative summary of results for the deterministic SVA and probabilistic novel *Fr 13* simulation of corrosion of ASTM A105 carbon-steel pipe are presented in Table 4-1. Ten thousand (10,000) r-MC samples were deemed sufficient as it was determined visually that the percentage of *Fr 13* failures approximately plateaued to a constant at this value (Appendix D).

The traditional SVA is read down column 3 where CR = 0.45 mm yr^{-1} is shown. The *Fr 13* simulation is read down column 4 in which a normal distribution has been used for both T and pH, namely, T = **RiskNormal** (353.15, 35.3, **RiskTruncate** (282.55, 423.75)), and pH = **RiskNormal** (5.15, 0.515, **RiskTruncate** (4.12, 6.18)). For example, for the *Fr 13* simulation, a r-MC sample for the temperature of the pipe-fluid = 376.90 K is shown which, in combination with pH = 4.51, gives a resulting risk factor for CR, p = 319.14. As $p > 0$, this scenario shows a corrosion rate greater than an acceptable (SVA) rate plus a practical tolerance of 20 %. This T-pH range is more realistic than that used by Collins et al. (2016) for pipe flows in which oil is normally produced as the dominant and continuous phase together with some gas and water dispersed homogenously (Arnold and Stewart, 1999; J. Y. G. Chu, Operations Manager, Upstream Production Services Pty Ltd., Australia, *pers. comm.*).

It can be seen from Table 4-1 that the *Fr 13* risk model is identical to the SVA in that all mathematical operations that link parameters are the same. The significant difference, however, is that the key input parameters T and pH are defined by distributions of values, and not single values as with the traditional deterministic SVA.

Importantly, however, the data shown in column 4 of Table 4-1 are for one only scenario of the 10,000 – a limitation of using tabulated data. However, the results for the 10,000 scenarios can be readily presented as a summary output probability distribution (Chandrakash and Davey, 2017).

A total of 4,360 failures were exposed in the 10,000 scenarios i.e. 43.6 %. These are summarised as Fig. 4-2 in which the *x*-axis is the computed value of *p* from Eq. (16) and the *y*-axis is the probability of *p* actually occurring (Vose, 2008). From the figure, it can be seen that the output distribution is normal, and that the area under the curve (~333 x 0.003) = one (1). The 4,360 failure scenarios are seen in the R of the figure for all $p > 0$.

(The 43.6 % failure rate calculated from the novel *Fr 13* risk model is an 15.5 % increase compared to the 28.1 % calculated from the initial *Fr 13* model. However, as both the distributions of *T* and the tolerance were different in both models, it is not prudent to compare them on a like-for-like basis).

A significant advantage of the *Fr 13* risk framework is that each and every scenario can be readily, separately identified, with the corresponding value of each contributing parameter identified (Zou and Davey, 2016; Chandrakash and Davey, 2017). To illustrate this, the contributing *T* and pH values that gave rise to unwanted *CR* in 10 selected failures in the 4,360 are presented in Table 4-2.

For example, row 10, (**bolded text**) failure 8 of the table shows the combination of $T = 376.90$ K and pH = 4.51 resulted in $CR = 2.08$ mm yr^{-1} with corresponding corrosion rate risk factor $p = 319.14$; this is the particular scenario highlighted in Table 4-1. A value of $CR_{max} = 4.79$ mm yr^{-1} was at $T = 378.47$ K and pH = 4.12 with a corresponding maximum value $p_{max} = 949.78$.

Importantly, it is not implied that the numerical values given in Tables 4-1 and 4-2 for *T*, pH and *CR* (and resulting *p*) need to be measured to these exactly - these values are reproduced exactly from those in the r-MC simulations.

4.6 Discussion

4.6.1 *Fr 13* simulations and free corrosion potential

The *Fr 13* simulation of the novel corrosion model of ASTM A105 carbon-steel pipe proved to be stable, and because the overall values of *CR* were similar to those reported by Collins et al. (2016) it was concluded that results were free of programming and computational errors.

Table 4-1: Comparative summary of the deterministic SVA with the novel probabilistic *Fr 13* simulations for corrosion of ASTM A105 carbon-steel pipe with a tolerance of 20 %. Column 3 is the SVA value. Column 4 is for one only of 10,000 simulated *Fr 13* scenarios. *CR* failure is defined for all $p > 0$ (the pH and *T* ranges were selected to mimic more realistic ranges which were based on industry advice (J. Y. G. Chu, Operations Manager, Upstream Production Services Pty Ltd., Australia, *pers. comm.*))

Row	Parameter	SVA[a]	*Fr 13 model*[b]	
1	**Inputs**			
2	*T* (K)	353.15	376.90[c]	**RiskNormal**(353.15,35.3, **RiskTruncate**(282.55,423.75))
3	*pH*	5.15	4.51[c]	**RiskNormal**(5.15,0.515, **RiskTruncate**(4.12,6.18))
4	**Constants**			
5	$\alpha_{a,Fe}$ (dimensionless)	0.4	0.4	constant
6	$\alpha_{c,Fe}$ (dimensionless)	0.6	0.6	constant
7	α_{a,H^+} (dimensionless)	0.6	0.6	constant
8	α_{c,H^+} (dimensionless)	0.4	0.4	constant
9	n_{Fe} (dimensionless)	2	2	constant
10	n_{H^+} (dimensionless)	1	1	constant
11	$e_{0,Fe}$ (A)	1.00E-07	1.00E-07	constant
12	e_{0,H^+} (A)	1.00E-07	1.00E-07	constant
13	A_E (m^2)	2.80E-03	2.80E-03	constant
14	γ_{Fe} (dimensionless)	0.3	0.3	constant
15	γ_{H^+} (dimensionless)	0.75	0.75	constant
16	$E°_{Fe}$ (V vs SCE)	-0.681	-0.681	constant
17	$E°_{H^+}$ (V vs SCE)	-0.241	-0.241	constant
18	$C_{s,Fe}$ (mol m^{-3})	9.99E-07	9.99E-07	constant/Solver
19	C_{s,H^+} (mol m^{-3})	1.00E-06	1.00E-06	constant
20	$C_{b,Fe}$ (mol m^{-3})	1.00E-06	1.00E-06	constant
21	D_{Fe} (m^2 s^{-1})	7.98E-10	7.98E-10	constant

22	D_{H+} (m^2 s^{-1})	9.47E-09	9.47E-09	constant
23	T_{ref} (K)	353.15	353.15	constant
24	$\delta_{N,Fe}$ (m)	7.23E-06	7.23E-06	constant
25	$\delta_{N,H+}$ (m)	1.67E-05	1.67E-05	constant
26	F (C mol^{-1})	96485	96485	constant
27	R (J mol^{-1} K^{-1})	8.314	8.314	constant
28	*%tolerance* (%)	-	20	
29	**Calculations**			
30	$C_{b,H+}$ (mol m^{-3})	7.08E-03	0.03	Conversion from pH
31	$j_{0,Fe}$ (A m^{-2})	3.57E-05	3.57E-05	Eq. (4.5a)
32	$j_{0,H+}$ (A m^{-2})	4.63E-08	1.53E-08	Eq. (4.5b)
33	$E_{rev,Fe}$ (V vs SCE)	-0.89	-0.91	Eq. (4.6a)
34	$E_{rev,H+}$ (V vs SCE)	-0.66	-0.69	Eq. (4.6b)
35	$j_{mt,Fe}$ (A m^{-2})	-5.86E-20	-6.26E-20	Eq. (4.9c)
36	$j_{mt,H+}$ (A m^{-2})	-0.39	-1.80	Eq. (4.9d)
37	$j_{ct,Fe}$ (A m^{-2})	0.39	1.80	Eq. (4.4a)
38	$j_{ct,H+}$ (A m^{-2})	5.18E-07	9.55E-07	Eq. (4.4b)
39	η_{Fe} (V vs SCE)	0.35	0.44	Eq. (4.7a)
40	η_{H+} (V vs SCE)	0.12	0.22	Eq. (4.7b)
41	E_{corr} (V vs SCE)	-0.54	-0.47	***Solver***
42	j_{Fe} (A m^{-2})	0.39	1.80	Eq. (4.11)
43	j_{H+} (A m^{-2})	-0.39	-1.80	Eq. (4.10)
44	j_T (A m^{-2})	-6.88E-07 (≈ 0)	6.73E-07 (≈ 0)	Eq. (4.10)
45	**Output**			
46	CR (mm yr^{-1})	0.45	2.08	Eq. (4.13)
47	p	-	319.14	Eq. (4.16)

[a] Traditional deterministic single point, or, single value assessment.
[b] One only of 10,000 scenarios.
[c] Values are reproduced from the r-MC sampling; it is not implied they are measured to this significance.

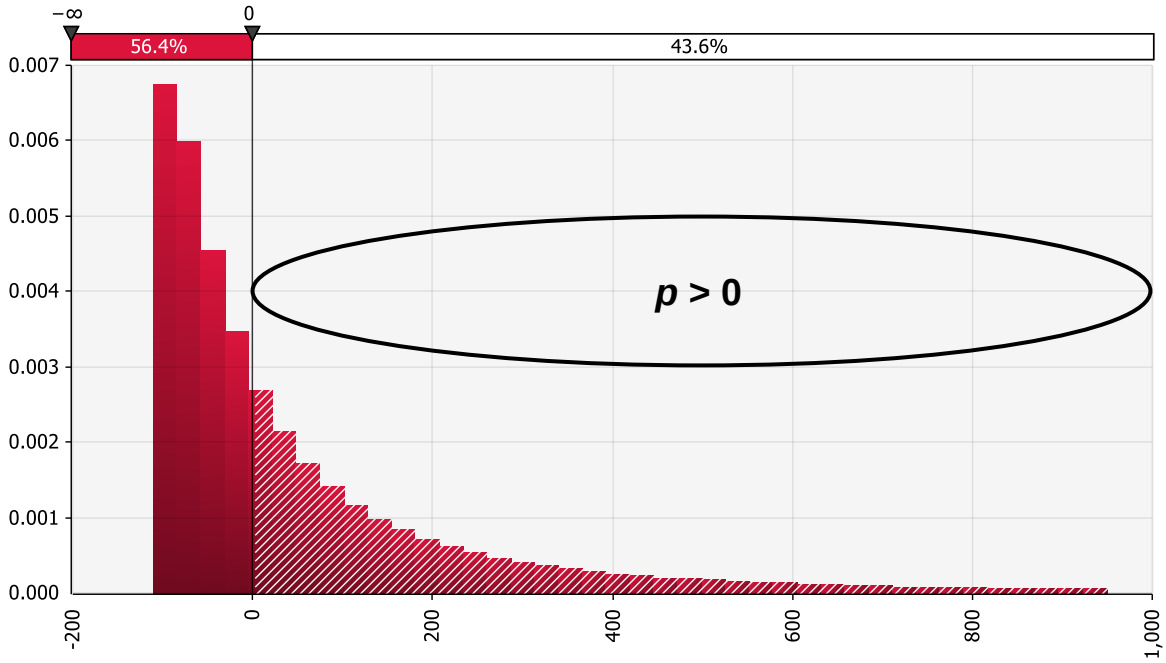

Fig. 4-2: *Fr 13* simulation of the corrosion rate risk factor, *p*, for corrosion with 10,000 scenarios and 20 % tolerance. The *x*-axis is the value of risk factor and the *y*-axis the probability of that value. To the R of the figure is shown the 43.6 % failure scenarios with unwanted corrosion > 0.45 mm yr^{-1} with $p > 0$. It can be seen that the output distribution is normal, and that the area under the curve (~333 x 0.003) = one (1)

Table 4-2: Ten (10) selected *Fr 13* failures in the 10,000 scenarios with 20 % tolerance

Failure	***T*** [b] **(K)**	**pH** [b] **(dimensionless)**	***CR'*** **(mm yr^{-1})**	***p*** **(dimensionless)**
1	312.24	5.07	0.54	0.02
2	352.35	5.02	0.61	16.16
3	418.96	4.96	0.69	35.06
4	324.35	4.90	0.79	57.57
5	319.51	4.84	0.92	84.96
6	326.87	4.70	1.27	164.20
7	325.55	4.61	1.55	225.96
8[a]	**376.90**	**4.51**	**2.08**	**319.14**
9	367.15	4.37	2.71	485.70
10	378.47	4.12	4.79	949.78

[a] Particular scenario of Table 4-1.

[b] Values are reproduced from the r-MC sampling; it is not implied they are measured to this significance.

Overriding however is that model predictions were significantly impacted by a value of the free corrosion potential, $E_{corr,}$ being dependent on combined fluctuations in pipe-fluid *T* and pH. For example, comparison with repeat simulations using the initial model of Collins et al. (2016) with the realistic distributions *T* = **RiskNormal** (353.15, 35.3, **RiskTruncate** (282.55, 423.75)) and pH = **RiskNormal** (5.15, 0.515, **RiskTruncate** (4.12, 6.18)) showed, for a mid-range *T* = 353.15 K and pH = 5.15 with constant E_{corr} = -0.556 V vs SCE, gave nonsensical (less than zero) values of *CR*. These repeat simulations underscored therefore the importance of treating E_{corr} as a function of combined pipe-fluid *T* and pH.

It is concluded therefore that predictive models for corrosion of carbon-steel pipe must take into account a free corrosion potential that is dependent on fluctuations in combined pipe-fluid *T* and pH.

If each of the *CR* simulations of Tables 4-1 and 4-2 is assumed as one day, there would be an unwanted rate of corrosion of the ASTM A105 steel pipe of > 0.45 mm yr^{-1} every (4,360/10,000 x 365.25 day/year ~) 160 days, averaged over the long term, because of natural fluctuations in pipe-fluid *T* and pH, despite a design safety margin (tolerance) of 20 %. There is however no reason to expect these predicted failures will be spaced equally in time.

It is acknowledged that the upper value used in the *T* distribution (423.75 K) might be considered high for SRB, since Pots et al. (2002) state that these bacteria normally function in the range 4 to 110, $^{\circ}$C (277.15 to 383.15, K) and Maxwell and Campbell (2006), 0 to 80, $^{\circ}$C (273.15 to 353.15, K). When the novel *Fr 13* model was run with the *T* range 0 to 110, $^{\circ}$C (273.15 to 383.15, K) with the same mean (353.15 K) and stdev (10 %), the percentage of failures stayed constant at 43.6 %.

However, the *T* range used is adequate for demonstration of the *Fr 13* risk model. (The range of values was based on the 2 x stdev in the assumed normal distribution to ensure 95.45 % of all r-MC samples fell within the distribution intervals).

It is evident that the range of *T* values could be readily delimited when more conditional data are available.

4.6.2 Mitigating pipe vulnerability to *Fr 13* failure

To investigate possible corrosion mitigation strategies, repeat simulations to quantify the impact of natural fluctuation in pH on *CR* at the minimum (282.55 K), mean (353.15

K), and maximum (423.75 K) pipe-fluid temperature were carried out. Results are presented as Fig. 4-3.

From the figure, it can be seen that, as *T* increases *CR* increases. (A limitation experienced however in using the commercial *Solver* (Trial & Error) convergence was a software constraint at ~4.9 < pH < ~5.10 and low *T* = 282.55 K, ~5.4 < pH < ~5.5 and mean *T* = 353.15 K, and ~5.7 < pH < 5.8 for high *T* = 423.75 K, in predicting *CR* as it systematically returned an 'error'. The reason for this was not transparent - and may not result from model formulation, but the *Solver* 'internal' method). Overall these predictions are however reliable and are a logical conclusion from the model corrosion kinetics.

An interesting insight from Fig. 4-3 is that at a fixed value of *T*, a decrease in pH results in an increase in carbon-steel pipe corrosion as reflected in an increase in the value of *CR*. For example, at fixed mean-value of *T* = 353.15 K a decrease in pH from 5.15 to 4.5 results in an increase in carbon-steel pipe corrosion of ~1.55 mm yr^{-1} i.e. ~347 % increase. In the pH range $5.6 \leq pH \leq 6.2$, the *CR* is seen not to be significantly impacted by pipe-fluid temperature (*T*).

It is concluded that the pH of the pipe-fluid is overriding compared with pipe-fluid *T* in impacting the corrosion rate in MIC.

This means that pipe vulnerability to *Fr 13* corrosion failure and any acidic corrosion in general could be minimised by increasing pH of the pipe-fluid. One way to practically do this could be by adding bases (e.g. potassium hydroxide, sodium hydroxide, sodium carbonate or potassium carbonate) (Kemmer, 1988). However, if the pipe-fluid pH is too high, anions can precipitate and form insoluble mineral scales that can lead to pipe fouling (Pichtel, 2016).

A practical value of tolerance of 20 % was included in the risk factor Eq. (16). This is a simple way of stating a level of safety in corrosion. However, this value should not be too large as it could result in plant operators believing that the carbon-steel pipes are less vulnerable to failure than they actually are. This could lead to steel pipe leaks or breaks, resulting in potential process or personnel loss.

To assess the impact of tolerance, the vulnerability of the ASTM A105 carbon-steel pipe to corrosion failure was investigated through repeat (second-tier) simulations over the range $0 \leq tolerance \leq 50$ %, maintaining a stdev = 10 % on parameters *T* and pH. These results are summarised in Fig. 4-4.

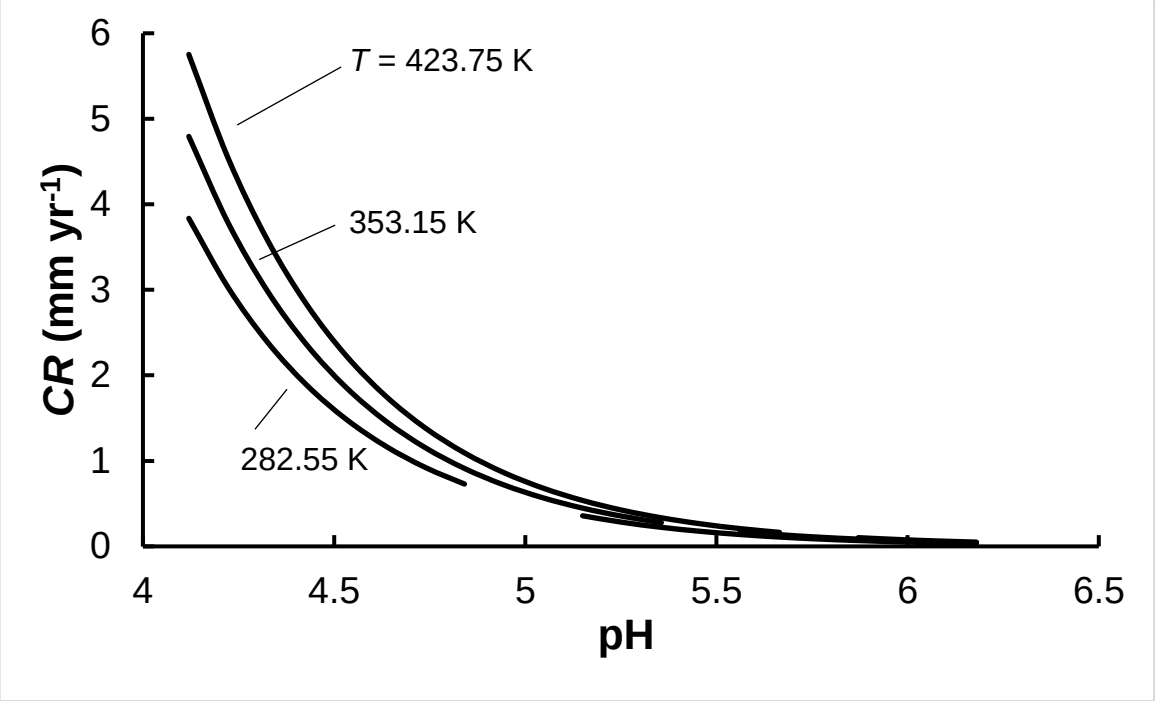

Fig. 4-3: Pipe-fluid pH vs corrosion rate (*CR*) for minimum, mean, and maximum values of the *Fr 13* temperature distribution

It can be seen in Fig. 4-4 that as tolerance is increased, the percentage of failures in unwanted corrosion of the steel pipe decreases, almost linearly. For example, at a minimum possible *% tolerance* = 0 %, the number of unwanted corrosion failures of the steel pipe is predicted to be a maximum at 50 %. At % *tolerance* = 50 % the number of unwanted failures of the carbon-steel pipe approaches 36 %.

Practically, decreasing *% tolerance* or design safety to maintain a desired value of *CR* implies increasingly strict controls on pipe-fluid *T* and pH. A suitable practical value could be decided on from accumulated expert knowledge. It is concluded however that the impact can be readily tested in the *Fr 13* analysis of corrosion.

4.6.3 Probability distributions and defining corrosion failure

The choice of distribution for corrosion parameters *T* and pH is best based on expert knowledge or experimental data. It is important only that the input (and therefore, the output) distributions are carefully selected so that they cover all practically possible values.

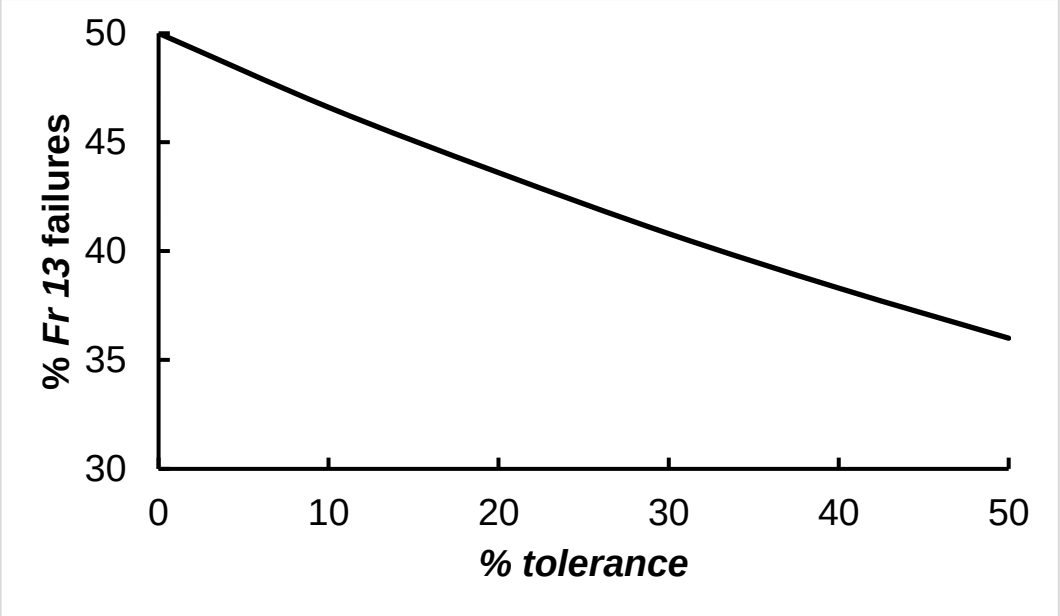

Fig. 4-4: Impact of % *tolerance* on corrosion rate (*CR*) against percentage of *Fr 13* failures per 10,000 scenarios

In the absence of unconditional data, the distributions selected were truncated normal. There are some 40 probability distribution types that could have been selected for the *Fr 13* risk assessment, including *beta subjective* (Davey and Cerf, 2003), *pert* (Davey et al., 2015) and *triangle* (Chandrakash and Davey, 2017). For the novel *Fr 13* corrosion model, it might be possible that distributions could be 'tailored' for particular metal-bacterial systems or geographical locations (*see* Davey et al., 2016; Lavigne and Davey, 2017). Regardless, distributions need to be selected such that the model outcomes are those that could be observed in practice.

The 'tipping point' from non-failure to failure in the novel *Fr 13* model for ASTM A105 carbon-steel pipe corrosion has been defined as any rate greater than that predicted in the traditional deterministic SVA of $CR = 0.45$ mm yr^{-1} (Table 4-1). Alternatively, however, failure could be defined as an actual reduction (%) in wall thickness of a wetted steel pipe. This may prove more convenient for particular application(s) or geographical locations, especially where significant corrosion data is available and which can be fitted to distributions (Vose, 2008). The risk model and definition of failure of the pipe can be readily adapted in the corrosion risk model.

Further, the model for ASTM A105 carbon-steel pipe corrosion appears generalizable and therefore applicable to a range of more complex biotic environments and different metals.

4.6.4 Limitations and results overview

Notably, the results from this *Fr 13* corrosion risk assessment are new and, importantly, quantitative. A novel insight is that the corrosion rate of the carbon-steel pipe in abiotic water is significantly impacted by naturally occurring, random fluctuations in *T* and pH of the pipe-fluid. These fluctuations can lead to pipe corrosion failure.

Significantly, this insight cannot be obtained from traditional SVA simulations or risk and hazard analyses. This is because the element of naturally occurring randomness is not explicit in these traditional assessments. The *Fr 13* model output is therefore more practical. Advantageously, it can be used to simulate every possible scenario, including corrosion failures, and any particular scenario can be identified, isolated and studied. Importantly, second-tier studies using the framework can be used to predict the impact on corrosion and pipe failure from any re-design of the physical system.

A shortcoming of the model however is that there is presently no biotic component, that is, a specific bacterial species modelled. The model needs to be refined to incorporate the impact of particular bacterial kinetics (Maxwell and Campbell, 2006) and species involved in micro-organism growth (sulphates, chlorides and hydrogen sulphide) on pipe-fluid *T* and pH for a particular pipe metal (Roberge, 2000), although ASTM A105 carbon-steel pipe is widely used globally.

These limitations may not be so problematic however, as the example scenario in Javaherdashti (2017) showed that a biotic environment containing SRB would have the same impact on the corrosion of carbon-steel as an abiotic one containing chlorides. This implies that the severity of carbon-steel corrosion in abiotic environments could be as great as in biotic environments. However, this statement should not be relied on in the absence of any controlled experimental work on biotic systems. Because the *Fr 13* risk model developed here is based on established unit-operations, and is generalizable, it is a natural 'starting point' from which to develop more complex biotic models.

It is concluded that the probabilistic corrosion model form when refined, could be used to quantitatively investigate the impact of proposed MIC intervention strategies in a range of micro-organism-metal systems.

4.7 Chapter summary and conclusions

1. A novel *Fr 13* model for corrosion of ASTM A105 carbon-steel pipe was synthesized by extending of the initial *Fr 13* model of Collins et al. (2016). This was done by considering the pipe free corrosion potential E_{corr}, a key corrosion parameter, as a function of combined internal pipe-fluid temperature (T) and pH to realistically simulate off-shore oil processing operations. This is important because the novel *Fr 13* model showed that E_{corr} is significantly impacted by natural fluctuations in the pipe-fluid environment and cannot be considered a constant.

2. Results show that with a mean temperature of 353.15 K and pH of 5.15 and a practical tolerance of 20 %, unwanted degradation of widely-used ASTM A105 carbon-steel pipe of > 0.45 mm yr^{-1} is expected to occur every 160 days (43.6 % of all cases), averaged over the long term, due to naturally occurring fluctuations in pipe-fluid T and pH. This insight is not available from traditional deterministic risk approaches.

3. Second-tier simulation studies highlight that vulnerability to corrosion failure of the carbon-steel pipe can be mitigated by increasing the pH of the pipe-fluid. One way to practically do this is by adding bases, however pipe-fouling scales can form if the pH becomes too high.

4. The model appears generalizable to a range of more complex biotic environment and different metals.

In the following chapter, Chapter 5, limitations of the model are discussed, together with future developments for MIC research.

CHAPTER FIVE

LIMITATIONS AND FUTURE DEVELOPMENT

5.1 Introduction

This thesis research has shown for the first time that the emerging *Fr 13* risk framework can be applied to gain new insight into, and help mitigate the risk of, the impact of naturally occurring random fluctuations in *T* and pH of the pipe-fluid on corrosion of ASTM A105 carbon-steel pipe. There are however limitations to the work.

In this chapter the key limitations are discussed, together with possible future developments to guide further research.

5.2 Limitations

The key shortcomings of the newly synthesized *Fr 13* model for corrosion are the present lack of: 1) a biotic component i.e. particular bacterial species modelling, and; 2) experimental validation.

5.2.1 Need for a biotic component

Maxwell and Campbell (2006) provide an example of an MIC model incorporating bacterial kinetics with simulation of an SRB biofilm within a given set of input parameters using the simplified equation:

$$Biofilm\ Development = Accumulation\ (A) - Removal\ (R) \tag{5.1}$$

The accumulation value *A* was calculated using Monod kinetics:

$$A = N_0 \times 10^{\frac{\mu(t-t_0)}{2.303}} \tag{5.2}$$

where N_0 is the biofilm inoculum per cm^2, μ is the specific growth rate of the micro-organism i.e. SRB, t is time, and t_0 is time at which the system is first inoculated with microbial cells. (*R* is calculated as logarithmic decreases of *A*, which is suitable for good (99.99 % effective) to poor (90 % effective) biocide performance).

N_0 was calculated by the following equation:

$$N_0 = \frac{(n \times v)}{a} \tag{5.3}$$

where *n* is the number of cells / ml of total fluids, *v* is the volume of total fluids per day (ml) (assuming continuous flow), and *a* is the water wet surface area (cm^2).

The authors concluded that combining bacterial kinetics with simplified MIC models provided an assessment of the lag period before MIC risk occurs. This in turn allowed for a more simplified model, as biological factors could be removed and fewer abiotic parameters were required.

Modelling the biofilm that usually forms when microbial cells attach themselves to a solid surface is an important part of MIC modelling, as it is usually under these biofilms in which MIC actually takes place. This is due to the micro-organisms getting an opportunity to stay in one place, which allows them to grow and produce corrosive species that initiate and accelerate corrosion.

Another example of a model that incorporates the impact of biofilms on MIC is the work of Xu et al. (2016), whose model included a parameter called the exchange current density for sulphate reduction $(j_{0(SO_4{}^{2-})})$, which they defined as the 'aggressiveness' of a sulphate-reducing bacteria (SRB) biofilm. This 'aggressiveness' was defined as the ability of an SRB biofilm to transfer electrons from an iron surface for sulphate reduction in the SRB cell. The parameter was dependent on many variables such as sessile cell density on the iron surface and the SRB's enzyme activities at different temperatures. It was possible to calibrate $j_{0(SO_4{}^{2-})}$ using experimental SRB pitting data.

5.2.2 Experimental validations

Javaherdashti (2017) in model studies showed that a biotic environment i.e. one containing SRB, would have the same impact on the corrosion of carbon-steel as a 'synthetic' abiotic one containing chlorides. This implied that the severity of carbon-steel corrosion in abiotic environments could be as great as in biotic environments.

Although this author's conclusion underscores the value of this thesis work, abiotic environments however should not be relied on in the absence of any controlled experimental work with biotic systems.

The synthesis of a biotic component plus experimental validation is needed. This is an important step as there is currently no commercial-scale real-world failure data to validate the *Fr 13* risk model.

As the types of micro-organisms are wide-ranging, experimental validation will need to be targeted, say, to widely used ASTM A105 pipe and SRB plus one or more other micro-organisms. This will also guide more realistic input parameter distributions.

5.2.3 An integrated process

There is strong anecdotal evidence that unexpected (surprise) failures are considered to be a part of normal chemical engineering processes. However, as the interconnectedness of processes and products is increased, the impacts of such surprise failures will be compounded. This is problematic as unexplained and non-equipment failure data are usually not disclosed publicly and therefore the true impact of these failures can be hidden (Zou and Davey, 2016). This compares for example with the significant equipment failure data contained in bases such as OREDA (2015).

It is acknowledged in the Blackett Review (Anon., 2012) that there is a need to develop theoretical and practical tools that can anticipate these problems when they occur.

The demonstration in this research to quantitatively simulate the potential accumulative effects of naturally occurring fluctuations in a steady-state corrosion model of ASTM A105 carbon-steel pipe under abiotic, synthetic conditions to determine and mitigate risk is therefore a significant step in the development of a *Fr 13* risk framework for a more integrated process.

5.3 Future developments

A major strength of the thesis work is that because the *Fr 13* risk model is predicated on established unit-operations (Foust et al., 1980; McCabe et al., 2001) and is generalizable, it is a natural ‘starting point’ from which to develop more complex biotic models.

5.3.1 Improving MIC syntheses

When refined and developed the *Fr 13* risk model for MIC could be used to quantitatively investigate the impact of proposed intervention strategies in a range of micro-organism-metal systems.

Some likely developments include:

- Addition of bacterial (biotic) kinetics (e.g. Maxwell and Campbell, 2006) and simulation of different micro-organisms e.g. sulphur/sulphide-oxidizing bacteria, iron/manganese-oxidizing bacteria, and; acid-producing bacteria (Chilingar, 2008, Javaherdashti, 2013; Xu et al., 2016)
- An increased number of pipe-fluid input parameters that might include: oxygen ingress (if the bacteria modelled was aerobic in some form), pressure, flow velocity, water quality (turbidity), and; salt concentration (chloride levels)
- A greater range of species/nutrients that can be involved in MIC initiation and growth, for example, sulphur (e.g. sulphates/sulphides), carbon (e.g. fatty acids), nitrogen (e.g. nitrates), chlorides and H_2S
- Various metals that are used where MIC is found. For example, a range of carbon alloys could be modelled to compare MIC susceptibility between them. Different pipe metals such as copper or zinc could also be modelled (Roberge, 2000)
- A 'global' model approach, which could involve linking numerous pipe systems within a piece of equipment or plant to determine the overall susceptibility as an integrated system to MIC. However, it might not be applicable because MIC can occur in localized sites which could lead to catastrophic failure at one site regardless of the susceptibility of the rest of the integrated system
- 'Tailored' models for specific geographical locations (*see* the work of Davey et al. (2016) for the Bass Strait and Lavigne and Davey (2017) for the Gulf of Mexico).

The combination of bacterial kinetics and developments listed would lead to a powerful risk assessment tool that could be relied on in the *design* and *synthesis* stages of a project. Simulations from the present stage of development of the *Fr 13* risk model can be relied on to guide this future work.

5.3.2 Time, cost, effort and benefit

As the results and recommendations of recent *Fr 13* work have not, to the author's knowledge, been implemented in the relevant industries, it is unknown at this stage what financial or safety returns would occur on a large scale.

However, simulations from the present research indicate that the time, cost, effort and benefit of applying the *Fr 13* risk assessment framework would be low compared to traditional risk assessment methodologies, which require multiple personnel for a period of hours (potentially up to a full working day).

In contrast to these established risk assessment methods, the *Fr 13* risk framework can be performed in the *design* and *synthesis* stages of a project as it is based on unit-operations. It should be relatively quick (a matter of hours) to set up a simulation(s) and, when performed correctly, would be easy-to-understand. Another benefit of the framework is that there is a quick turnaround of information regarding key input and output parameters and possible second-tier unit-operation design changes.

A caution inherent in all model designs (Richardson et al., 1979) however is that: 1) No one model will provide a complete picture of the system being analysed; 2) Data used to synthesize the model could be incomplete - especially because of the reliance on distributions - an advantage however is that these can be updated and modified with experience and later validated experimentally, and; 3) Model simulations can be misused by operators who don't fully understand how to correctly set up and run the simulation - this could lead to poor decision-making and possible equipment inefficiencies or failure.

The *Fr 13* risk framework could be used in conjunction with traditional risk assessments just before the design of the system is 'locked down', and afterwards, with a view to modifying the physical system to reduce vulnerability to the possible impact of unexpected accumulation of fluctuations in key input parameters.

A major benefit of *Fr 13* is that it will add to a deeper understanding of how apparently steady-state processes can unexpectedly give different outcomes.

In the final chapter, Chapter 6, conclusions available from this thesis research are summarised.

CHAPTER SIX

CONCLUSIONS

6.1 Conclusions

The following can be concluded from this research:

1. Although the *Fr 13* risk framework has been successfully applied to risk of pitting of externally exposed metal (AISI 316L) in off-shore oil and gas structures as impacted by naturally occurring fluctuations in sea temperature and salinity (< 20 m depth), it was not known if the framework could provide new insight into microbiologically influenced corrosion (MIC) of internal pipe metals. However, as modelling of direct MIC is uniquely complex, a limited research program was therefore undertaken to investigate how random, naturally occurring fluctuations in steady-state pipe-fluid parameters *T* and pH can impact failure of widely-used ASTM A105 carbon-steel pipe due to general corrosion, with a view to extending the model to include MIC in future research . An initial model based on a three-electrode corrosion cell and potentiostat experimental setup was selected to test the methodology. Pipe failure was defined as a corrosion rate greater than an acceptable design rate

2. Results from an initial *Fr 13* model for corrosion of ASTM A105 carbon-steel pipe (Collins et al., 2016) showed that with a temperature of 293.15 K and pH of 5.15 and a practical tolerance of 50 % as a design margin of safety, an unacceptable MIC of carbon-steel pipe can occur in 28.1 % of all scenarios. If every scenario is thought of as one day there would be approximately 103 unacceptable rates of corrosion each year averaged over the long term. These failures would not be expected to be spaced equally in time however

3. A drawback of the initial *Fr 13* model was that a key parameter E_{corr} (free corrosion potential) was taken as a single value when in fact it is a multivariable function of *T* and pH. The initial *Fr 13* model was therefore extended by considering E_{corr} as a function of combined internal pipe-fluid temperature (*T*) and pH to realistically simulate off-shore oil processing operations. This was important because the extended (novel) *Fr 13* model showed that E_{corr} is significantly impacted by natural fluctuations in the pipe-fluid environment and cannot be considered a constant. The *T* range was also modified to more

accurately model temperatures found in oil pipe flows. Results showed that with a mean temperature of 353.15 K and pH of 5.15 and a practical tolerance of 20 %, unwanted corrosion of widely-used ASTM A105 carbon-steel pipe of > 0.45 mm yr^{-1} is expected to occur every 160 days (43.6 % of all cases), averaged over the long term, due to naturally occurring fluctuations in pipe-fluid *T* and pH (Collins and Davey, 2018)

4. Overall, *Fr 13* simulations of the two models underscored that the apparent steady-state corrosion of ASTM A105 carbon-steel pipe should be more considered as a combination of successful and failed operations. This is new information is not readily available from traditional risk and hazard approaches, with or without sensitivity analyses

5. Second-tier *Fr 13* simulation studies highlight that vulnerability to corrosion failure of the carbon-steel pipe can be mitigated by increasing the pH of the pipe-fluid. One way to practically do this is by adding bases, however pipe-fouling scales can form if the pH becomes too high

6. A shortcoming of the novel *Fr 13* model is that there is presently no biotic component. However, the model can be refined in later iterations to incorporate the impact of particular bacterial kinetics and species involved in micro-organism growth (sulphates, chlorides and hydrogen sulphide) on pipe-fluid *T* and pH for a particular pipe metal in a specific geographical location

7. It is concluded that the *Fr 13* framework is applicable to corrosion of ASTM A105 carbon-steel pipe. Further, the model appears generalizable to a range of micro-organism-metal systems. If developed properly, the risk framework could provide a new decision-making tool in both *design* and *synthesis* stages to give new knowledge and insights into understanding unit-operation behaviour outcomes.

The research is original and is not incremental work. Findings will be of immediate benefit and interest to a range of risk analysts and design engineers involved in pipe metals selection and mitigating MIC in pipe flows.

APPENDICES

APPENDICES A - D

APPENDIX A – A definition of some important terms used in this research

Abiotic	Not relating to living organisms *see* Biotic
Anode	The site in an electrochemical cell where oxidation occurs
Biocide	A chemical agent that is used to either inactivate or control unwanted micro-organisms through chemical means
Biofilm	A collection of microbial cells (algal, fungal, or bacterial) and extracellular products encased in a matrix, that can be attached to either an inert or living surface
Biofouling	The unwanted accumulation of micro-organisms, algae and fungi in process equipment
Biotic	Relating to living organisms *see* Abiotic
Cathode	The site in an electrochemical cell where reduction occurs
Corrosion potential	The equilibrium potential of a metal in an electrochemical cell without external electrical current
Corrosion rate (*CR*)	The rate at which a metal in a defined environment corrodes. Generally expressed as mm yr^{-1}
Cut	Volumetric ratio of a certain fluid component compared to the overall fluid volume
EPS	Extracellular Polymeric Substance(s). Sticky macro-molecules produced by micro-organisms that allow them to attach to solid surfaces and stay in a single place in the system by way of a thin, slimy film matrix of cells
Eukaryotic	Uni- or multi-cellular organisms with cells that have a membrane-bound nucleus and multiple chromosomes (Nelson and Cox, 2000) *see* Prokaryotic
Failure	A scenario in which the design value for success is not achieved
Fr 13	*see Friday 13th Syndrome*
Friday 13th Syndrome	A surprise event resulting from accumulation of naturally occurring fluctuations in a unit-operation (*see* Chandrakash and Davey, 2017)

Fr 13 simulation	Novel, probabilistic simulation for a predicted model output with probability distribution of values as inputs (developed by Davey and Cerf, 2003)
Genera	Plural form of genus (taxonomic rank used to classify organisms in biology. Comes above species, but below family) (Brock and Madigan, 1991)
Gram staining	A common microbiological technique to identify and characterize micro-organisms, primarily bacteria. The method involves applying a violet dye to a sample of cells on a slide, which turn the cells purple. They are then flushed with an iodine solution, followed by an organic solvent. *Gram-positive* cells retain the original purple colour as they have a single cell wall which is too thick to be easily penetrated by the solvent. *Gram-negative* cells, on the other hand, lose the purple colour as their cells walls are thinner and can be easily penetrated by the solvent. These Gram-negative cells are then strained with another dye which turns them red (Madigan et al., 2003)
Latin Hypercube	Sampling technique where the input(s) probability distribution is split into *n* intervals of equal probability. This ensures values are sampled to cover the entire range (Vose, 2008)
Methanogen	Strictly anaerobic micro-organisms that produce methane as the main product of their metabolism (Whitman et al., 2006)
MIC	Microbiologically Influenced Corrosion - corrosion of metal initiated by macro- or micro-organism activity (Roberge, 2000)
Overpotential	The difference between a redox half-reaction's reversible (equilibrium) potential and the potential measured experimentally
Oxidation	The loss of electrons or increase in oxidation state by an atom, molecule, or ion - always occurs concurrently with reduction in a 'redox' reaction *see* Reduction
Pigging	Use of a mechanical device called a 'pig' (Pipeline Inspection Gadget) to clean a pipeline. An advantage is that the flow of fluid in a pipeline doesn't have to be stopped while the pig is used (Flemming, 2002). A chemical (biocidal) pig may be used as a follow up
Planktonic	Micro-organisms that are freely floating in a medium (Roberge, 2000). Opposite of Sessile

Probability	A numeric measure of the likelihood of a particular outcome of a stochastic process scenario
Prokaryotic	Single-cell organisms that lack a membrane-bound nucleus and any other specialized organelles, and have only one chromosome (Nelson and Cox, 2000) *see* Eukaryotic
Reduction	The gain of electrons or decrease in oxidation state by an atom, molecule, or ion *see* Oxidation
Second-tier (studies)	Repeat simulations of the *Fr 13* assessment that are used to reduce risk through the investigation of intervention strategies and the potential re-design of the physical plant or unit-operation. Can be applied at either the *design* or *synthesis* stages (Davey, 2015 a; Abdul-Halim and Davey, 2016)
Sessile	Micro-organisms that are anchored in a fixed spot, e.g. in a biofilm (Roberge, 2000). Opposite of Planktonic
SRB	Sulphate-reducing bacteria. Bacteria that obtain energy by reducing sulphate (SO_4^{2-}) to sulphide while oxidising organic compounds or hydrogen molecules (H_2)
Single Value Assessment (SVA)	Model computations that use traditional chemical engineering single or point values as the value for an input (Davey and Cerf, 2003)
Stochastic process	A system of numerical values in a well-defined random process
Tolerance	Measure of over-design for safety
Uncertainty	A lack of knowledge, or level of ignorance, about parameters that characterize the physical system or process being modelled. It is sometimes reducible through further measurement, careful study, or through consulting more experts (Vose, 2008)
Unit-operation	A step in a process that involves a physical or chemical change taking place e.g. heating, mixing, distillation, cooling, etc.
Variability	The effect of chance on an outcome. It is a function of the system and cannot be reduced through either further study or measurement. However, it can be reduced by changing the physical system (Vose, 2008)

APPENDIX B - Fish bone diagram for *Fr 13* simulation of corrosion of ASTM A105 carbon-steel pipe

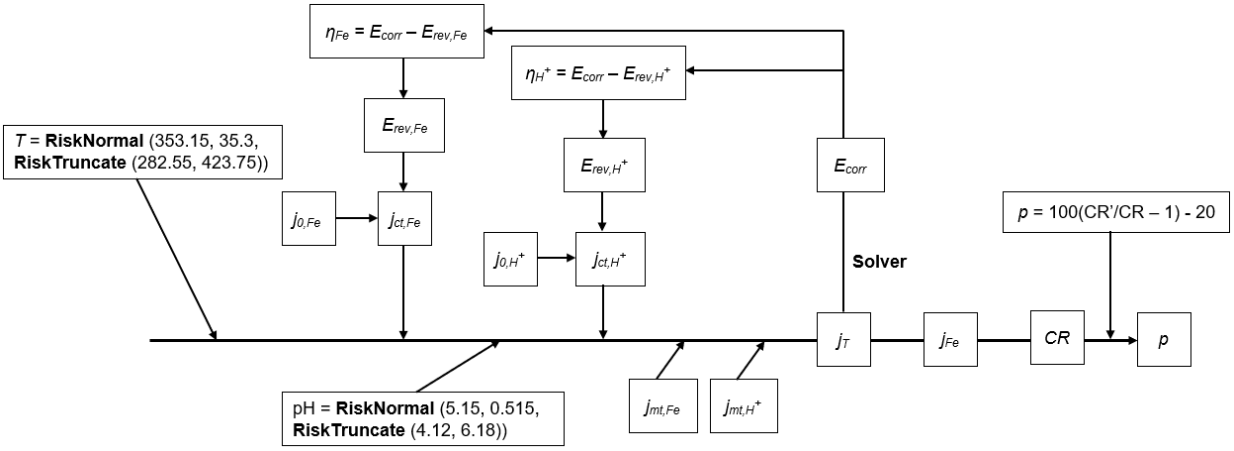

Fig. B-1: Fish bone diagram [6] for the steady-state, 1-step, novel *Fr 13* model for corrosion of ASTM A105 carbon-steel pipe (*see* discussion in Chapter 4, section 4.4.2)

[6] Also titled an Ishikawa diagram (after Kaoru Ishikawa, 1968).

APPENDIX C - Refereed publications from this research

1. Collins, S.D., Davey, K.R., 2018. A novel *Fr 13* risk assessment of corrosion of carbon-steel pipe in de-aerated water. Chemical Engineering Science – *submitted* CES-D-18-00449, Feb.

2. Collins, S.D., Davey, K.R., Chu, J.Y.G., O'Neill, B.K., 2016. A new quantitative risk assessment of Microbiologically Influenced Corrosion (MIC) of carbon steel pipes used in chemical engineering. In: CHEMECA 2016: Chemical Engineering - Regeneration, Recovery and Reinvention, Sept. 25-28, Adelaide, Australia, paper 3386601. ISBN: 9781922107831

CES-D-18-00449 - Feb

Chemical Engineering Science

A novel *Fr 13* risk assessment of corrosion of carbon-steel pipe in de-aerated water

Samuel D. Collins, Kenneth R. Davey
School of Chemical Engineering,
The University of Adelaide, Adelaide, SA 5005, Australia

To whom correspondence should be addressed:
K R (Ken) Davey
PhD FIChemE CEng CSci
School of Chemical Engineering
The University of Adelaide, SA 5005, Australia
Email: kenneth.davey@adelaide.edu.au

ABSTRACT

Microbiologically influenced corrosion (MIC) insidiously corrodes carbon-steel pipe and is a major problem globally. However, the impact of naturally occurring, random (stochastic) fluctuations in bulk temperature (T) and pH of the internal pipe-environment on MIC has not been addressed and therefore represents a potential risk. Here we synthesize a simplified probabilistic *Fr 13* risk assessment (Chem. Eng. Sci. 171 (2017) 1-18) and use it to investigate MIC of widely used ASTM A105 carbon-steel pipe with an abiotic (synthetic) environment containing sulphate, chloride and hydrogen sulphide. We demonstrate, based on independent experimental data, that despite a design safety margin (*tolerance*) of 20 %, unwanted corrosion of the inside wall of the pipe of > 0.45 mm yr^{-1} can occur every 61 days, averaged over the long term, due to the impact of natural fluctuations in the pipe-fluid T and pH on the free (equilibrium) corrosion potential (E_{corr}) of the system. This insight is not available from traditional risk approaches. The work also highlights the need for E_{corr} to be treated as a function of combined T and pH. We use this model in second-tier studies to explore intervention strategies and show that pH of the pipe-environment should be increased where practical to limit MIC, and any acidic corrosion. Results are contrasted with traditional deterministic simulations. Because the form of the simplified MIC model is generalizable it should permit developments to a more complex biotic environment, and different metals. Findings will be of immediate benefit and interest to a range of risk analysts, and in practical operations involving carbon-steel pipe flows.
[Word count = 259]

Keywords:
Steel-pipe corrosion; Microbiologically Influenced Corrosion (MIC); Microbial corrosion; ASTM A105 carbon-steel pipe; Probabilistic risk modelling; *Fr 13* risk modelling

HIGHLIGHTS

- Microbiologically Influenced Corrosion (MIC) of carbon pipes a global problem.
- Probabilistic *Fr 13* risk model applicable to simplified (abiotic) corrosion.
- Stochastic fluctuations in *T* and pH significantly impact internal pipe corrosion.
- Increasing pH of the pipe-fluid environment can be used to mitigate corrosion.
- Model is general and can be extended for biotic species and different metals.
- Results immediate benefit to risk analysts and pipe-fluid operations.

1. Introduction

Microbiologically influenced corrosion (MIC) is an insidious and unwanted degradation of metals, such as widely used ASTM A105 carbon-steel pipe (Roberge, 2000). It is caused by the presence of particular micro-organisms (Zhao, 2008; Javaherdashti, 2013) and occurs when these attach themselves to surfaces through physical adhesion, then release metabolic products that change the electrochemical conditions at the surface/fluid interface. These changes can lead to the initiation of corrosion (Moura et al., 2013).

MIC can be occur on above- and below-ground process equipment and in internal pipe-fluid environments (Jacobson, 2007) that transport water-based fluids such water-oil-chemical ‘cuts’. Typically, MIC occurs at low points in pipe internals where fluid flow is low. The particular micro-organisms of interest are sulphate-reducing bacteria (SRB), but also fungi, algae and protozoa (Pope et al., 1989; Zhao, 2008).

MIC impacts globally in off-shore and on-shore chemical engineering gas and oil industries, water treatment plants and, nuclear power plants with stainless and carbon-steel tanks and piping (Jack, 2002; Zhao, 2008). MIC accounts for some 20 % of overall corrosion (Flemming, 1996), and; is estimated to cost AUD$7 billion annually in Australia (Javaherdashti and Raman-Singh, 2001).

MIC poses a practical risk because it can initiate unexpectedly and, eventually it can cause sudden and unexpected failure of pipes. Current MIC risk mitigation strategies can be broadly classified as either physical or chemical (Roberge, 2000). Physical mitigation includes flushing or ‘pigging’ with a mechanical PIG (Pipeline Inspection Gadget) whilst chemical methods include the addition of both ionic (e.g. Tetrakis-HydroxymethylPhosphonium Sulphate (THPS)) and organic (e.g. glutaldehyde) biocides (Zhao, 2008; Moura, 2013). MIC risk can also be mitigated by careful selection of pipe materials (Javaherdashti, 2013), cathodic protection, or, protective coatings - although these later two are used mainly to mitigate external corrosion (Flemming, 2002). Additionally, the increasing of process flows (e.g. > 2 m s^{-1}) can sometimes be used to limit micro-organism growth (Roberge, 2000; Pots et al., 2002).

A clear understanding however of the role of bacteria in MIC has been slow to emerge. This is most likely because of the microscopic-scale involved and because the influences on corrosion mechanisms of the bacteria adhering to surfaces are not uniquely understood, and therefore difficult to model (Videla and Herrera,

2005). Model approaches include those of Maxwell and Campbell (2006), Smith et al. (2011), Xu et al. (2016), Javaherdashti (2017) and Skovhus et al. (2017). These underscore a complex interplay of parameters such as pipe-fluid pH, temperature (*T*), salinity, nutrient availability, flow against pipe surface(s), pigging frequency, and; biocide treatment(s) on micro-organism activity.

Major drawbacks with these models however include: 1) they are highly dependent on specific micro-organism–metal systems, and are therefore not generalizable; 2) model parameters can be complex and inter-dependent on processes not directly related to micro-organism activity, and, importantly; 3) they do not account for the impact of naturally occurring, random fluctuations in *T* and pH of the pipe-fluid environment.

Importantly, Davey and co-workers (e.g. Zou and Davey, 2016; Chandrakash and Davey, 2017) have demonstrated that these naturally occurring, random (stochastic) fluctuations in the value of process parameters can unexpectedly accumulate and impact significant change in process output behaviour - including failure in plant and product. To underscore the unexpected element, they titled their risk framework *Fr 13* (*Friday 13th*). Case studies of their probabilistic framework to 1-step operations include loss of thermal efficiency in a coal-fired boiler (Davey, 2015) and, failure to remove whey deposits in Clean-In-Place (CIP) milk processing (Davey et al., 2015). More recently, to advance their risk framework for progressively, multi-step and complex (in the sense of 'integrated', not 'complicated') processes they demonstrated its usefulness to 2-step membrane fouling with combined ultrafiltration-osmotic distillation (UF-OD) (Zou and Davey, 2016), and; a 3-step microbiological raw milk pasteurization (Chandrakash and Davey, 2017). Findings overall have revealed no methodological complications in application - and it was concluded the risk framework was generalizable.

A significant advantage of the *Fr 13* risk framework is that it can be used in 'second-tier' studies to reduce risk through simulations of intervention strategies and re-design of physical plant, or operating practices. It can be applied at both *synthesis* and *analysis* stages. As both the facts about the process and the effects of random fluctuations in input parameters are separated, it is claimed (Abdul-Halim and Davey, 2016) to be more mathematically correct than alternative probabilistic risk methods such as those of Aven and others (Aven, 2010; Milazzo and Aven, 2012) whose analyses restrict attention to only the most credible scenarios. The recent 'fuzzy logic' model of Javaherdashti (2017) is not conventional as it effectively dispenses with mathematics and therefore it is not based on established unit operations widely used in chemical engineering. Significantly, based on simulation of corrosion of carbon-steel the author concluded there is no difference (preference) 'in the corrosion behaviour of carbon-steel in both biotic and abiotic systems', and that, 'carbon-steel can be corroded with almost the same possibility being exposed to sulphate-reducing bacteria or synthetic sea water'. A general drawback with fuzzy logic models however is that they cannot be extrapolated reliably (de Reus, 1994). Importantly, the recent Blackett Review (Anon., 2012) highlighted that low-probability high-impact failures are an emerging concern to industry, and governments.

Although the *Fr 13* framework has been successfully applied to risk of pitting of externally exposed metal (AISI 316L) in off-shore oil and gas structures as impacted by naturally occurring fluctuations in sea temperature and salinity (< 20 m depth) (Davey et al., 2016; Lavigne and Davey, 2017), it was not known if the framework could provide new insight into microbiologically influenced corrosion of internal pipe metals. However, because modelling of direct MIC would be uniquely complex, it was planned that a general model for corrosion should be synthesized and understood that could be extended. Collins et al. (2016) developed a limited probabilistic *Fr 13* risk synthesis of corrosion based on the independent, abiotic experimental work of

Smith et al. (2011). They showed, for the first time, that some 28.1 % of all abiotic corrosion would be greater than an acceptable rate of pipe corrosion of 0.5 mm yr^{-1}, averaged over the long-term, due to the accumulated impact of random fluctuations in pipe-fluid *T* and pH.

A major drawback with this work, however, involved a simplified treatment of the free (equilibrium) corrosion potential (E_{corr}). This is the potential at which there is a balance in the transfer of charge (electrons) to create a current density of zero for the system. It was assumed, and not tested, that E_{corr} was constant (-0.616 V vs SCE) irrespective of the impact of fluctuations in the value of pipe-fluid *T* and pH. Further, the range of pipe-fluid *T* and pH used was not typical for practical oil flows in carbon-steel pipe operations. This therefore represents a potential risk.

1.1. Purpose of this study

Here we extend the underlying abiotic synthesis of Collins et al. (2016) to more realistically simulate risk of corrosion of widely used ASTM A105 carbon-steel pipe. This is done by treating the free corrosion potential, E_{corr}, as a function of pipe *T* and pH over a more practical range for flows in oil pipe-lines. The aim was to gain quantitative new insight that might demonstrate the applicability of the *Fr 13* framework to corrosion. A justification is that an enhanced risk understanding will lead to improved design and safety in pipe flow.

Results reveal a significant dependence of E_{corr} on combined *T* and pH of the pipe-fluid and are used to quantitatively evaluate intervention strategies that might be used to mitigate corrosion failures. We show that for a given ambient flow, corrosion could be decreased through increasing the pH of the pipe-fluid.

This new synthesis is simulated using spread-sheeting techniques with a convergence criterion to compute unique values of E_{corr} for combined impact of natural fluctuations in pipe-fluid *T* and pH. A comparison of results is made with the model of Collins et al. (2016).

All symbols used are carefully defined in the Nomenclature.

2. Materials and methods

The underlying independent experimental work of Smith et al. (2011) was carried out with a three-electrode cell in which a rotating disk was used as the working-electrode (WE) together with a sample of steel pipe that was embedded in the tip. A counter-electrode (CE), made from platinised titanium, was used as the electron sink/source, and a saturated calomel electrode (SCE) reference-electrode (RE) was used for measurement of potential. ‘Synthetic-water’ (Smith et al., 2011) containing sulphate, chloride and hydrogen sulphide, was used to simulate MIC, Fig. 1.

insert Fig. 1

It was assumed that the electrons formed by the oxidation of iron in the steel pipe were consumed by the reduction of protons in the following half-reactions

$$Fe \rightarrow Fe^{2+} + 2e^{-} \quad (1)$$

$$H^+ + e^- \rightarrow \tfrac{1}{2}H_2 \quad (2)$$

Because of the nature of electron transport, the transfer of charge (electrons) was assumed to occur only at the surface between the steel pipe (WE) and the synthetic-water, Fig. 2.

insert Fig. 2

The overall corrosion reaction was given by

$$Fe + 2H^+ \rightarrow Fe^{2+} + H_2 \quad (3)$$

2.1. *A novel corrosion model*

The established Butler-Volmer equation (Gu et al., 2009) can be used to predict current density for each of the electrical species due to charge transfer (Roberge, 2000), namely

$$j_{ct,Fe} = j_{0,Fe}\left(exp\left(\frac{\alpha_{a,Fe}\cdot n_{Fe}\cdot F}{R\cdot T}\cdot \eta_{Fe}\right) - exp\left(\frac{-\alpha_{c,Fe}\cdot n_{Fe}\cdot F}{R\cdot T}\cdot \eta_{Fe}\right)\right) \quad (4a)$$

$$j_{ct,H^+} = j_{0,H^+}\left(exp\left(\frac{\alpha_{a,H^+}\cdot n_{H^+}\cdot F}{R\cdot T}\cdot \eta_{H^+}\right) - exp\left(\frac{-\alpha_{c,H^+}\cdot n_{H^+}\cdot F}{R\cdot T}\cdot \eta_{H^+}\right)\right) \quad (4b)$$

Fe in Eq. (4a) denotes oxidation of iron, and H^+ in Eq. (4b), proton reduction.

The exchange current density is that at equilibrium, and for each species, respectively, is given by (Newman and Thomas-Alyea, 2004)

$$j_{0,Fe} = \frac{e_{0,Fe}}{A_E}\cdot\left(\frac{c_{s,Fe}}{c_{b,Fe}}\right)^{\gamma_{Fe}} \quad (5a)$$

$$j_{0,H^+} = \frac{e_{0,H^+}}{A_E}\cdot\left(\frac{c_{s,H^+}}{c_{b,H^+}}\right)^{\gamma_{H^+}} \quad (5b)$$

The reversible (equilibrium) potential is calculated using the Nernst equation (Roberge, 2000), where the activity of each species is represented by the surface concentration. This is a reasonable assumption for the pipe surface because: 1) the concentration profile for each species is formed from the surface out to the bulk of the solution, and; 2) the electrolyte solution is dilute. Therefore

$$E_{rev,Fe} = E^\circ_{Fe} + \frac{2.3\cdot R\cdot T}{n_{Fe}\cdot F}\cdot \log\left(c_{s,Fe}\right) \quad (6a)$$

$$E_{rev,H^+} = E^\circ_{H^+} + \frac{2.3\cdot R\cdot T}{n_{H^+}\cdot F}\cdot \log\left(c_{s,H^+}\right) \quad (6b)$$

When equilibrium is achieved between oxidation and reduction, a balance in the transfer of charge is created. The potential at which this happens is the free corrosion potential (E_{corr}). The overpotential (η) for each species then is

$$\eta_{Fe} = E_{corr} - E_{rev,Fe} \quad (7a)$$

$$\eta_{H^+} = E_{corr} - E_{rev,H^+} \tag{7b}$$

The corrosive mass transfer at the pipe surface is obtained from

$$\frac{j_{mt,Fe}}{n_{Fe} \cdot F} = -D_{Fe}\left(\frac{c_{b,Fe} - c_{s,Fe}}{\delta_{N,Fe}}\right) \tag{8a}$$

$$\frac{j_{mt,H^+}}{n_{H^+} \cdot F} = -D_{H^+}\left(\frac{c_{b,H^+} - c_{s,H^+}}{\delta_{N,H^+}}\right) \tag{8b}$$

Eqs. (8a) and (8b) can be rearranged to give

$$j_{mt,Fe} = (n_{Fe} \cdot F) \cdot \left(-D_{Fe}\left(\frac{c_{b,Fe} - c_{s,Fe}}{\delta_{N,Fe}}\right)\right) \tag{9a}$$

$$j_{mt,H^+} = (n_{H^+} \cdot F) \cdot \left(-D_{H^+}\left(\frac{c_{b,H^+} - c_{s,H^+}}{\delta_{N,H^+}}\right)\right) \tag{9b}$$

However, a drawback with Eqs. (9a) and (9b) resulting from adaption of the synthesis of Smith et al. (2011) is that there is no explicit term to predict that as temperature increases, D_{Fe} and D_{H^+} must increase, and therefore *CR* must increase also.

A mathematically convenient, and robust, way to deal with this necessary addition to the model is to use a temperature-correction suggested by Nesic et al. (1996) such that Eqs. (9a) and (9b) become, respectively:

$$j_{mt,Fe} = (n_{Fe} \cdot F) \cdot \left(-D_{Fe}\left(\frac{T}{T_{ref}}\right)\left(\frac{c_{b,Fe} - c_{s,Fe}}{\delta_{N,Fe}}\right)\right) \tag{9c}$$

$$j_{mt,H^+} = (n_{H^+} \cdot F) \cdot \left(-D_{H^+}\left(\frac{T}{T_{ref}}\right)\left(\frac{c_{b,H^+} - c_{s,H^+}}{\delta_{N,H^+}}\right)\right) \tag{9d}$$

where T_{ref} is the value of the SVA mean = 80 °C (353.15 K).

Because the number of electrons produced in oxidation of iron in the pipe is balanced by reduction of protons, the total current density (j_T) must be zero i.e.

$$j_T = j_{Fe} + j_{H^+} = \left(j_{ct,Fe} + j_{mt,Fe}\right) + \left(j_{ct,H^+} + j_{mt,H^+}\right) = 0 \tag{10}$$

The overall current density for iron oxidation can be computed by the addition of the current density for iron oxidation due to charge transfer, and the current density for iron oxidation due to mass transfer

$$j_{Fe} = j_{ct,Fe} + j_{mt,Fe} \tag{11}$$

This overall current density for iron oxidation was used by Collins et al. (2016) to determine a corrosion rate (*CR*) (Gu et al., 2009) based on molecular weight and density of the metal such that

$$CR = \frac{M_{Fe}}{2F \cdot \rho_{Fe}} \cdot j_{Fe} \tag{12}$$

Eq. (12) can be simplified for a wide range of temperature to

$$CR = 1.155 j_{Fe} \quad (13)$$

Eqs. (4a) through (13) define the model for corrosion of carbon-steel pipe.

To realistically solve this model for widely used ASTM A105 carbon-steel pipe however, E_{corr} must be treated as a multi-parameter function of pipe-fluid T and pH.

2.2. Solution

Solution of the MIC model with E_{corr} as a function of pipe-fluid T and pH is carried out as follows

1. Each of T (K) and pH is specified
2. $j_{0,Fe}$ and $j_{0,H+}$ (A m^{-2}) are obtained from, respectively, Eqs. (5a) and (5b) and substituted, respectively, into Eqs. (4a) and (4b)
3. $E_{rev,Fe}$ and $E_{rev,H+}$ (V vs SCE) are computed from, respectively, Eqs. (6a) and (6b) and substituted, respectively, into Eqs. (7a) and (7b)
4. η_{Fe} and η_{H+} (V vs SCE) are obtained from, respectively, Eqs. (7a) and (7b) and substituted respectively into, Eqs. (4a) and (4b)
5. $j_{mt,Fe}$ and $j_{mt,H+}$ (A m^{-2}) are computed from, respectively, Eqs. (9c) and (9d)
6. $j_{ct,Fe}$ and $j_{ct,H+}$ (A m^{-2}) are computed from, respectively, Eqs. (4a) and (4b) and are, together with $j_{mt,Fe}$ and $j_{mt,H+}$, substituted into Eq (10)
7. E_{corr} (V vs SCE) is computed by employing a convergence criterion on Eq. (10) such that $j_T = 0$
8. E_{corr} is substituted into Eq. (7a) to obtain η_{Fe}
9. η_{Fe} is substituted into Eq. (4a) to obtain $j_{ct,Fe}$
10. $j_{ct,Fe}$ is substituted into Eq. (11) to obtain j_{Fe}
11. j_{Fe} (A m^{-2}) is substituted into Eq. (13) to obtain CR (mm yr^{-1}).

The computations can be readily performed in Microsoft Excel™ with, for example, the *Solver* function used for step-7 such that a target cell is set to $j_T = 0$ - with an absolute value for practical convergence of 0.001 V vs SCE. Excel is convenient as it is widely available and is generally readily understood, thereby streamlining communication.

3. Traditional single value assessment (SVA) solution

A traditional chemical engineering, deterministic and single value assessment (SVA) (Sinnott, 2005; Davey, 2015) of the model is as follows: for example, for water at a temperature T = 353.15 K, pH = 5.15 (which is equivalent to $C_{b,H^+} = 10^{-pH} \times 10^3 = 10^{-5.15} \times 10^3 = 7.08 \times 10^{-3}$ mol m^{-3}, an initial 'guess' (Smith et al., 2011) of the values $C_{s,Fe} = 1 \times 10^{-4}$ mol m^{-3}, $C_{b,Fe} = 1 \times 10^{-6}$ mol m^{-3} and E_{corr} = -0.556 V vs SCE is made to give $j_{0,Fe}$ (Eq. (5a)), $j_{0,H+}$ (Eq. (5b)), $E_{rev,Fe}$ (Eq. (6a)), $E_{rev,H+}$ (Eq. (6b)), η_{Fe} (Eq. (7a)), η_{H+} (Eq. (7b)), $j_{mt,Fe}$

(Eq. (9c)), and; $j_{mt,H+}$ (Eq. (9d)). Values for $j_{0,Fe}$, $E_{rev,Fe}$, and η_{Fe} are used to give $j_{ct,Fe}$ (Eq. (4a)). Values for $j_{0,H+}$, $E_{rev,H+}$ and η_{H+} are substituted into $j_{ct,H+}$ (Eq. (4b)) and $j_{ct,Fe}$, $j_{ct,H+}$, $j_{mt,Fe}$ and $j_{mt,H+}$ substituted into Eq. (10).

The *Solver* loop converges to give E_{corr} = -0.54 V vs SCE, from Eq. (5a), $j_{0,Fe}$ = 3.57 x 10^{-5} A m^{-2}, from Eq. (5b), $j_{0,H+}$ = 4.63 x 10^{-8} A m^{-2}, from Eq. (6a), $E_{rev,Fe}$ = -0.89 V vs SCE, from Eq. (6b), $E_{rev,H+}$ = -0.66 V vs SCE , from Eq. (7a), η_{Fe} = 0.35 V vs SCE, and from Eq. (7b), η_{H+} = 0.12 V vs SCE. Substitution of values of $j_{0,Fe}$, $E_{rev,Fe}$, and η_{Fe} into Eq. (4a) is used to give $j_{ct,Fe}$ = 0.39 A m^{-2}, whilst substitution of values of $j_{0,H+}$, $E_{rev,H+}$, and η_{H+} into Eq. (4b) give $j_{ct,H+}$ = 5.18 x 10^{-7} A m^{-2}.

From Eq. (9a), $j_{mt,Fe}$ = -5.86 x 10^{-20} A m^{-2}, and from Eq. (9b), $j_{mt,H+}$ = -0.39 A m^{-2} is computed. From Eq. (11), addition of $j_{ct,Fe}$ and $j_{mt,Fe}$ is used to give j_{Fe} = 0.39 A m^{-2}.

The predicted iron corrosion rate is then CR = 0.45 mm yr^{-1} (Eq. (13)).

4. *Fr 13* risk model

4.1. Risk factor and failure

In contrast to the deterministic SVA solution, in the probabilistic *Fr 13* risk simulation of the corrosion model, a corrosion risk factor P is defined by an 'off-specification' or value greater than the value (e.g. Davey, 2015; Davey at al., 2016) of an acceptable corrosion rate such that

$$P = CR' - CR \tag{14}$$

where *CR'* is the instantaneous rate of corrosion (or mathematically more strictly, the *CR* obtained in a particular probabilistic simulation). However, a mathematically more convenient form (Abdul-Halim and Davey, 2016; Chandrakash and Davey, 2017) is

$$p = 100\left(\frac{CR'}{CR} - 1\right) \tag{15}$$

Eq. (15) is computationally convenient because it is dimensionless and because corrosion rates greater than an acceptable value can be readily identified by all values $p > 0$.

Generally, an engineering design specification includes some measure of tolerance i.e. a design margin of safety. The corrosion risk factor of Eq. (15) can therefore be written as

$$p = 100\left(\frac{CR'}{CR} - 1\right) - \%tolerance \tag{16}$$

The practical upshot of Eq. (16) is that for corrosion rates greater than an acceptable rate plus a tolerance, then $p > 0$ and corrosion is seen to be a 'failure'.

Eqs. (4a) through (13) plus (16) define the probabilistic *Fr 13* model for corrosion of the carbon-steel pipe with E_{corr} as a function of pipe-fluid T and pH.

4.2. Fr 13 *simulation*

In contrast to the traditional deterministic SVA, the probabilistic *Fr 13* risk simulation defines input parameters as distributions of values to mimic naturally occurring fluctuations, together with the probability of a particular value actually physically occurring. This means that the output behaviour will be a distribution of probabilities of particular outcomes. A refined Monte Carlo (r-MC) with *Latin Hypercube* sampling of the distributions ensures sampling covers the entire range of the distributions. ('Pure' MC cannot be relied on because it can over- and under-estimate from parts of the distribution (Vose, 2008)).

The probability distributions for the pipe-fluid parameters *T* and pH, in the absence of conditional data, for a large enough sample size are assumed normal and truncated, namely **RiskNormal** (mean, stdev, **RiskTruncate** (minimum, maximum)) (Vose, 2008). A standard deviation around the mean value in the distribution is assumed at stdev = 10 %, with the distributions truncated with a 2 x stdev about the mean to limit the minimum and maximum values of the system parameters to that that could occur practically i.e. **RiskNormal** (mean, stdev, **RiskTruncate** (minimum = mean – 2 x stdev, maximum = mean + 2 x stdev)). This means that nearly all r-MC samples (95.45 %) will fall within these intervals (Sullivan, 2004).

For example, for pipe-fluid temperature, *T* = **RiskNormal** (353.15, 35.3, **RiskTruncate** (282.55, 423.75)), which sets a mean = 353.15, stdev = 35.3, and minimum = 282.55 and maximum = 423.75, K. This is a practical way to say that in operation the temperature of the pipe-fluid does vary randomly but not outside this range. To recognize the natural variability in sensitivity to pH, it is assumed pH = **RiskNormal** (5.15, 0.515, **RiskTruncate** (4.12, 6.18)).

A schematic for the resulting *Fr 13* model of corrosion of ASTM A105 carbon-steel pipe is presented as Fig. 3. Importantly, the schematic highlights that input parameters used to mimic the naturally occurring fluctuations in the pipe environment in *T* and pH are distributions.

insert Fig. 3

To ensure that the output distribution of the mean is sufficiently normal, a minimum number of samples is needed (Vose, 2008) - this is usually some 1,000 to 50,000 (e.g. Zou and Davey, 2016; Chandrakash and Davey, 2017). This number can be determined when a plot of percentage of *Fr 13* failures versus number of simulations plateaus to a constant. (This can also be established by visual inspection of the output distribution).

Importantly, with a sufficient number of simulations it means that all possible practical combinations of scenarios that could occur with MIC will have been reproduced, including unwanted corrosion rates of the steel pipe as failures.

In the absence of hard i.e. unconditional data, and to demonstrate the model simulation, a *%tolerance* = 20 % was assumed.

The simulations were carried out using standard Microsoft Excel spread-sheeting with a commercially available add-on *@Risk* version 7.5 (Palisade Corporation™). Conveniently, the distributions defining the naturally occurring fluctuations in *T* and pH could be entered, viewed, copied, pasted and manipulated as Excel formulae (Chandrakash and Davey, 2017).

5. Results

Table 1 presents a comparative summary of results of the traditional deterministic SVA and the new probabilistic *Fr 13* simulation of corrosion of the carbon-steel pipe.

Ten thousand (10,000) r-MC samples were found sufficient.

insert Table 1

The traditional SVA is read down column 3 where CR = 0.45 mm yr^{-1} is shown. The *Fr 13* simulation is read down column 4 in which a normal distribution has been used for both T and pH, namely, T = **RiskNormal** (353.15, 35.3, **RiskTruncate** (282.55, 423.75)), and pH = **RiskNormal** (5.15, 0.515, **RiskTruncate** (4.12, 6.18)). For example, for the *Fr 13* simulation, a r-MC sample for the temperature of the pipe-fluid = 376.90 K is shown which, in combination with pH = 4.51, gives a resulting risk factor for CR, p = 319.14. As $p > 0$, this scenario shows a corrosion rate greater than an acceptable (SVA) rate plus a practical tolerance of 20 %. This T-pH range is more realistic than that used by Collins et al. (2016) for pipe flows in which oil is normally produced as the dominant and continuous phase together with some gas and water dispersed homogenously (Arnold and Stewart, 1999; J. Y. G. Chu, Operations Manager, Upstream Production Services Pty Ltd., Australia, *pers. comm*.).

It can be seen from Table 1 that the *Fr 13* risk model is identical to the SVA in that all mathematical operations that link parameters are the same. The significant difference, however, is that the key input parameters T and pH are defined by distributions of values, and not single values as with the traditional deterministic SVA.

Importantly, however, the data shown in column 4 of Table 1 are for one only scenario of the 10,000 – a limitation of using tabulated data. However, the results for the 10,000 scenarios can be readily presented as a summary output probability distribution (Chandrakash and Davey, 2017).

A total of 4,360 failures were exposed in the 10,000 scenarios i.e. 43.6 %. These are summarised as Fig. 4 in which the x-axis is the computed value of p from Eq. (16) and the y-axis is the probability of p actually occurring (Vose, 2008). From the figure, it can be seen that the output distribution is normal, and that the area under the curve (~333 x 0.003) = one (1). The 4,360 failure scenarios are seen in the R of the figure for all $p > 0$.

insert Fig. 4

A significant advantage of the *Fr 13* risk framework is that each and every scenario can be readily, separately identified, with the corresponding value of each contributing parameter identified (Zou and Davey, 2016; Chandrakash and Davey, 2017). To illustrate this, the contributing T and pH values that gave rise to unwanted CR in 10 selected failures in the 4,360 are presented in Table 2.

insert Table 2

For example, row 10, (**bolded text**) failure 8 of the table shows the combination of T = 376.90 K and pH = 4.51 resulted in CR = 2.08 mm yr^{-1} with corresponding corrosion rate risk factor p = 319.14; this is the

particular scenario highlighted in Table 1. A value of CR_{max} = 4.79 mm yr^{-1} was at T = 378.47 K and pH = 4.12 with a corresponding maximum value p_{max} = 949.78.

Importantly, it is not implied that the numerical values given in Tables 1 and 2 for T, pH and CR (and resulting p) need to be measured to these exactly - these values are reproduced exactly from those in the r-MC simulations.

6. Discussion

6.1. Fr 13 *simulations and free corrosion potential*

The *Fr 13* simulation of the novel corrosion model proved to be stable, and because the overall values of *CR* were similar to those reported by Collins et al. (2016) it was concluded that results were free of programming and computational errors.

Overriding however is that model predictions were significantly impacted by a value of the free corrosion potential, $E_{corr,}$ being dependent on combined fluctuations in pipe-fluid T and pH. For example, comparison with repeat simulations using the simplified model of Collins et al. (2016) with the realistic distributions T = **RiskNormal** (353.15, 35.3, **RiskTruncate** (282.55, 423.75)) and pH = **RiskNormal** (5.15, 0.515, **RiskTruncate** (4.12, 6.18)) showed, for a mid-range T = 353.15 K and pH = 5.15 with constant E_{corr} = -0.556 V vs SCE, gave nonsensical (less than zero) values of *CR*. These repeat simulations underscored therefore the importance of treating E_{corr} as a function of combined pipe-fluid T and pH.

It is concluded therefore that predictive models for corrosion of carbon-steel pipe must take into account a free corrosion potential that is dependent on fluctuations in combined pipe-fluid T and pH.

If each of the *CR* simulations of Tables 1 and 2 is assumed as one day, there would be an unwanted rate of corrosion of the ASTM A105 steel pipe of > 0.45 mm yr^{-1} due to MIC every (4,360/10,000 x 365.25 day/year ~) 160 days, averaged over the long term, because of natural fluctuations in pipe-fluid T and pH, despite a design safety margin (tolerance) of 20 %. There is however no reason to expect these predicted failures will be spaced equally in time.

It is acknowledged that the upper value used in the T distribution (423.75 K) might be considered high for SRB, since Pots et al. (2002) state that these bacteria normally function in the range 4 to 110, °C (277.15 to 383.15, K) and Maxwell and Campbell (2006), 0 to 80, °C (273.15 to 353.15, K). However the T range used is adequate for demonstration of the *Fr 13* risk model. (The range of values was based on the 2 x stdev in the assumed normal distribution to ensure 95.45 % of all r-MC samples fell within the distribution intervals).

It is evident that the range of T values could be readily delimited when more conditional data are available.

6.2. Mitigating pipe vulnerability to Fr 13 *failure*

To investigate possible MIC mitigation strategies, repeat simulations to quantify the impact of natural fluctuation in pH on *CR* at the minimum (282.55 K), mean (353.15 K), and maximum (423.75 K) pipe-fluid temperature were carried out. Results are presented as Fig. 5.

insert Fig. 5

From the figure, it can be seen that, as *T* increases *CR* increases. (A limitation experienced however in using the commercial *Solver* (Trial & Error) convergence was a software constraint at ~4.9 < pH < ~5.10 and low *T* = 282.55 K, ~5.4 < pH < ~5.5 and mean *T* = 353.15 K, and ~5.7 < pH < 5.8 for high *T* = 423.75 K, in predicting *CR* as it systematically returned an 'error'. The reason for this was not transparent - and may not result from model formulation, but the *Solver* 'internal' method). Overall these predictions are however reliable and are a logical conclusion from the model corrosion kinetics.

Another interesting insight from Fig. 5 is that, at a fixed value of *T*, a decrease in pH results in an increase in carbon-steel pipe corrosion as reflected in an increase in the value of *CR*. For example, at fixed mean-value of *T* = 353.15 K a decrease in pH from 5.15 to 4.5 results in an increase in carbon-steel pipe corrosion of ~1.55 mm yr^{-1} i.e. ~347 % increase. In the pH range 5.6 ⩽ pH ⩽ 6.2, the *CR* is seen not to be significantly impacted by pipe-fluid temperature (*T*).

It is concluded that the pH of the pipe-fluid is overriding compared with pipe-fluid *T* in impacting the corrosion rate.

This means that pipe vulnerability to *Fr 13* corrosion failure and any acidic corrosion in general could be minimised by increasing pH of the pipe-fluid. One way to practically do this could be by adding bases (e.g. potassium hydroxide, sodium hydroxide, sodium carbonate or potassium carbonate) (Kemmer, 1988). However, if the pipe-fluid pH is too high, anions can precipitate and form insoluble mineral scales that can lead to pipe fouling (Pichtel, 2016).

A practical value of tolerance of 20 % was included in the risk factor Eq. (16). This is a simple way of stating a level of safety in corrosion. However, this value should not be too large as it could result in plant operators believing that the carbon-steel pipes are less vulnerable to failure than they actually are. This could lead to steel pipe leaks or breaks, resulting in potential process or personnel loss.

To assess the impact of tolerance, the vulnerability of the ASTM A105 carbon-steel pipe to corrosion failure was investigated through repeat (second-tier) simulations over the range $0 \leq tolerance \leq 50$ %, maintaining a stdev = 10 % on parameters *T* and pH. These results are summarised in Fig. 6.

insert Fig. 6

It can be seen in Fig. 6 that as tolerance is increased, the percentage of failures in unwanted corrosion of the steel pipe decreases, almost linearly. For example, at a minimum possible *% tolerance* = 0 %, the number of unwanted corrosion failures of the steel pipe is predicted to be a maximum at 50 %. At % *tolerance* = 50 % the number of unwanted failures of the carbon-steel pipe approaches 36 %.

Practically, decreasing *% tolerance* or design safety to maintain a desired value of *CR* implies increasingly strict controls on pipe-fluid *T* and pH. A suitable practical value could be decided on from accumulated expert knowledge. It is concluded however that the impact can be readily tested in the *Fr 13* analysis of corrosion.

6.3. Probability distributions and defining corrosion failure

The choice of distribution for corrosion parameters T and pH is best based on expert knowledge or experimental data. It is important only that the input (and therefore, the output) distributions are carefully selected so that they cover all practically possible values.

In the absence of unconditional data, the distributions selected were truncated normal. There are some 40 probability distribution types that could have been selected for the *Fr 13* risk assessment, including **BetaSubjective** (Davey and Cerf, 2003), **Pert** (Davey et al., 2015) and **Triangle** (Chandrakash and Davey, 2017). For the *Fr 13* corrosion model, it might be possible that distributions could be 'tailored' for particular metal-bacterial systems or geographical locations (*see* Davey et al., 2016; Lavigne and Davey, 2017). Regardless, distributions need to be selected such that the model outcomes are those that could be observed in practice.

The 'tipping point' from non-failure to failure in the probabilistic *Fr 13* model for pipe corrosion has been defined as any rate greater than that predicted in the traditional deterministic SVA of $CR = 0.45$ mm yr^{-1} (Table 1). Alternatively, however, failure could be defined as an actual reduction (%) in wall thickness of a wetted steel pipe. This may prove more convenient for particular application(s) or geographical locations, especially where significant corrosion data is available, and which can be fitted to distributions (Vose, 2008). The risk model and definition of failure of the pipe can be readily adapted in the corrosion risk model.

Further, the model for steel pipe corrosion appears generalizable and therefore applicable to a range of more complex biotic environments and different metals.

6.4. Limitations and results overview

Notably, the results from this *Fr 13* corrosion risk assessment are new and, importantly, quantitative. A novel insight is that the corrosion rate of the carbon-steel pipe in abiotic water is significantly impacted by naturally occurring, random fluctuations in T and pH of the pipe-fluid. These fluctuations can lead to pipe corrosion failure.

Significantly, this insight cannot be obtained from traditional SVA simulations or risk and hazard analyses. This is because the element of naturally occurring randomness is not explicit in these traditional assessments. The *Fr 13* model output is therefore more practical. Advantageously, it can be used to simulate every possible scenario, including corrosion failures, and any particular scenario can be identified, isolated and studied. Importantly, second-tier studies using the framework can be used to predict the impact on corrosion and pipe failure from any re-design of the physical system.

A shortcoming of the model however is that there is presently no biotic component, that is, a specific bacterial species modelled. The model needs to be refined to incorporate the impact of particular bacterial kinetics (Maxwell and Campbell, 2006) and species involved in micro-organism growth (sulphates, chlorides and hydrogen sulphide) on pipe-fluid T and pH for a particular pipe metal (Roberge, 2000), although ASTM A105 carbon-steel pipe is widely used globally.

These limitations may not be so problematic however, as the example scenario in Javaherdashti (2017) showed that a biotic environment containing SRB would have the same impact on the corrosion of carbon-steel

as an abiotic one containing chlorides. This implies that the severity of carbon-steel corrosion in abiotic environments could be as great as in biotic environments. However, this statement should not be relied on in the absence of any controlled experimental work on biotic systems. Because the *Fr 13* risk model developed here is based on established unit-operations, and is generalizable, it is a natural 'starting point' from which to develop more complex biotic models.

It is concluded that the probabilistic corrosion model form when refined, could be used to quantitatively investigate the impact of proposed MIC intervention strategies in a range of micro-organism-metal systems.

7. Conclusions

The probabilistic *Fr 13* risk framework is amenable to simplified corrosion of widely used carbon-steel pipe ASTM A105.

Importantly, the pipe free corrosion potential E_{corr} a key corrosion parameter, must be viewed as a function of combined internal pipe-fluid temperature (T) and pH to realistically simulate off-shore oil processing operations. This is because it is significantly impacted by natural fluctuations in the pipe-fluid environment and cannot be considered a constant.

Based on independent experimental data, unwanted degradation of widely used ASTM A105 carbon-steel pipe of > 0.45 mm yr^{-1} is expected to occur every 160 days (43.6 % of all cases), averaged over the long term, due to naturally occurring fluctuations in pipe-fluid T and pH, despite a design safety margin (tolerance) of 20 %. This insight is not available from traditional deterministic risk approaches. Second-tier simulation studies highlight that vulnerability to corrosion failure of the carbon-steel pipe can be mitigated by increasing the pH of the pipe-fluid.

Because the model appears generalizable it could be applied to a range of biotic micro-organism-metal systems.

Findings will be of immediate benefit and interest to a range of risk analysts and design engineers involved in pipe metals selection and mitigating MIC in pipe flows.

Acknowledgements

The authors gratefully acknowledge the practical guidance from Dr J. Y. G. (James) Chu, FIChemE, Operations Manager, Upstream Production Services Pty Ltd., Australia, and; Dr Olivier Lavigne, Materials Scientist, Sandvik Hyperion, Sandvik Espanola, S.A., Spain, in preparing this paper.

Nomenclature

The number in parentheses refers to the equation in which the symbol is first used or defined.

A_E	electrode surface area (m^2) (5a)
CR	corrosion rate (mm yr^{-1}) (12)
$C_{b,Fe}$	concentration iron species in bulk electrolyte (= 1 x 10^{-6} mol m^{-3}) (5a)
$C_{b,H+}$	concentration proton species in bulk electrolyte (= 10^{-pH} x 1000 mol m^{-3}) (5b)
$C_{s,Fe}$	concentration of iron species at pipe surface (= 10^{-4} mol m^{-3}) (5a)
$C_{s,H+}$	concentration of proton species at pipe surface (= 10^{-6} mol m^{-3}) (5b)
D_{Fe}	diffusion coefficient of iron species (= 7.98 x 10^{-10} m^2 s^{-1}) (8a)
D_{H+}	diffusion coefficient or proton species (= 9.47 x 10^{-9} m^2 s^{-1}) (8b)
E	potential (V vs SCE) (6)
$e_{0,Fe}$	exchange current density transfer parameter for iron species (= 1 x 10^{-7} A) (5a)
$e_{0,H+}$	exchange current density transfer parameter for proton species (= 1 x 10^{-7} A) (5b)
E_{corr} (V vs SCE)	free (equilibrium) corrosion potential (V vs SCE) (7a)
$E_{rev,Fe}$ (V vs SCE)	reversible potential for iron species (V vs SCE) (6a)
$E_{rev,H+}$ (V vs SCE)	reversible potential for proton species (V vs SCE) (6b)
$E°_{Fe}$ (V vs SCE)	standard (equilibrium) potential for iron species (= -0.681 V vs SCE) (6a)
$E°_{H+}$ (V vs SCE)	standard (equilibrium) potential for proton species (= -0.241 V vs SCE) (6b)
F	Faraday constant (= 96,485 C mol^{-1}) (4a)
j	current density (A m^{-2}) (4a)
$j_{ct,Fe}$	current density due to charge transfer for iron species (A m^{-2}) (4a)
$j_{ct,H+}$	current density due to charge transfer for proton species (A m^{-2}) (4b)
$j_{mt,Fe}$	current density due to mass transfer for iron species (A m^{-2}) (8a)
$j_{mt,H+}$	current density due to mass transfer for proton species (A m^{-2}) (8b)
$j_{0,Fe}$	exchange current density for iron species (A m^{-2}) (4a)
$j_{0,H+}$	exchange current density for proton species (A m^{-2}) (4b)
M_{Fe}	molecular weight of iron (= 55.85 g mol^{-1}) (12)
n_{Fe}	number of electrons transferred in oxidation (iron) process (4a)
n_{H+}	number of electrons transferred in reduction (proton) process (4b)
p	corrosion rate risk factor (dimensionless) (15)
R	universal gas constant (= 8.314 J mol^{-1} K^{-1}) (4a)
T	temperature of pipe-fluid (K) (4a)
T_{ref}	reference temperature (= 353.15 K) (9c)

Greek Symbols

$\alpha_{a,Fe}$	anodic transfer symmetry function for iron species (= 0.4 dimensionless) (4a)
$\alpha_{a,H+}$	anodic transfer symmetry function for proton species (= 0.6 dimensionless) (4b)
$\alpha_{c,Fe}$	cathodic transfer symmetry function for iron species (= (1 - $\alpha_{a,Fe}$) = 0.6 dimensionless) (4a)
$\alpha_{c,H+}$	cathodic transfer symmetry function for proton species (= (1 - $\alpha_{a,H+}$) = 0.4 dimensionless) (4b)
$\delta_{N,Fe}$	Nernst diffusion layer thickness for iron species (= 7.23 x 10^{-6} m) (8a)
$\delta_{N,H+}$	Nernst diffusion layer thickness for proton species (= 1.67 x 10^{-5} m) (8b)
η_{Fe} (V vs SCE)	overpotential for iron species (V vs SCE) (4a)
η_{H+} (V vs SCE)	overpotential for proton species (V vs SCE) (4b)
ρ_{Fe}	density of iron (= 7,850 kg m^{-3}) (12)
γ_{Fe}	concentration sensitivity parameter for iron species (= 0.3 dimensionless) (5a)
γ_{H+}	concentration sensitivity parameter for proton species (= 0.75 dimensionless) (5b)

Subscripts

a	anodic symmetry function
c	cathodic symmetry function
T	total system parameter

Other

%tolerance	practical tolerance over design corrosion rate *CR* (%) (16)
CE	counter-electrode Fig. 1
RE	reference-electrode Fig. 1
SCE	saturated calomel electrode Fig. 1
WE	working-electrode Fig. 1

Superscript

‘	particular r-MC scenario (14)

References

Abdul-Halim, N., Davey, K.R., 2016. Impact of suspended solids on Fr 13 failure of UV irradiation for inactivation of *Escherichia coli* in potable water production with turbulent flow in an annular reactor. Chemical Engineering Science 143, 55-62. http://dx.doi.org/10.1016/j.ces.2015.12.017

Anon., 2012. Blackett Review of High Impact Low Probability Risks. Government Office for Science (UK). http://bis.gov.uk/assets/goscience/docs/b/12-519-blackett-review-high-impact-low-probability-risks.pdf (last accessed 12.50 pm, Dec. 7, 2017).

Arnold, K., Stewart, M., 1999. Surface Production Operations Volume 1: Design of Oil-Handling Systems and Facilities, second edition, Gulf Publishing Company, Houston, USA, pp. 101. ISBN: 0884158217

Aven, T., 2010. On how to define, understand and describe risk. Reliability Engineering and System Safety 95, 623-631. http://dx.doi.org/10.1016/j.ress.2010.01.011

Chandrakash, S., Davey, K.R., 2017. Advancing the *Fr 13* risk framework to an integrated three-step microbiological failure synthesis of pasteurization of raw milk containing *Mycobacterium avium* subsp. *Paratuberculosis* (*MAP*). Chemical Engineering Science 171, 1-18. http://dx.doi.org/10.1016/j.ces.2017.05.020

Collins, S.D., Davey, K.R., Chu, J.Y.G., O'Neill, B.K., 2016. A new quantitative risk assessment of Microbiologically Influenced Corrosion (MIC) of carbon steel pipes used in chemical engineering. In: CHEMECA 2016: Chemical Engineering – Regeneration, Recovery and Reinvention, Adelaide, Sept. 25 – 28, 2016, paper 3386601, pp. 209-217. ISBN: 9781922107831. http://search.informit.com.au/documentSummary;dn=405489164746545;res=IELENG

Davey, K.R., 2015. A novel *Friday 13th* risk assessment of fuel-to-steam efficiency of a coal-fired boiler. Chemical Engineering Science 127, 133-142. http://dx.doi.org/10.1016/j.ces.2015.01.031

Davey, K.R., Cerf, O., 2003. Risk modelling - An explanation of *Friday 13th Syndrome* (failure) in well-operated continuous sterilisation plant. In: Proc. 31st Australasian Chemical Engineering Conference (Product and Processes for the 21st Century), Adelaide, Sept. 28 – Oct. 1, 2003, paper 115, pp. 757-763. ISBN: 9780863968295

Davey, K.R., Chandrakash, S., O'Neill, B.K., 2015. A *Friday 13th* failure assessment of clean-in-place removal of whey protein deposits from metal surfaces with auto-set cleaning times. Chemical Engineering Science 126, 106-115. http://dx.doi.org/10.1016/j.ces.2014.12.013

Davey, K.R., Lavigne, O., Shah, P., 2016. Establishing an atlas of risk of pitting of metals at sea – demonstrated for stainless steel AISI 316L in the Bass Strait. Chemical Engineering Science 140, 71-75. http://dx.doi.org/10.1016/j.ces.2015.10.008

De Reus, N.M., 1994. Assessment of benefits and drawbacks of using fuzzy logic, especially in fire control systems. Report No. ADA285428, Fysisch En Elektronisch Lab TNO, The Hague, Netherlands.

Flemming, H.C., 1996. Economical and technical overview. In: Microbially Influenced Corrosion of Materials – Scientific and Technological Aspects, Heitz, E., Flemming, H.C., Sand, W. (Eds.), Springer-Verlag, Berlin, Germany. ISBN: 3540604324

Flemming, H.C., 2002. Biofouling in water systems – cases, causes and countermeasures. Applied Microbiology and Biotechnology 59, 629-640.

Gu, T., Zhao, K., Nesic, S., 2009. A new mechanistic model for MIC based on a biocatalytic cathodic sulfate reduction theory. In: Corrosion 2009, Atlanta, Mar. 22 - 26, 2009, paper 09390, pp. 1-12. ISSN: 03614409

Jack, T.R., 2002. Biological Corrosion Failures. In: ASM Handbook Volume 11: Failure Analysis and Prevention, Becker, W.T., Shipley, R.J. (Eds.), ASM International, Materials Park, USA, pp. 881-898. ISBN: 9780871707048

Jacobson, G.A., 2007. Corrosion at Prudhoe Bay: A lesson on the line. Materials Performance 46, 26-34.

Javaherdashti, R., 2013. Microbiologically Influenced Corrosion. In: Corrosion and Materials in the Oil and Gas Industries, Javaherdashti, R., Nwaoha C., Tan H. (Eds.), CRC Press, Boca Raton, USA, pp. 47-128. ISBN: 9781466556256

Javaherdashti, R., 2017. Microbiologically Influenced Corrosion – An Engineering Insight, second edition, Springer International Publishing, Cham, Switzerland, pp. 29-79. ISBN: 9783319443041

Javaherdashti, R., Raman-Singh, R.K., 2001. Microbiologically influenced corrosion of stainless steels in marine environments: A materials engineering approach. In: Proc. Engineering Materials, Melbourne, Sept. 23 – 26, 2001, pp. 299-304. ISBN: 186585118

Kemmer, F.N. (Ed.), 1988. The Nalco Water Handbook, McGraw-Hill, New York, USA, pp. 22.7. ISBN: 0070458723

Lavigne, O., Davey, K.R., 2017. Mitigating the impact of metal roughness on the risk of pitting of stainless steel alloy AISI 316L in the Gulf of Mexico. Chemical Engineering Science – *in preparation.*

Maxwell, S., Campbell, S., 2006. Monitoring the mitigation of MIC risk in pipelines. In: Corrosion 2006, San Diego, Mar. 12 - 16, 2006, paper 06662, pp. 1-16. ISSN: 03614409

Milazzo, M.F., Aven, T., 2012. An extended risk assessment approach for chemical plants applied to a study related to pipe ruptures. Reliability Engineering and System Safety 99, 183-192. http://dx.doi.org/10.1016/j.ress.2011.12.001

Moura, M. C., Pontual, E. V., Paiva, P. M. G., Coelho, L. C. B. B., 2013. An outline to corrosive bacteria. In: Microbial Pathogens and Strategies for Combating Them Volume 1: Science, Technology and Education. Méndez-Vilas, A., (Eds.), Formatex Research Center, Badajoz, Spain, pp. 11-22. ISBN: 9788493984397

Nesic, S., Postlethwaite, J., Olsen, S., 1996. An electrochemical model for prediction of corrosion of mild steel in aqueous carbon dioxide solutions. Corrosion 52, 280-294. ISSN: 00109312

Newman, J., Thomas-Alyea, K.E., 2004. Electrochemical Systems, third edition, John Wiley & Sons, Inc., Hoboken, USA, pp. 214-216. ISBN: 9780471477563

Pichtel, J., 2016. Oil and gas production wastewater: Soil contamination and pollution prevention. Applied and Environmental Soil Science 2016, 1-25. http://dx.doi.org/10.1155/2016/2707989

Pope, D.H., Duquette, D., Wayner, P.C., Jr., Arland, H.J., 1989. Microbiologically Influenced Corrosion: A State-of-the-Art Review, second edition, Materials Technology Institute of the Chemical Process Industries, St. Louis, USA, pp. 1-76. ISBN: 1877914096

Pots, B.F.M., John, R.C., Rippon, I.J., Thomas, M.J.J.S., Kapusta, S.D., Girgis, M.M., Whitman, T., 2002. Improvements on DeWaard-Milliams corrosion prediction and applications to corrosion management. In: Corrosion 2002, Denver, Apr. 7 – 11, 2002, paper 02235, pp. 1-19. ISSN: 03614409

Roberge, P.R., 2000. Handbook of Corrosion Engineering, McGraw-Hill, New York, USA, pp. 35-54, 187-220, 335-336, 1047-1059. ISBN: 0070765162

Sinnott, R.K., 2005. Chemical Engineering Design, fourth edition, Butterworth-Heinemann, UK, pp. 756–764. ISBN: 9780080492551

Skovhus, T.L., Andersen, E.S., Hillier, E., 2017. Management of microbiologically influenced corrosion in Risk-Based Inspection analysis. In: The Society of Petroleum Engineers International Oilfield Corrosion Conference and Exhibition, May 9-10, Aberdeen, Scotland, paper 179930. ISSN: 19301855

Smith, P., Roy, S., Swailes, D., Maxwell, S., Page, D., Lawson, J., 2011. A model for the corrosion of steel subjected to synthetic produced water containing sulfate, chloride and hydrogen sulphide. Chemical Engineering Science 66, 5775-5790. http://dx.doi.org/10.1016/j.ces.2011.07.033

Sullivan, M., 2004. Statistics – Informed Decision Making Using Data, Pearson Education, New Jersey, USA. ISBN: 0130618640

Videla, H.A., Herrera, L.K., 2005. Microbiologically influenced corrosion: looking to the future. International Microbiology 8, 169-180. ISBN: 1851666265

Vose, D., 2008. Risk Analysis - A Quantitative Guide, third edition, John Wiley & Sons, Chichester, UK, pp. 43, 45-47. ISBN: 0470512849

Xu, D., Li, Y., Gu, T., 2016. Mechanistic modeling of biocorrosion caused by biofilms of sulfate reducing bacteria and acid producing bacteria. Bioelectrochemistry 110, 52-58. http://dx.doi.org/10.1016/j.bioelechem.2016.03.003

Zhao, K., 2008. Investigation of microbiologically influenced corrosion (MIC) and biocide treatment in anaerobic salt water and development of a mechanistic MIC model. PhD thesis, The Russ College of Engineering and Technology of Ohio University, USA.

Zou, W., Davey, K.R., 2016. An integrated two-step *Fr 13* synthesis - demonstrated with membrane fouling in combined ultrafiltration-osmotic distillation (UF-OD) for concentrated juice. Chemical Engineering Science 152, 213-226. http://dx.doi.org/10.1016/j.ces.2016.06.020

Table 1

Comparative summary of the deterministic SVA with the new probabilistic *Fr 13* simulations for corrosion of carbon-steel pipe with a tolerance of 20 %. Column 3 is the SVA value. Column 4 is for one only of 10,000 simulated *Fr 13* scenarios. *CR* failure is defined for all $p > 0$.

Row	Parameter	SVA[a]	*Fr 13 model*[b]	
1	**Inputs**			
2	T (K)	353.15	376.90[c]	**RiskNormal**(353.15,35.3, **RiskTruncate**(282.55,423.75))
3	*pH*	5.15	4.51[c]	**RiskNormal**(5.15,0.515, **RiskTruncate**(4.12,6.18))
4	**Constants**			
5	$\alpha_{a,Fe}$ (dimensionless)	0.4	0.4	constant
6	$\alpha_{c,Fe}$ (dimensionless)	0.6	0.6	constant
7	$\alpha_{a,H+}$ (dimensionless)	0.6	0.6	constant
8	$\alpha_{c,H+}$ (dimensionless)	0.4	0.4	constant
9	n_{Fe} (dimensionless)	2	2	constant
10	n_{H+} (dimensionless)	1	1	constant
11	$e_{0,Fe}$ (A)	1.00E-07	1.00E-07	constant
12	$e_{0,H+}$ (A)	1.00E-07	1.00E-07	constant
13	A_E (m^2)	2.80E-03	2.80E-03	constant
14	γ_{Fe} (dimensionless)	0.3	0.3	constant
15	γ_{H+} (dimensionless)	0.75	0.75	constant
16	$E°_{Fe}$ (V vs SCE)	-0.681	-0.681	constant
17	$E°_{H+}$ (V vs SCE)	-0.241	-0.241	constant
18	$C_{s,Fe}$ (mol m^{-3})	9.99E-07	9.99E-07	constant/Solver
19	$C_{s,H+}$ (mol m^{-3})	1.00E-06	5.19E-03	constant
20	$C_{b,Fe}$ (mol m^{-3})	1.00E-06	1.00E-06	constant
21	D_{Fe} (m^2 s^{-1})	7.98E-10	7.98E-10	constant
22	D_{H+} (m^2 s^{-1})	9.47E-09	9.47E-09	constant
23	T_{ref} (K)	353.15	353.15	constant
24	$\delta_{N,Fe}$ (m)	7.23E-06	7.23E-06	constant
25	$\delta_{N,H+}$ (m)	1.67E-05	1.67E-05	constant
26	F (C mol^{-1})	96485	96485	constant
27	R (J mol^{-1} K^{-1})	8.314	8.314	constant
28	*%tolerance* (%)	-	20	
29	**Calculations**			
30	$C_{b,H+}$ (mol m^{-3})	7.08E-03	0.03	Conversion from pH
31	$j_{0,Fe}$ (A m^{-2})	3.57E-05	3.57E-05	Eq. (5a)
32	$j_{0,H+}$ (A m^{-2})	4.63E-08	1.53E-08	Eq. (5b)

33	$E_{rev,Fe}$ (V vs SCE)	-0.89	-0.91	Eq. (6a)
34	$E_{rev,H+}$ (V vs SCE)	-0.66	-0.69	Eq. (6b)
35	η_{Fe} (V vs SCE)	-5.86E-20	-6.26E-20	Eq. (7a)
36	η_{H+} (V vs SCE)	-0.39	-1.80	Eq. (7b)
37	$j_{mt,Fe}$ (A m^{-2})	0.39	1.80	Eq. (9c)
38	$j_{mt,H+}$ (A m^{-2})	5.18E-07	9.55E-07	Eq. (9d)
39	$j_{ct,Fe}$ (A m^{-2})	0.35	0.44	Eq. (4a)
40	$j_{ct,H+}$ (A m^{-2})	0.12	0.22	Eq. (4b)
41	E_{corr} (V vs SCE)	-0.54	-0.47	***Solver***
42	j_{Fe} (A m^{-2})	0.39	1.80	Eq. (10)
43	j_{H+} (A m^{-2})	-0.39	-1.80	Eq. (10)
44	j_T (A m^{-2})	-6.88E-07 (≈ 0)	6.73E-07 (≈ 0)	Eq. (10)
45	**Output**			
46	*CR* (mm yr^{-1})	0.45	2.08	Eq. (13)
47	*p*	-	319.14	Eq. (16)

[a] Traditional deterministic single point, or, single value assessment.

[b] One only of 10,000 scenarios.

[c] Values are reproduced from the r-MC sampling; it is not implied they are measured to this significance.

Table 2

Ten (10) selected *Fr 13* failures in the 10,000 scenarios with 20 % tolerance.

Failure	***T*** [b] **(K)**	**pH** [b] **(dimensionless)**	***CR'*** **(mm yr^{-1})**	***p*** **(dimensionless)**
1	312.24	5.07	0.54	0.02
2	352.35	5.02	0.61	16.16
3	418.96	4.96	0.69	35.06
4	324.35	4.90	0.79	57.57
5	319.51	4.84	0.92	84.96
6	326.87	4.70	1.27	164.20
7	325.55	4.61	1.55	225.96
8[a]	**376.90**	**4.51**	**2.08**	**319.14**
9	367.15	4.37	2.71	485.70
10	378.47	4.12	4.79	949.78

[a] Particular scenario of Table 1.

[b] Values are reproduced from the r-MC sampling; it is not implied they are measured to this significance.

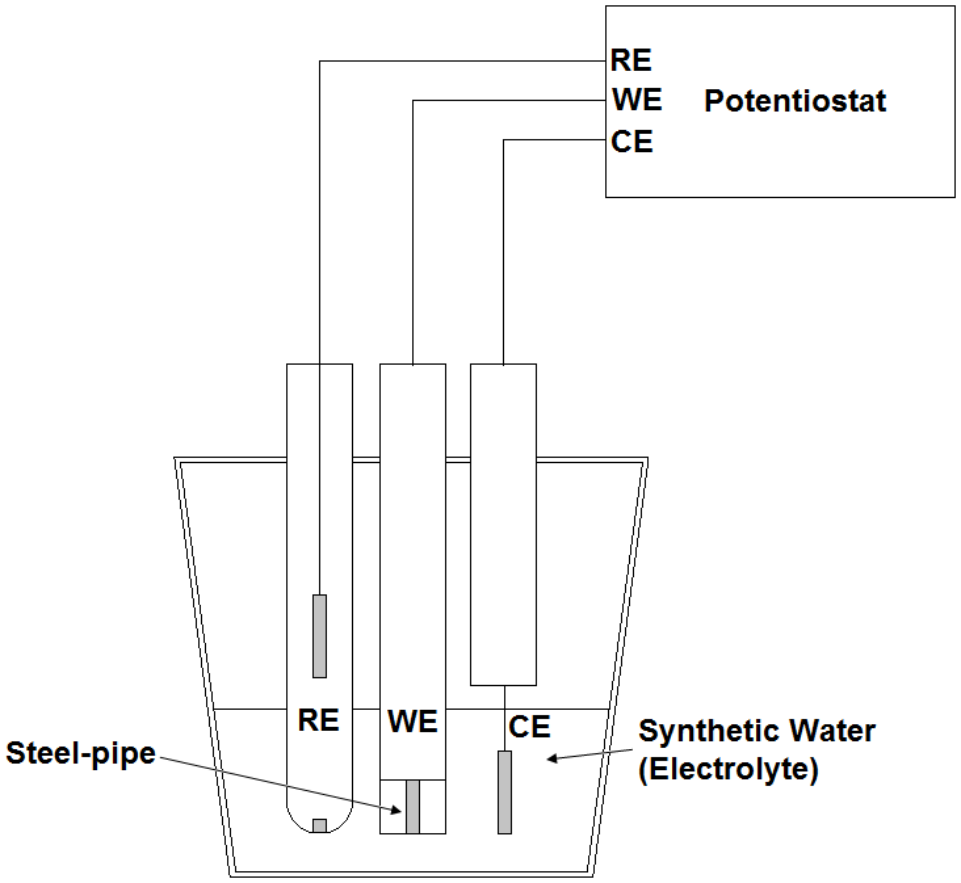

Fig. 1. Schematic of experimental three-electrode corrosion cells and potentiostat with synthetic-water containing sulphate, chloride and hydrogen sulphide to mimic MIC (adapted from Smith et al., 2011).

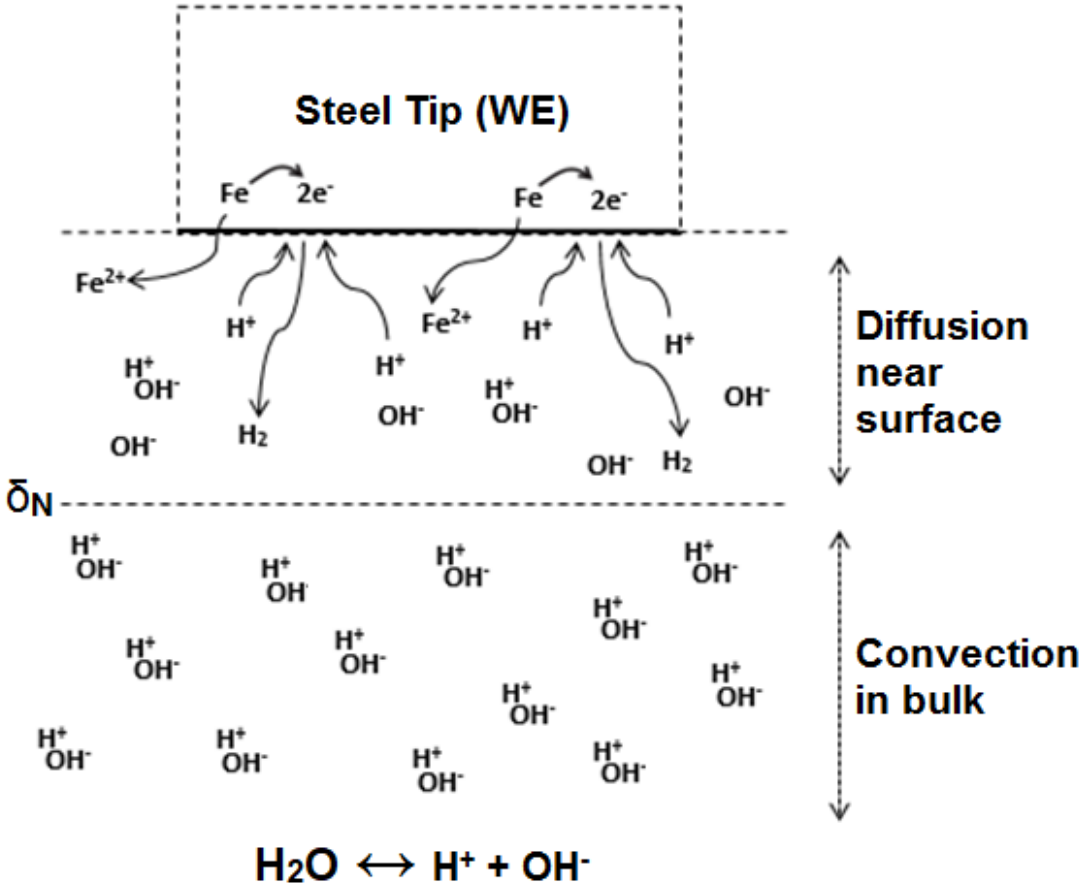

Fig. 2. Corrosion of surface interactions of steel pipe with deaerated, low conductivity synthetic-water containing sulphate, chloride and hydrogen sulphide (adapted from Smith et al., 2011).

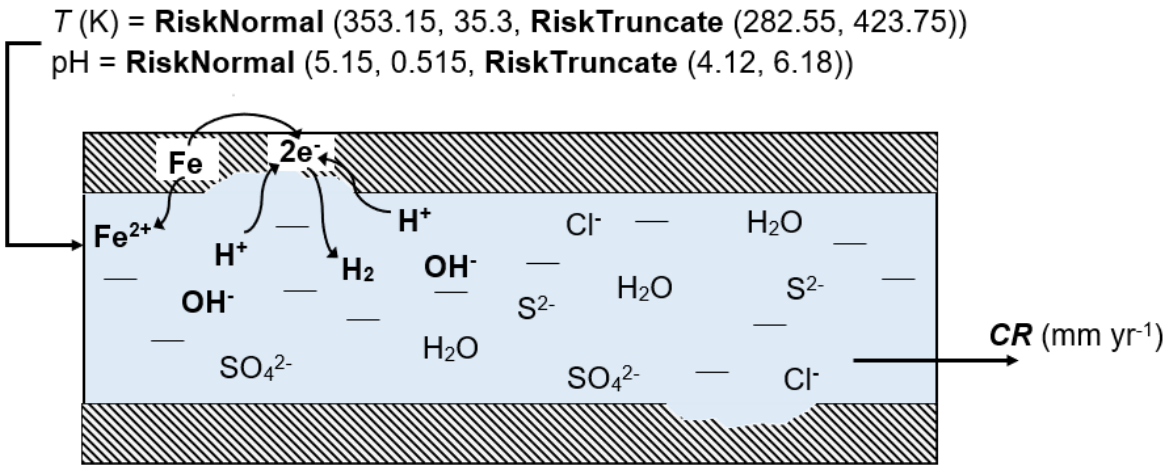

Fig. 3. *Fr 13* corrosion model of carbon-steel pipe.

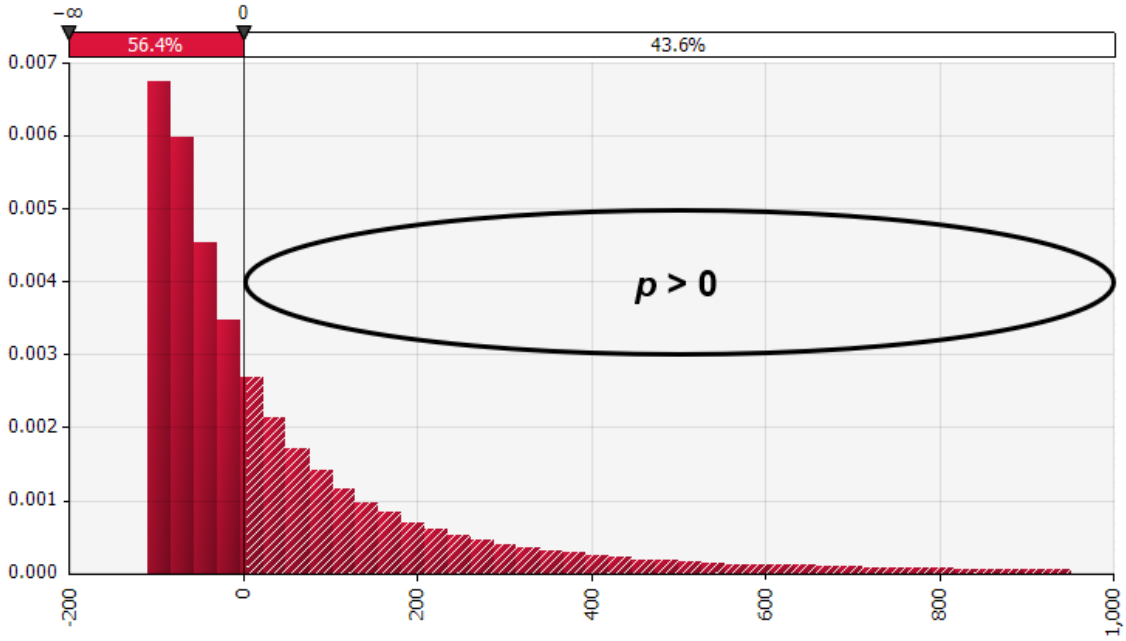

Fig. 4. *Fr 13* simulation of the corrosion rate risk factor, *p*, for MIC with 10,000 scenarios and 20 % tolerance. The *x*-axis is the value of risk factor and the *y*-axis the probability of that value. To the R of the figure is shown the 43.6 % failure scenarios with unwanted corrosion > 0.45 mm yr^{-1} with $p > 0$.

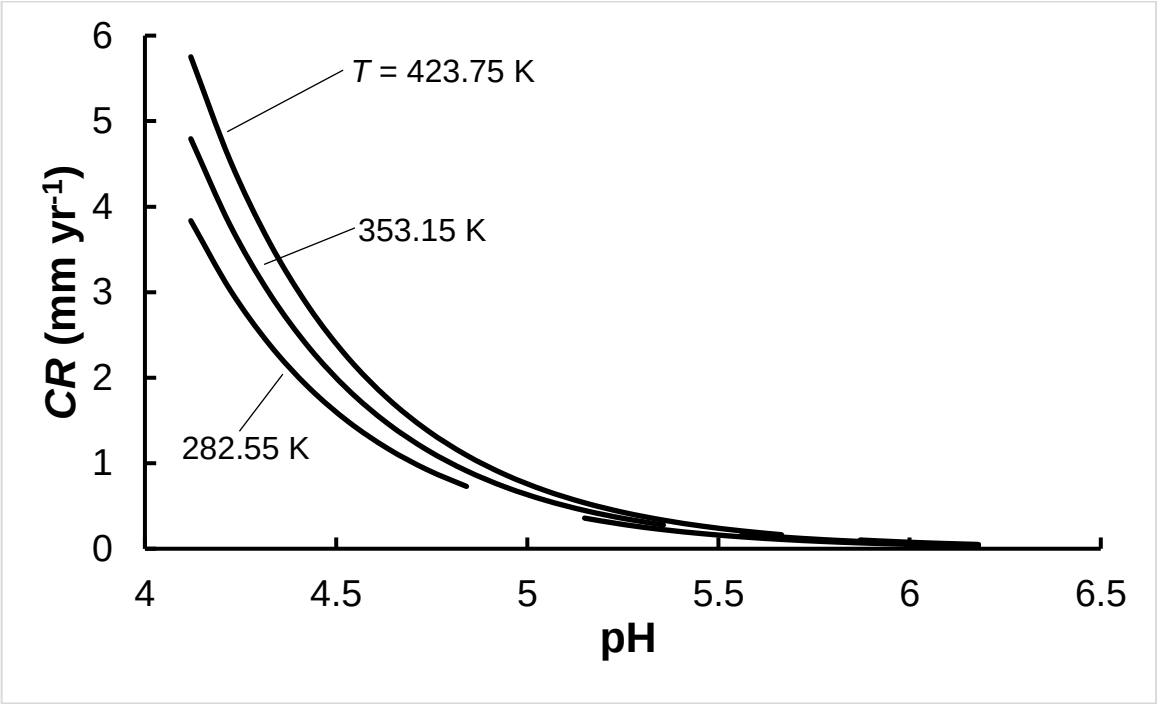

Fig. 5. Pipe-fluid pH vs corrosion rate (*CR*) for minimum, mean, and maximum values of the *Fr 13* temperature distribution.

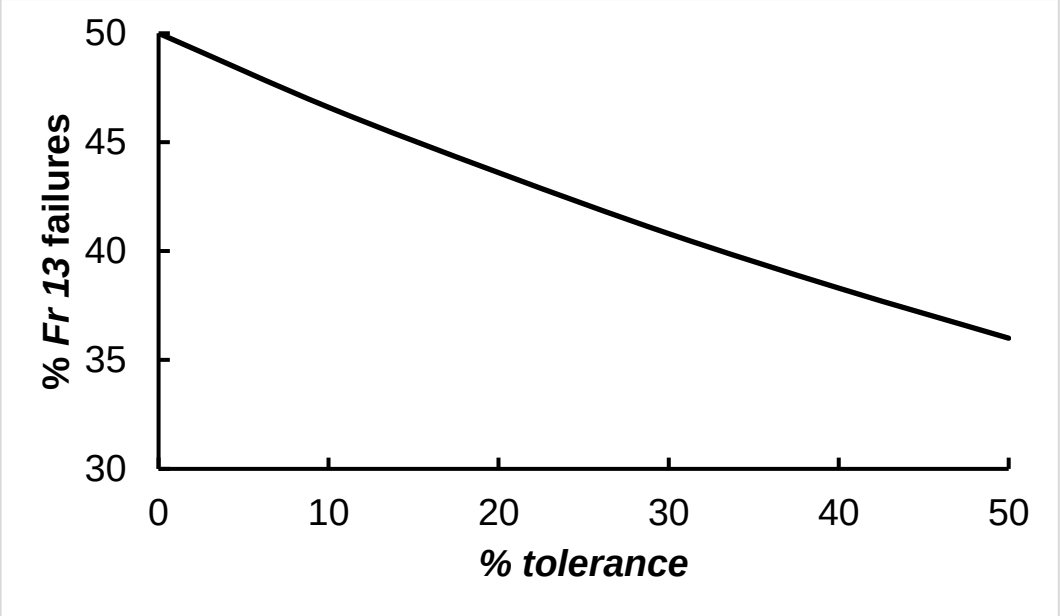

Fig. 6. Impact of % *tolerance* on corrosion rate (*CR*) against percentage of *Fr 13* failures per 10,000 scenarios.

chemeca CONFERENCE
25 – 28 September 2016
Adelaide Convention Centre
Adelaide, Australia

Paper no. 3386601

Chemeca 2016
25 – 28 September 2016, Adelaide, Australia

A new quantitative risk assessment of Microbiologically Influenced Corrosion (MIC) of carbon steel pipes used in chemical engineering

Samuel D Collins, Kenneth R Davey*, James Y G Chu and Brian K O'Neill

School of Chemical Engineering, Faculty of Engineering, Computer and Mathematical Sciences, The University of Adelaide, SA 5005, Australia

*Corresponding author. Email: kenneth.davey@adelaide.edu.au

Abstract: Microbiologically Influenced Corrosion (MIC) is corrosion initiated by microbial activity that can lead to failure of metals used in chemical engineering plants. Predictive models developed in recent decades however have major drawbacks in that they are highly dependent on specific microorganism–metal systems, and therefore are not generalizable, and importantly do not address the impact of naturally occurring random fluctuations in the environment on corrosion. Here we demonstrate a simplified, new MIC unit-operations model based on electrochemical/microbiological principles to predict the corrosion rate of carbon steel pipelines. We quantitatively investigate for the first time the risks that naturally occurring random fluctuations in environmental parameters have on MIC initiation and propagation. We use the new model to investigate the potential for MIC mitigation strategies. Results and findings will be of wide interest and immediate benefit to a range of industries involved in metals selection and in mitigating MIC in flow of fluid through process equipment.

Keywords: carbon-steel pipe corrosion; Fr 13; Fr 13 risk modelling; microbial corrosion; Microbiologically Influenced Corrosion (MIC); rate of corrosion of pipe.

1 Introduction

Microbiologically influenced corrosion (MIC) is the insidious and unwanted metal pitting and deterioration caused by the metabolic activity of micro-organisms in wide-spread steady-state batch-continuous and continuous processes (Jacobson, 2007). MIC can lead to unexpected (surprise) failure in chemical engineering unit-operations and processing plants.

Many industries globally are impacted by MIC, including offshore and onshore chemical engineering gas and oil industries, particularly in the Bass Strait (Exxon Mobil Australia, 2015; Davey and Lavigne, 2016); water treatment plant, including piping and heat exchangers, and; nuclear power plants with stainless and carbon steel tanks and piping, and aluminium and bronze cooling tubes (Jack, 2002).

MIC can be controlled through two (2) key approaches, broadly classified as either *physical* or *chemical*. Physical methods include cleaning, such as flushing or backwashing, and UV radiation (Abdul-Halim and Davey, 2015). Chemical methods include cleaning with biocides and 'pigging' (Flemming, 2002). Protection can also be built into a system by selecting materials that do not support microbial growth, or the use of cathodic protection, or, protective coatings. Operating conditions can sometimes be modified to limit micro-organism growth (Roberge, 2000).

Because of the microscopic nature of MIC, development of a clear understanding of the role of the micro-organisms has been slow to emerge (Videla and Herrera, 2005). A number of models have been developed in recent decades to simulate MIC in industrial settings (De Waard et al., 1991; Pots et al., 2002; Maxwell and Campbell, 2006; Gu et al., 2009). A major drawback however is that these are highly dependent on specific micro-organism–metal systems and are therefore not generalizable. Another is that they fail to account for the impact of naturally occurring random fluctuations in fluid temperature and pH.

However Davey and co-workers (e.g. Abdul-Halim and Davey, 2015; Chandrakash et al., 2015; Davey, 2015; Davey et al., 2015; Davey et al., 2013; Davey, 2011; Davey and Cerf, 2003) have developed a new risk

framework to address the impact of these naturally occurring random fluctuations, and quantitatively assess how they can accumulate and cause failure within-system.

1.1 This research

Here we synthesize a new simplified and generalized but justifiable, MIC unit-operations model based on the experimental work of Smith et al. (2011) to predict the corrosion rate of carbon steel pipe in industrial settings. We solve this using the probabilistic Friday 13th (*Fr 13*) risk framework of Davey and co-workers for the first time. A comparison is then made with more traditional chemical engineering solutions.

The aim is to gain quantitative, new insights into MIC, and to investigate preventative intervention strategies. It is hoped that findings can be generalized to a range of micro-organism–metal systems.

Outcomes will be of immediate interest to risk analysts, and corrosion and design engineers.

2 Material and methods

2.1 A simplified unit-operations MIC model

Consider a three-electrode cell and potentiostat arrangement (Smith et al., 2011), Figure 1.

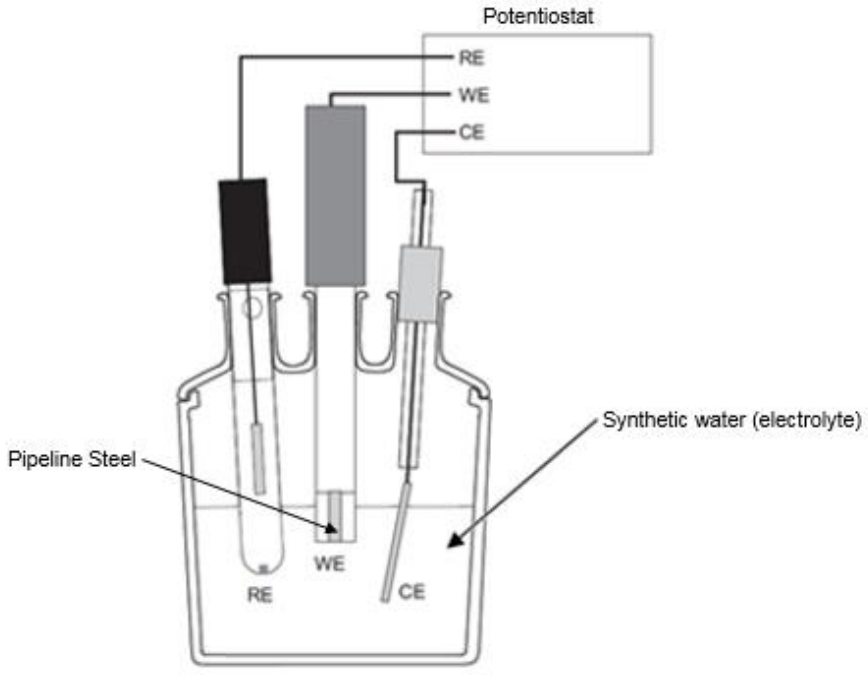

Figure 1: Schematic of experimental three-electrode corrosion cells and potentiostat with synthetic water (electrolyte) to mimic MIC bacterial activity (Adapted from Smith et al., 2011).

A rotating disk electrode is used as the working electrode (WE) with the tip containing a sample of pipeline steel. A counter electrode (CE), made from platinised titanium, is used as the electron sink/source, and a saturated calomel electrode (SCE) reference electrode (RE) is used for potential measurement. Synthetic water (containing sulphate, chloride and hydrogen sulphide) is used in which micro-organism growth and MIC is simulated.

2.2 Charge Transfer

If it is assumed that the electrons formed by the oxidation of iron in the steel are consumed by the reduction of protons then we can write

$$Fe \rightarrow Fe^{2+} + 2e^{-} \qquad (1)$$

$$H^{+} + e^{-} \rightarrow \tfrac{1}{2}H_2 \qquad (2)$$

The transfer of charge (electrons) occurs only at the surface between the steel (WE) and the synthetic water because of the nature of electron transport; this is shown schematically, Figure 2.

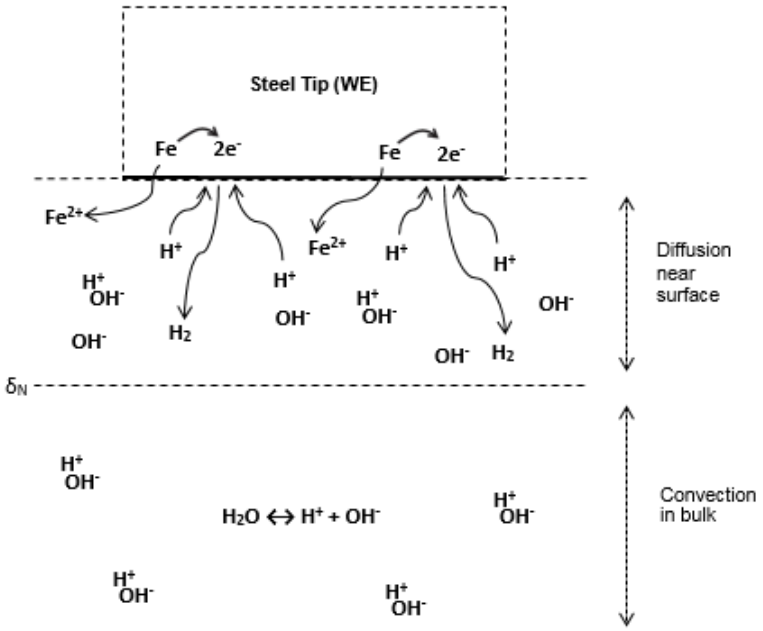

Figure 2: Schematic of surface interactions of pipe steel with deaerated, low conductivity water (Adapted from Smith et al., 2011)

The overall corrosion reaction is given by

$$Fe + 2H^+ \rightarrow Fe^{2+} + H_2 \tag{3}$$

The charge transfer at the steel surface can be described by the Butler-Volmer equation (Gu et al., 2009) for current density due to oxidation of iron (anodic process)

$$j_{ct,H^+} = j_{0,H^+}\left(exp\left(\frac{\alpha_{a,H^+}\cdot n_{H^+}\cdot F}{R\cdot T}\cdot \eta_{H^+}\right) - exp\left(\frac{-\alpha_{c,H^+}\cdot n_{H^+}\cdot F}{R\cdot T}\cdot \eta_{H^+}\right)\right) \tag{4}$$

where the exchange current density (Nesic et al., 1996) is

$$j_{0,H^+} = j_{0,H^+}^{ref}\exp\left(-\Delta H_{H^+}/_R\left(1/_T - 1/_{T_R}\right)\right) \tag{5}$$

All symbols used are carefully defined in the Nomenclature.
The overpotential is given by

$$\eta_{H^+} = E_{corr} - E_{rev,H^+} \tag{6}$$

The reversible potential is calculated using the Nernst equation (Roberge, 2000)

$$E_{rev,H^+} = E^{\circ}{}_{H^+} + \frac{2.3\cdot R\cdot T}{n_{H^+}\cdot F}\cdot \log\left(c_{s,H^+}\right) \tag{7}$$

2.2 Mass Transfer

The mass transfer at the steel surface is described by a flux balance arising from the dependency on diffusion and charge consumption

$$\frac{j_{mt,H^+}}{n_{H^+}\cdot F} = -D_{H^+}\left(\frac{c_{b,H^+} - c_{s,H^+}}{\delta_{N,H^+}}\right) \tag{8}$$

which can be rearranged to isolate the current density due to mass transfer to give

$$j_{mt,H^+} = (n_{H^+}\cdot F)\cdot\left(-D_{H^+}\left(\frac{c_{b,H^+} - c_{s,H^+}}{\delta_{N,H^+}}\right)\right) \tag{9}$$

Because the number of electrons produced in the oxidation of iron is balanced by the reduction of protons (seen in (3), the total current in the system i.e. the sum of the current due to oxidation and reduction, must be zero, namely

$$j_T = j_{Fe} + \left(j_{ct,H^+} + j_{mt,H^+}\right) = j_{Fe} + j_{H^+} = 0 \tag{10}$$

(10) can be rearranged to give

$$j_{Fe} = -j_{H^+} \tag{11}$$

The current density due to iron oxidation can be converted to corrosion rate using molecular weight and density (Gu et al., 2009) to yield

$$CR = \frac{M_{Fe}}{2F \cdot \rho_{Fe}} \cdot j_{Fe} \tag{12}$$

which can be simplified to

$$CR = 1.155 j_{Fe} \tag{13}$$

(1) through (13) define the simplified unit-operations model for MIC of pipe steel.

3 Deterministic single value assessment (SVA)

A traditional chemical engineering, deterministic and single value assessment (SVA) (Sinnott, 2005; Davey, 2015) of the unit-operations model for corrosion is carried out as follows: for water at a temperature T = 293.15 K, pH = 5.15, $C_{b,H+}$ = 7.08 x 10^{-3} mol m^{-3} and with assumed E_{corr} = -0.616 V vs. SCE, from (5) $j_{0,H+}$ = 0.050 A m^{-2}, from (7) $E_{rev,H+}$ = -0.590 V vs. SCE and from (6), η_{H+} = -0.0264 V vs. SCE. Substitution of these values into (4) gives $j_{ct,H+}$ = -0.0493 A m^{-2}.

From (9), $j_{mt,H+}$ = -0.387 A m^{-2}. From (10), addition of $j_{ct,H+}$ and $j_{mt,H+}$ gives j_{H+} = -0.437 A m^{-2}. Therefore, from (11), j_{Fe} = 0.437 A m^{-2}.

Converting iron oxidation corrosion current density to corrosion rate gives CR = 0.504 mm yr^{-1} (13).

3.1 *Fr 13* Risk Simulation

In contrast to this traditional SVA, the probabilistic *Fr 13* risk simulation of Davey and co-workers (Davey, 2015; Davey et al., 2015; Abdul-Halim and Davey, 2015) considers input parameters as distributions of values to mimic naturally occurring fluctuations, together with the probability of a particular value actually physically occurring. This means that the output will be a distribution of probabilities of particular outcomes. Because all practically possible inputs are simulated, the output will include unwanted outcomes i.e. 'failed' operations in which unwanted (intolerable) levels of MIC occurs.

A refined Monte Carlo (r-MC) (with *Latin Hypercube*) sampling of the distributions ensure sampling covers the entire range of the distributions. Pure MC cannot be relied on because it can over- and under-estimate from parts of the distribution (Vose, 2008).

In the *Fr 13* simulation, a MIC corrosion risk factor P can be defined by an off-specification from a tolerable corrosion rate

$$P = CR' - CR \tag{14}$$

where *CR'* is the instantaneous rate of corrosion (or mathematically more strictly, the *CR* obtained in a particular probabilistic simulation). However, a mathematically more convenient form (Abdul-Halim & Davey, 2015; Davey, 2015; Davey et al., 2015) is

$$p = 100\left(\frac{CR'}{CR} - 1\right) \tag{15}$$

(15) is computationally convenient because it is dimensionless and because corrosion rates greater than tolerable, that is failures, can be readily identified for all values $p > 0$.

Generally, the design specification includes some measure of tolerance i.e. design safety. The corrosion risk factor of (15) can therefore be written as

$$p = 100\left(\frac{CR'}{CR} - 1\right) - \%tolerance \qquad (16)$$

The practical upshot of (16) is that for corrosion rates greater than acceptable plus a tolerance, then $p > 0$, and the rate of corrosion is seen to be a failure.

(1) through (13) plus (16) defines the probabilistic *Fr 13* model for MIC corrosion of the steel pipe. If a sufficiently large sample size is made the output will simulate all possible outcomes. This sample size can be readily established from a plateau in the plot of number of failures versus number of samples (e.g. Davey, 2015). Importantly, it is seen all the mathematical operations of the SVA and *Fr 13* simulation are identical. In the absence of hard i.e. unconditional data and to demonstrate the model simulation a *%tolerance* = 50 % is assumed.

4 Results

Table 1 presents a summary comparison of results from the traditional SVA and new *Fr 13* simulation of Microbiologically Influenced Corrosion (MIC) of carbon steel pipe at a mid-range value of T = 293.15 K, and pH = 5.15 (rows 2 and 3, respectively). These are the key parameters which naturally fluctuate. The physical system is fixed by the parameter values shown in rows 5 through 18 of the table. The traditional SVA is read down column 2 where the corrosion rate CR = 0.504 mm yr^{-1} is shown.

The *Fr 13* simulation is read down column 4 in which a normal distribution has been used for both T and pH, namely, **RiskNormal** (mean, stdev, **RiskTruncate** (minimum, maximum)). For example, for T, this gives a mean = 293.15, stdev = 29.3, K, and minimum = 290.15 and maximum = 298.15, K. This is a practical way to say that in operation the temperature of the electrolyte does vary randomly but not outside this range. To recognize the natural variability in sensitivity to pH of the MIC it is assumed pH = **RiskNormal** (5.15, 0.515, **RiskTruncate** (4.64, 5.67)). It is not implied that values in Table 1 for T and pH need to be measured to these exactly; these are reproduced as the exact value sampled randomly in the r-MC simulations.

Ten thousand (10,000) r-MC samples were found sufficient. This means that all possible practical combinations of scenarios that could occur with MIC will have been simulated, including unacceptable rates of corrosion of the steel pipe as failures. The simulations were carried out using Microsoft Excel™ spread sheeting with a commercially available add-on @Risk (version 5.5 Palisade Corporation).

Importantly, however, the data shown in column 4 of Table 1 are for one only scenario of the 10,000 – a limitation of using tabulated data. A total of 2,810 failures were revealed in in the 10,000 scenarios i.e. 28.1 %. These are summarised as Figure 3. The x-axis is the computed value of p from (15) and the y-axis is the probability of p actually occurring (Vose, 2008). From the figure, it can be seen the area under the curve (275 x ~0.0036) = one (1). The figure shows the 2,810 failure scenarios to the right of the figure i.e. $p > 0$.

5 Discussion

The simulations proved stable. If each scenario is thought of as one day there would be an unacceptable rate of corrosion due to MIC every (10,000/365.25/2,810/365.25 =) 0.28 years on average over the long term with a tolerance of 50 %. There is no reason to expect these events will be equally spaced in time however. This insight is not available from traditional solutions such as the SVA.

The number of occasions that the acceptable corrosion rate would be exceeded will of course increase with tighter tolerance, and vice versa. Repeat simulations showed that with a design %*tolerance* respectively, 25 % and 75 %, there would be an unacceptable corrosion rate, respectively, each 0.26 and 0.48 years on average.

A significant advantage of the *Fr 13* framework over traditional solutions is that each and every scenario can be identified (Davey, 2015; Zou and Davey, 2016). The actual combination of T and pH that gave rise to an unacceptable rate of corrosion in 10 widespread failure values in the 2,810 with a 50 % tolerance is presented in Table 2. For example, failure 9 of the table shows a combination of T = 297.92 K and pH = 4.93 with resulting p = 6.80. This is the scenario shown in Table 1. A maximum corrosion rate of CR_{max} = 1.504 mm yr^{-1} was found at T = 291.73 and pH = 4.64 with a corresponding maximum value of the corrosion rate risk factor of p_{max} = 148.36. The table also shows that the corrosion rate overall increases with lower pH. A potential application of this insight could be that steps should be taken to increase the pH of the system wherever practical.

Importantly however, is that the value of the corrosion rate risk factor p will be determined directly by the probability distributions used to define the key MIC parameters. In the absence of unconditional data, truncated normal distributions have been used to simulate the naturally occurring fluctuations in the value of T and pH in MIC. To establish better distributions some experimenting is needed or expert knowledge drawn upon.

Table 1: Summary comparison of traditional SVA with the new *Fr 13* simulation of MIC with a tolerance of 50 %. Column 2 is the SVA value. *Fr 13* values of column 3 are for one only of 10,000 simulated scenarios. Failure is defined for all $p > 0$.

Row	Parameter	SVA	*Fr 13* simulation	
1	*Variable Inputs*			
2	T (K)	293.15	297.92†	**RiskNormal**(293.15,29.3,**RiskTruncate**(290.15,298.15))
3	pH	5.15	4.93†	**RiskNormal**(5.15,0.515,**RiskTruncate**(4.64,5.67))
4	*Constants*			
5	E_{corr} (V vs. SCE)	-0.616	-0.616	Constant
6	$\alpha_{a,H+}$ (dimensionless)	0.6	0.6	Constant
7	$\alpha_{c,H+}$ (dimensionless)	0.4	0.4	Constant
8	n_{H+} (dimensionless)	1	1	Constant
9	$j^{ref}_{0,H+}$ (A m^{-2})	0.05	0.05	Constant
10	ΔH_{H+} (J mol^{-1})	30000	30000	Constant
11	T_R (K)	293.15	293.15	Constant
12	$E°_{H+}$ (V vs SCE)	-0.241	-0.241	Constant
13	$C_{s,H+}$ (mol m^{-3})	0.000001	0.000001	Constant
14	D_{H+} (m^2 s^{-1})	9.47E-09	9.47E-09	Constant
15	$\delta_{N,H+}$ (m)	0.0000167	0.0000167	Constant
16	F (C mol^{-1})	96485	96485	Constant
17	R (J mol^{-1} K^{-1})	8.314	8.314	Constant
18	*%tolerance* (%)	-	50	
19	*Calculations*			
20	$C_{b,H+}$ (mol m^{-3})	0.0071	0.0117	Conversion from pH
21	$j_{0,H+}$ (A m^{-2})	0.0500	0.0609	Eq. (5)
22	$E_{rev,H+}$ (V vs SCE)	-0.5896	-0.5953	Eq. (7)
23	η_{H+} (V vs SCE)	-0.0264	-0.0207	Eq. (6)
24	$j_{ct,H+}$ (A m^{-2})	-0.0493	-0.0466	Eq. (4)
25	$j_{mt,H+}$ (A m^{-2})	-0.3873	-0.6379	Eq. (9)
26	j_{H+} (A m^{-2})	-0.4365	-0.6845	Eq. (10)
27	j_{Fe} (A m^{-2})	0.4365	0.6845	Eq. (11)
28	*Output*			
29	CR (mm yr^{-1})	0.5042	0.7906†	Eq. (13)
30	p	-	6.80	Eq. (16)

† Values tabulated are computed from the r-MC sampling; it is not implied they need to be measured to this order.

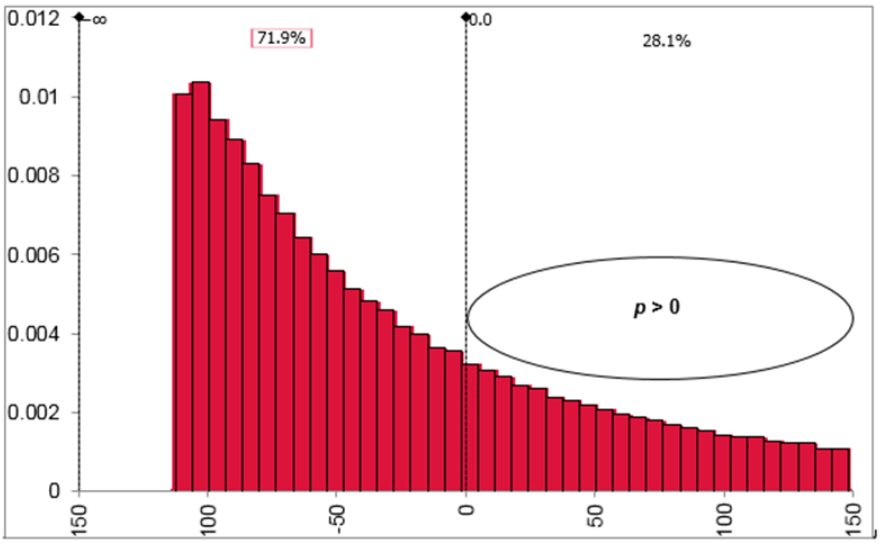

Figure 3: *Fr 13* simulation of the corrosion rate risk factor for MIC with 10,000 scenarios. The figure shows the 2,810 failure scenarios to the right of the figure i.e. $p > 0$.

Table 2: Ten (10) failures in the 2,810 scenarios with 50 % tolerance. The bold text denotes the particular scenario in Table 1.

Failure	T † (K)	pH † (dimensionless)	CR (mm yr^{-1})	p (dimensionless)
1	297.83	4.64	1.50	147.21
2	297.17	4.66	1.44	135.84
3	297.34	4.67	1.39	126.66
4	296.92	4.69	1.34	115.42
5	294.49	4.70	1.31	109.07
6	291.20	4.80	1.06	60.86
7	294.71	4.85	0.94	37.39
8	296.00	4.90	0.86	19.93
9	**297.92**	**4.93**	**0.79**	**6.80**
10	294.14	4.96	0.76	0.01

† Values are computed from the r-MC sampling; it is not implied they need to be measured to this order.

It might be that distributions can be 'tailored' for particular systems or geographical locations. Regardless, distributions need to be carefully considered so that the model give outcomes that can be observed in real situations where MIC occurs. The present work has nevertheless demonstrated the benefits and new insights from the probabilistic framework.

The model can be refined iteratively, and; to include different pipeline metals.

6 Conclusions

Microbiologically influenced corrosion (MIC) of carbon-steel pipeline has been shown to be amenable to a quantitative probabilistic risk framework.

Based on a simplified unit-operations model for synthetic micro-organism growth, an unacceptable MIC of carbon steel pipe would occur every 0.28 years averaged over the long term with a design tolerance of 50 % due to the impact of naturally occurring fluctuations in environment temperature and pH. This insight is not available from traditional risk methods.

The model form appears generalizable to a range of micro-organism–metal systems. A refined model could be used to quantitatively investigate MIC preventative intervention strategies.

Findings will be of wide interest to a range of designers and risk researchers involved in metals selection and in mitigating MIC in process equipment.

Nomenclature

Numbers in parentheses after the description refer to the equation in which the symbol is first used or defined

CR	Corrosion rate, mm yr^{-1} (12, 13)
$C_{b,H+}$	Concentration of species in bulk electrolyte = 10^{-pH} x1000 mol m^{-3} (8)
$C_{s,H+}$	Concentration of species at steel surface = 10^{-6} mol m^{-3} (8)
D_{H+}	Diffusion coefficient = 9.47 x 10^{-9} m^2 s^{-1} (8)
E	Potential, V (6)
E_{corr} (V vs. SCE)	Free corrosion potential = -0.616 V (6)
E_{rev} (V vs. SCE)	Reversible potential for species, V (7)
$E°_{H+}$ (V vs. SCE)	Standard (equilibrium) potential = -0.241 V (7)
F	Faraday constant = 96,485 C mol^{-1} (4)
ΔH_{H+}	Enthalpy of activation = 30,000 J mol^{-1} for proton reduction (5)
$J_{0,H+}$	Exchange current density, A m^{-2} (4)
$j^{ref}_{0,H+}$	Reference exchange current density = 5 x 10^{-2} A m^{-2} (5)
M_{Fe}	Molecular weight = 55.85 g mol^{-1} (12)
n_{H+}	Number of electrons transferred in the process (4)
p	Corrosion rate risk factor, dimensionless (16)
R	Universal gas constant = 8.314 J mol^{-1} K^{-1} (4)
%tolerance	Practical tolerance over design corrosion rate *CR*, % (16)
T	Temperature of electrolyte, K (4)
T_R	Reference temperature = 293.15 K (5)

Greek Symbols

$\alpha_{a,H+}$	Anodic transfer symmetry function = 0.6 dimensionless (4)
$\alpha_{c,H+}$	Cathodic transfer symmetry function = (1 - $\alpha_{a,H+}$) = 0.4 dimensionless (4)
$\delta_{N,H+}$	Nernst diffusion layer thickness = 1.67 x 10^{-5} m (8)
η_{H+} (V vs. SCE)	Overpotential, V (7)
ρ_{Fe}	Density of iron = 7,850 kg m^{-3} (12)

Subscripts

a	Anodic symmetry function
c	Cathodic symmetry function
T	Total system parameter

Superscript

‘	Particular r-MC scenario (14)

References

Abdul-Halim, N., Davey, K.R. (2015), *A Friday 13th risk assessment of ultraviolet irradiation for potable water in turbulent flow*, Food Control, **50**, 770-777.

Chandrakash, S., Davey, K.R., O’Neill, B.K. (2015), *An Fr 13 risk analysis of failure in a global food process – Illustration with milk processing*, Asia-Pacific Journal of Chemical Engineering, **10**, 526-541.

Davey, K.R. (2011), *Introduction to fundamentals and benefits of Friday 13th risk modelling technology for food manufacturers*, Food Australia, **63**, 192-197.

Davey, K.R. (2015), *A novel Friday 13th risk assessment of fuel-to-steam efficiency of a coal-fired boiler*, Chemical Engineering Science, **127**, 133-142.

Davey, K.R., Cerf, O. (2003), *Risk modelling - An explanation of Friday13th syndrome (failure) in well-operated continuous sterilisation plant*, in: *Proceedings of the 31st Australasian Chemical Engineering Conference (Product and Processes for the 21st Century)*, Adelaide, Sept. 28 – Oct. 1, 2003.

Davey, K.R., Chandrakash, S., O'Neill, B.K. (2013), *A new risk analysis of Clean-In-Place milk processing*, Food Control, **29**, 248-253.

Davey, K.R., Chandrakash, S., O'Neill, B.K. (2015), *A Friday 13th failure assessment of clean-in-place removal of whey protein deposits from metal surfaces with auto-set cleaning times*, Chemical Engineering Science, **126**, 106-115.

Davey, K.R., Lavigne, O., Shah, P. (2016), *Establishing an atlas of risk of pitting of metals at sea – demonstrated for stainless steel AISI 316L in the Bass Strait*, Chemical Engineering Science, **140**, 71-75.

De Waard, C., Lotz, U., Miliams, D.E. (1991), *Predictive model for CO2 corrosion engineering in wet natural gas pipelines*, Corrosion, **47**, 976–985

ExxonMobilAustralia, (2015), Bass Strait. ExxonMobil (Australia) http://www.exxonmobil.com.au/Australia-English/PA/about_what_gipps_bs.aspx (viewed 7 Jun 2016).

Flemming, H.C. (2002), *Biofouling in water systems – cases, causes and countermeasures*, Applied Microbiology and Biotechnology, **59**, 629-640.

Gu, T., Zhao, K., Nesic, S. (2009), *A New Mechanistic Model for MIC Based on a Biocatalytic Cathodic Sulfate Reduction Theory*, in *CORROSION 2009*, Atlanta, March 22 - 26, 2009

Jacobson, G.A. (2007), *Corrosion at Prudhoe Bay: A lesson on the line,* Materials Performance **46**, 26-34.

Jack, T.R. (2002), *Biological Corrosion Failures*, in Becker, W.T., Shipley, R.J., "ASM Handbook Volume 11: Failure Analysis and Prevention", ASM International, Materials Park, Ohio, pp. 881-898.

Maxwell, S., Campbell, S. (2006), *Monitoring the Mitigation of MIC Risk in Pipelines*, in *CORROSION 2006*, San Diego, March 12 - 16, 2006.

Nesic, S., Postlethwaite, J., Olsen, S. (1996), *An electrochemical model for prediction of corrosion of mild steel in aqueous carbon dioxide solutions*, Corrosion, **52**, 280-294.

Pots, B.F.M., John, R.C., Rippon, I.J., Thomas, M.J.J.S., Kapusta, S.D., Girgis, M.M., Whitman, T. (2002), *Improvements on DeWaard-Milliams corrosion prediction and applications to corrosion management*, in *CORROSION 2002*, Denver, April 7 – 11, 2002.

Roberge, P.R. (2000), *Handbook of Corrosion Engineering*, McGraw-Hill, New York. pp. 35-54, 187-220, 335-336, 1047-1059.

Sinnott, R.K. (2005), *Chemical Engineering Design*, fourth edition, Butterworth-Heinemann, Jordan Hill, Great Britain, pp. 756–764.

Smith, P., Roy, S., Swailes, D., Maxwell, S., Page, D., Lawson, J. (2011), *A model for the corrosion of steel subjected to synthetic produced water containing sulfate, chloride and hydrogen sulphide*, Chemical Engineering Science, **66**, 5775-5790.

Videla, H.A., Herrera, L.K. (2005), *Microbiologically influenced corrosion: looking to the future*, International Microbiology, **8**, 169-180.

Vose, D. (2008), *Risk Analysis - A Quantitative Guide*, third edition, John Wiley & Sons, Chichester, UK. pp. **43**, 45-47.

Zou, W., Davey, K.R. (2016), *An integrated two-step Fr 13 synthesis - demonstrated with membrane fouling in combined ultrafiltration-osmotic distillation (UF-OD) for concentrated juice*, Chemical Engineering Science, *in press* 14 June.

Presenting author biography

Sam Collins is a graduate of The University of Adelaide and is currently a postgraduate student with researcher Davey in the School of Chemical Engineering, The University of Adelaide, Australia.

K R (Ken) Davey FIChemE CEng FAIFST CSci received his PhD from Melbourne University and worked as a Postdoctoral Researcher with CSIRO and subsequently at The University of Adelaide. He has published more than 120 refereed articles and patents and received numerous awards for his work. He has consulted widely in chemical/biochemical engineering and lectured in a number of Universities internationally. He is involved in interdisciplinary research in (bio) chemical process engineering and in the development of new quantitative risk assessments for improved efficiencies, reliability and safety.

APPENDIX D – Plot of percentage of *Fr 13* failures versus number of simulations - Novel *Fr 13* model for corrosion of ASTM A105 carbon-steel pipe (The red line denotes 10,000 simulations)

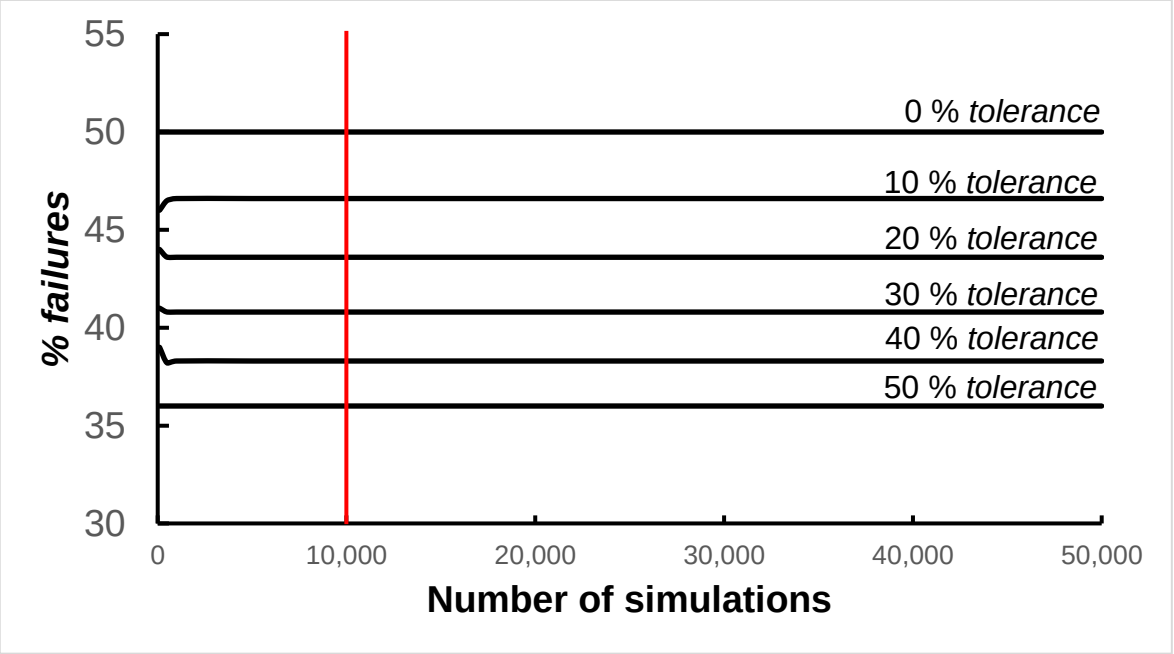

NOMENCLATURE

The equation or figure number given after description refers to that in which the symbol is first used or defined.

A_E	electrode surface area (2.80×10^{-3} m^2) (4.5a)
CR	corrosion rate (mm yr^{-1}) (3.13)
$C_{b,Fe}$	concentration iron species in bulk electrolyte ($= 1 \times 10^{-6}$ mol m^{-3}) (4.5a)
$C_{b,H+}$	concentration proton species in bulk electrolyte ($= 10^{-pH} \times 1000$ mol m^{-3}) (3.9)
$C_{s,Fe}$	concentration of iron species at carbon steel-pipe surface ($= 1 \times 10^{-4}$ mol m^{-3}) (4.5a)
$C_{s,H+}$	concentration of proton species at carbon steel-pipe surface ($= 1 \times 10^{-6}$ mol m^{-3}) (3.7)
D_{Fe}	diffusion coefficient of iron species ($= 7.98 \times 10^{-10}$ m^2 s^{-1}) (4.8a)
D_{H+}	diffusion coefficient or proton species ($= 9.47 \times 10^{-9}$ m^2 s^{-1}) (3.9)
E	potential (V vs SCE) (3.7)
$e_{0,Fe}$	exchange current density transfer parameter for iron species ($= 1 \times 10^{-7}$ A) (4.5a)
$e_{0,H+}$	exchange current density transfer parameter for proton species ($= 1 \times 10^{-7}$ A) (4.5b)
E_{corr} (V vs SCE)	free corrosion potential (V vs SCE) (3.8)
$E_{rev,Fe}$ (V vs SCE)	reversible potential for iron species (V vs SCE) (4.6a)
$E_{rev,H+}$ (V vs SCE)	reversible potential for proton species (V vs SCE) (3.7)
$E°_{Fe}$ (V vs SCE)	standard (equilibrium) potential for iron species ($= -0.681$ V vs SCE) (4.6a)

$E°_{H+}$ (V vs SCE)	standard (equilibrium) potential for proton species (= -0.241 V vs SCE) (3.7)
F	Faraday constant (= 96,485 C mol^{-1}) (3.4)
ΔH_{H+}	Enthalpy of activation (= 30,000 J mol^{-1} for proton reduction) (3.6)
j	current density (A m^{-2}) (3.4)
$j_{ct,Fe}$	current density due to charge transfer for iron species (A m^{-2}) (4.4a)
$j_{ct,H+}$	current density due to charge transfer for proton species (A m^{-2}) (3.5)
$j_{mt,Fe}$	current density due to mass transfer for iron species (A m^{-2}) (4.8a)
$j_{mt,H+}$	current density due to mass transfer for proton species (A m^{-2}) (3.9)
$j_{0,Fe}$	exchange current density for iron species (A m^{-2}) (4.5a)
$j_{0,H+}$	exchange current density for proton species (A m^{-2}) (3.5)
$j^{ref}_{0,H+}$	reference exchange current density for proton species (= 5 x 10^{-2} A m^{-2}) (3.6)
M_{Fe}	molecular weight of iron (= 55.85 g mol^{-1}) (3.13)
n_{Fe}	number of electrons transferred in oxidation (iron) process (4.4a)
n_{H+}	number of electrons transferred in reduction (proton) process (3.5)
p	corrosion rate risk factor (dimensionless) (3.16)
R	universal gas constant (= 8.314 J mol^{-1} K^{-1}) (3.4)
T	temperature of pipe-fluid (K) (3.4)
T_R	Reference temperature (Chapter 3 model) (= 293.15 K) (3.6)
T_{ref}	Reference temperature (Chapter 4 model) (= 353.15 K) (4.9c)

Greek Symbols

$\alpha_{a,Fe}$	anodic transfer symmetry function for iron species (= 0.4 dimensionless) (4.4a)

$\alpha_{a,H+}$	anodic transfer symmetry function for proton species (= 0.6 dimensionless) (3.5)
$\alpha_{c,Fe}$	cathodic transfer symmetry function for iron species (= (1 - $\alpha_{a,H+}$) = 0.6 dimensionless) (4.4a)
$\alpha_{c,H+}$	cathodic transfer symmetry function for proton species (= (1 - $\alpha_{a,H+}$) = 0.4 dimensionless) (3.5)
$\delta_{N,Fe}$	Nernst diffusion layer thickness for iron species (= 7.23 x 10^{-6} m) (4.8a)
$\delta_{N,H+}$	Nernst diffusion layer thickness for proton species (= 1.67 x 10^{-5} m) (3.9)
η_{Fe} (V vs SCE)	overpotential for iron species (V vs SCE) (4.4a)
η_{H+} (V vs SCE)	overpotential for proton species (V vs SCE) (3.5)
ρ_{Fe}	density of iron (= 7,850 kg m^{-3}) (3.13)
γ_{Fe}	concentration sensitivity parameter for iron species (= 0.3 dimensionless) (4.5a)
γ_{H+}	concentration sensitivity parameter for proton species (= 0.75 dimensionless) (4.5b)

Subscripts

a	anodic symmetry function
c	cathodic symmetry function
T	total system parameter (3.11)

Other

%tolerance	practical tolerance over design corrosion rate *CR* (%) (3.17)

CE	counter-electrode (Fig. 3-1)
RE	reference-electrode (Fig. 3-1)
SCE	saturated calomel electrode (Fig. 3-1)
WE	working-electrode (Fig. 3-1)

Superscript

‘	particular r-MC scenario (3.15)

REFERENCES

Abdul-Halim, N., Davey, K.R., 2015. A Friday 13th risk assessment of ultraviolet irradiation for potable water in turbulent flow. Food Control 50, 770-777. http://dx.doi.org/10.1016/j.foodcont.2014.10.036

Abdul-Halim, N., Davey, K.R., 2016. Impact of suspended solids on *Fr 13* failure of UV irradiation for inactivation of *Escherichia coli* in potable water production with turbulent flow in an annular reactor. Chemical Engineering Science 143, 55-62. http://dx.doi.org/10.1016/j.ces.2015.12.017

Abdul-Halim, N., 2017. A Quantitative Risk Assessment of *Fri 13* Failure Modelling for Ultraviolet Irradiation for Potable Water Production. PhD Research thesis, The University of Adelaide.

Alberts, B., Johnson, A., Lewis, J., Raff, M., Roberts, K., Walter, P., 2002. Molecular Biology of the Cell. 4th ed. Garland Science, New York, USA, pp. G-2, G-14. ISBN: 0815340729

Allison, P.W., Sahar, R.N.R.R., Guan, O.H., Hain, T.S., Vance, I., Thompson, M.J., 2008. The investigation of microbial activity in an offshore oil production pipeline system and the development of strategies to manage the potential for microbially influenced corrosion. In: CORROSION 2008, Mar. 16-20, New Orleans, USA, paper 08651. ISBN: 086512008CP

Amundson, N.R., Aris, R., Varma, A., 1980. The Mathematical Understanding of Chemical Engineering Systems. Pergamon Press, Oxford, UK, pp. 30, 278-282, 342-366. ISBN: 9780080238364

Anon., 1972. Bacteria have destroyed 10% of the world's crude. World Oil 174, Feb, pp. 28-29.

Anon., 2012. Blackett Review of High Impact Low Probability Risks. Government Office for Science (UK). http://bis.gov.uk/assets/goscience/docs/b/12-519-blackett-review-high-impact-low-probability-risks.pdf, viewed 11 Jan, 2015, 13:00 h.

Arnold, K., Stewart, M., 1999. Surface Production Operations Volume 1: Design of Oil-Handling Systems and Facilities. 2nd ed. Gulf Publishing Company, Houston, USA, pp. 101. ISBN: 0884158217

Aven, T., 2010. On how to define, understand and describe risk. Reliability Engineering and System Safety 95, 623-631. http://dx.doi.org/10.1016/j.ress.2010.01.011

Bastin, E.S., 1926. The problem of the natural reduction of sulphates. Bulletin of the American Association of Petroleum Geologists 10, 1270-99. ISSN: 01491423

Beech, I.B., Sunner, J.A., 2007. Sulphate-reducing bacteria and their role in corrosion of ferrous materials. In: Barton, L.L., Hamilton, W.A., ed. Sulphate-reducing Bacteria – Environmental and Engineered Systems. Cambridge University Press, New York, USA, pp. 459-482. ISBN: 978-0-521-85485-6

Beijerinck, M.W., 1895. Ueber *Spirillum desulphuricans* als ursache von sulfat-reduction. Zantralblatt für Bakteriologie und Parasitenkunde 1, 1-9, 49-59, 104-14.

Breakell, J.E., Siegwart, M., Foster, K., 2005. Management of Accelerated Low Water Corrosion in Steel Maritime Structures. Alden Press, London, UK. ISBN: 978-0860176343

Brock, T.D., Madigan, M.T., 1991. Biology of Microorganisms. 6th ed. Prentice-Hall, Englewood Cliffs, USA, pp. 839. ISBN: 0130838179

Bubela, B., 1983. Combined effects of temperature and other environmental stresses on microbiologically enhanced oil recovery (MEOR). In: Proceedings of the 1982 International Conference on Microbial Enhancement of Oil Recovery, May 16-21, Afton, USA.

Chandrakash, S., 2012. A new risk analysis in Clean-In-Place (CIP) milk processing. Master Research thesis, The University of Adelaide, pp. 101.

Chandrakash, S., Davey, K.R., 2017. Advancing the *Fr 13* risk framework to an integrated three-step microbiological failure synthesis of pasteurization of raw milk containing *Mycobacterium avium* subsp. *Paratuberculosis* (*MAP*). Chemical Engineering Science 171, 1-18. http://dx.doi.org/10.1016/j.ces.2017.05.020

Chandrakash, S., Davey, K.R., O'Neill, B.K., 2015. An *Fr 13* risk analysis of failure in a global food process – Illustration with milk processing. Asia-Pacific Journal of Chemical Engineering 10, 526-541. http://dx.doi.org/10.1002/apj.1887

Characklis, W.G., Marshall, K.C., 1990. Biofilms. John Wiley and Sons, New York, USA. ISBN: 978-0471826637

Chexal, V.K., Horowitz, J.S., Munson, D.P., Shye, K., Spalaris, C.S., 1997. Using predictive technology to control corrosion in raw cooling water systems. In: Proceedings of the International Corrosion Conference, date unknown, Pittsburgh, USA, paper IWC-97-84.

Chilingar, G. V., Mourhatch, R., Al-Qahtani, G. D., 2008. The Fundamentals of Corrosion and Scaling for Petroleum & Environmental Engineers. 1st ed. Gulf Publishing Company, Houston, USA. ISBN: 9781933762302

Collins, S.D., Davey, K.R., 2018. A *Fr 13* risk assessment of microbiologically influenced corrosion (MIC) of carbon-steel pipe. Chemical Engineering Science – *submitted* CES-D-18-00449, Feb.

Collins, S.D., Davey, K.R., Chu, J.Y.G., O'Neill, B.K., 2016. A new quantitative risk assessment of Microbiologically Influenced Corrosion (MIC) of carbon steel pipes used in chemical engineering. In: CHEMECA 2016: Chemical Engineering – Regeneration, Recovery and Reinvention, Sept. 25-28, Adelaide, Australia, paper 3386601. ISBN: 9781922107831

Costerton, J.W., Colwell, R.R., 1977. Native Aquatic Bacteria: Enumeration, Activity and Ecology, Special Technical Publication 695. American Society for Testing and Materials, Philadelphia, USA, pp. 5. ISBN-13: 9780803105263

Crolet, J.L., 1993. Mechanisms of uniform corrosion under corrosion deposits. Journal of Materials Science 28, 2589-606. ISSN: 0022-2461

Davey, K.R., 2010. A novel proposal to advance the discipline and to quantitatively safeguard important hygienic bio-processes. In: Proceedings of the 40th Australasian Chemical Engineering Conference (Engineering at the Edge) - CHEMECA 2010: Engineering at the Edge, Sept. 26-29, Adelaide, Australia, paper 0495. ISBN: 9780858259713

Davey, K.R., 2011. Introduction to fundamentals and benefits of Friday 13th risk modelling technology for food manufacturers. Food Australia 63, 192-197. ISSN: 1032598

Davey, K.R., 2015 a. A novel Friday 13th risk assessment of fuel-to-steam efficiency of a coal-fired boiler. Chemical Engineering Science 127, 133-142. http://dx.doi.org/10.1016/j.ces.2015.01.031

Davey, K.R., 2015 b. Development and illustration of a computationally convenient App for simulation of transient cooling of fish in ice slurry at sea. LWT – Food Science and Technology 60, 308-314. https://doi.org/10.1016/j.lwt.2014.08.022

Davey, K.R., 2018. A seminal *Fr 13* failure model of a generic process with feed-stream, reactor, separator and recycle with purge. Chemical Engineering Science – *in preparation*.

Davey, K.R., Cerf, O., 2003. Risk modelling - An explanation of Friday 13th Syndrome (failure) in well-operated continuous sterilisation plant. In: Proceedings of the 31st Australasian Chemical Engineering Conference (Product and Processes for the 21st Century), Sept. 28–Oct. 1, Adelaide, Australia, paper 61. ISBN: 9780863968295

Davey, K.R., Chandrakash, S., O'Neill, B.K., 2013. A new risk analysis of Clean-In-Place milk processing. Food Control 29, 248-253. http://dx.doi.org/10.1016/j.foodcont.2012.06.014

Davey, K.R., Chandrakash, S., O'Neill, B.K., 2015. A Friday 13th failure assessment of clean-in-place removal of whey protein deposits from metal surfaces with auto-set cleaning times. Chemical Engineering Science 126, 106-115. http://dx.doi.org/10.1016/j.ces.2014.12.013

Davey, K.R., Lavigne, O., Shah, P., 2016. Establishing an atlas of risk of pitting of metals at sea – demonstrated for stainless steel AISI 316L in the Bass Strait. Chemical Engineering Science 140, 71-75. http://dx.doi.org/10.1016/j.ces.2015.10.008

De Waard, C., Lotz, U., Miliams, D.E., 1991. Predictive model for CO_2 corrosion engineering in wet natural gas pipelines. Corrosion 47, 976–985. http://dx.doi.org/10.5006/1.3585212

De Romero, M., Duque, Z., de Rincón, O., Pérez, O., Araujo, I., Martinez, A., 2000. Online monitoring systems of microbiologically influenced corrosion on Cu-10% Ni alloy in chlorinated, brackish water. In: CORROSION 99, Apr. 25-30, San Antonio, USA. ISSN: 00109312

Dillion, C.P., 1982. Forms of Corrosion: Recognition and Prevention. NACE International, Houston, USA. ISBN: 0915567873

Donlan, R. M., Costerson, J. W., 2002. Biofilms: Survival mechanisms of clinically relevant microorganisms. Clinical Microbiology Reviews 15, 167-193. http://dx.doi.org/10.1128/CMR.15.2.167-193.2002

Eckford, R.E., Fedorak, P.M., 2004. Using nitrate to control microbially-produced hydrogen sulphide in oil field waters. In: Vazquez-Duhalt, R., Quintero-Ramírez, R., ed. Petroleum Biotechnology - Developments and Perspectives. Elsevier, Amsterdam, the Netherlands, pp. 307-340. ISBN: 9780444516992

Electric Power Research Institute, 1999. CHECWorks™ Cooling Water Applications. In: CWUG-1999, 1999, Palo Alto, USA.

Enning, D., Garrelfs, J., 2014. Corrosion of iron by sulphate-reducing bacteria: New views of an old problem. Applied and Environmental Microbiology 80, 1226-1236. http://dx.doi.org/10.1128/AEM.02848-13

Flemming, H.C., 1996. Economical and technical overview. In: Heitz, E., Flemming, H.C., Sand, W., ed. Microbially Influenced Corrosion of Materials. Springer-Verlag, Berlin, Germany. ISBN: 3540604324

Flemming, H.C., 2002. Biofouling in water systems – cases, causes and countermeasures. Applied Microbiology and Biotechnology 59, 629-640. http://dx.doi.org/10.1007/s00253-002-1066-9

Foust, A.S., Wenzel, L.A., Clump, W.C., Maus, L., Andersen, L.B., 1980. Principles of Unit Operations. 2nd ed. John Wiley and Sons, New York, USA. ISBN: 0471268976

Gaines, R.H., 1910. Bacterial activity as a corrosive influence in the soil. The Journal of Industrial and Engineering Chemistry 2, 128-130. http://dx.doi.org/10.1021/ie50016a003

Geesey, G. G., 1993. Biofilm Formation. In: Kobrin, G., ed. A Practical Manual on Microbiologically Influenced Corrosion. NACE International, Houston, USA, pp. 21, 101, 103. ISBN: 1877914568

Geesey, G., Beech, I., Bremer, P., Webster, B.J., Wells, D.B., 2000. Biocorrosion. In: Bryers, J.D., ed. Biofilms II: Process Analysis and Applications. Wiley, New York, USA, pp. 281-325. ISBN: 9780471296560

Ghasem, N., Henda, R., 2008. Principles of Chemical Engineering Processes. CRC Press, UK. ISBN: 9781420080131

Gu, T., Zhao, K., Nesic, S., 2009. A New Mechanistic Model for MIC Based on a Biocatalytic Cathodic Sulfate Reduction Theory. In: CORROSION 2009, Mar. 22-26, Atlanta, USA, paper 09390. ISSN: 03614409

Gubner, R., Beech, I.B., 1999. Statistical assessment of the risk of biocorrosion in tidal waters. In: CORROSION 1999, Apr. 25-30, Houston, USA, paper 184. ISBN: 99184 1999 CP

Haimes, Y.Y., 2009. On the complex definition of risk: A systems-based approach. Risk Analysis 29, 1647-1654. http://dx.doi.org/10.1111/j.1539-6924.2009.01310.x

Hansson, C. M., 2010. The impact of corrosion on society. Metallurgical and Materials Transactions A 42, 2952-2962. http://dx.doi.org/10.1007/s11661-011-0703-2

Harrison, J.J., Turner, R. Ceri, H., 2005. Persister cells, the biofilm matrix and tolerance to metal cations in biofilm and planktonic *Pseudomonas aeruginosa*. Environmental Microbiology 7, 981-94. http://dx.doi.org/10.1111/j.1462-2920.2005.00777.x

Hathurusingha, P.I., Davey, K.R., 2016. Chemical taste taint accumulation in RAS farmed fish - A *Fr 13* risk assessment demonstrated with geosmin (GSM) and 2-methylisoborneol (MIB) in barramundi (*Lates calcarifer*). Food Control 60, 309-319. http://dx.doi.org/10.1016/j.foodcont.2015.08.014

Hays, G. F., 2012. Now is the Time. World Corrosion Organization. http://corrosion.org/wco_media/nowisthetime.pdf ; http://corrosion.org/

Holman, J.P., 2010. Heat Transfer. 10th edition. McGraw-Hill, UK. ISBN: 9780073529363

Iverson, W.P., 1966. Direct evidence for the cathodic depolarization theory of bacterial corrosion. Science 151, 986-988. ISSN: 00368075; 10959203

Jack, T.R., 1999. Monitoring microbial fouling and corrosion problems in industrial systems. Corrosion Reviews 17, 1-32. https://doi.org/10.1515/CORRREV.1999.17.1.1

Jack, T.R., 2002. Biological Corrosion Failures. In: Becker, W.T., Shipley, R.J., ed. ASM Handbook Volume 11: Failure Analysis and Prevention. ASM International, Materials Park, Ohio, pp. 881-898. ISBN: 9780871707048

Jacobson, G.A., 2007. Corrosion at Prudhoe Bay: A lesson on the line. Materials Performance 46, Aug., pp. 26-34. ISSN: 00941492

Javaherdashti, R., 2013. Microbiologically influenced corrosion. In: Javaherdashti, R., Nwaoha C., Tan, H., ed. Corrosion and Materials in the Oil and Gas Industries. CRC Press, Boca Raton, USA, pp. 47-128. ISBN: 9781466556256

Javaherdashti, R., 2017. Microbiologically Influenced Corrosion – An Engineering Insight. 2nd ed. Springer International Publishing, Cham, Switzerland, pp. 29-79. ISBN: 9783319443041

Javaherdashti, R., Raman-Singh, R.K., 2001. Microbiologically Influenced Corrosion of Stainless Steels in Marine Environments: A Materials Engineering Approach. In: Proceedings of Engineering Materials 2001, Sept. 23-26, Melbourne, Australia.

Jones, L. W., 1988. Corrosion and Water Technology for Petroleum Producers. OGCI Publications, Tulsa, USA. ISBN: 0930972090

Kemmer, F.N., ed. 1988. The Nalco Water Handbook. McGraw-Hill, New York, USA, pp. 22.7. ISBN: 0070458723

Koch, G. H., Brongers, M. P. H., Thompson, N. G., Virmani, Y. P., Payer, J. H., 2001. Corrosion costs and preventative strategies in the United States. Report no. FHWA-RD-01-156, Federal Highway Administration, Washington, D.C.

Lavigne, O., Davey, K.R., 2017. Mitigating the impact of metal roughness on the risk of pitting of stainless steel alloy AISI 316L in the Gulf of Mexico – *in preparation.*

Le Faou, A., Rajagopal, B.S., Daniels, L., Fauque, G., 1990. Thiosulphate, polythionates and elemental sulfur assimilation and reduction in the bacterial world. FEMS Microbiology Reviews 75, 351-82. http://dx.doi.org/10.1111/j.1574-6968.1990.tb04107.x

Lewin, R.A., Andersen, R.A., 2017. Algae. Encyclopaedia Britannica. https://www.britannica.com/science/algae, viewed 31 Oct, 2017, 12:32 h.

Lutey, R.W., Stein, A., 1999. A Review and Comparison of MIC Indices (Models). In: Proceedings of the International Water Conference, Oct. 22-26, Pittsburgh, USA, paper IWC-01-04. ISSN: 00749575

Madigan, M.T., Martinko, J.M., Parker, J., 2003. Brock Biology of Microorganisms. 10th ed. Pearson Education, Upper Saddle River, USA, pp. 58-59. ISBN: 0-13-066271-2

Magot, M., Basso, O., Tardy-Jacquenod, C., Caumetter, P., 2004. *Desulfovibrio bastinii* sp. nov.and *Desulfovibrio gracilis* sp. nov., moderately halophilic, sulfate-reducing bacteria isolated from deep subsurface oilfield water. International Journal of Systematic and Evolutionary Microbiology 54, 1693-7. http://dx.doi.org/10.1099/ijs.0.02977-0

Malard, E., Kervadec, D., Gil, O., Lefevre, Y., Malard, S., 2008. Interactions between steels and sulphide-producing bacteria – Corrosion of carbon steels and low-alloy steels in natural seawater. Electrchimica Acta 54, 8-13. http://dx.doi.org/10.1016/j.electacta.2008.05.075

Maxwell, S., Campbell, S., 2006. Monitoring the Mitigation of MIC Risk in Pipelines. In: CORROSION 2006, Mar. 12-16, San Diego, USA, paper 06662. ISSN: 03614409

McCabe, W.L., Smith, J.C., Harriott, P., 2001. Unit Operations of Chemical Engineering. 6th ed. McGraw-Hill, New York, USA. ISBN: 0070393664

Melchers, R.E., 2009. Experiments, science and intuition in the development of models for the corrosion of steel infrastructure. In: The 49th Annual Conference of the Australasian Corrosion Association 2009: Corrosion and Prevention 2009, Nov. 15-18, Coffs Harbour, Australia, paper 35. ISSN: 14420139

Milazzo, M.F., Aven, T., 2012. An extended risk assessment approach for chemical plants applied to a study related to pipe ruptures. Reliability Engineering and System Safety 99, 183-192. http://dx.doi.org/10.1016/j.ress.2011.12.001

Mohanty, S.S., Das, T., Mishra, S.P., Chaudhury, G.R., 2000. Kinetics of SO_4^{2-} reduction under different growth media by sulfate reducing bacteria. Biometals 13, 73-76. http://dx.doi.org/10.1023/A:1009240203326

Moore, D., Ahmadjian, V., Alexopoulos, C.J., 2017. Fungus. Encyclopaedia Britannica. https://www.britannica.com/science/fungus, viewed 31 Oct, 2017, 12:35 h.

Moura, M. C., Pontual, E. V., Paiva, P. M. G., Coelho, L. C. B. B., 2013. An outline to corrosive bacteria. In: Méndez-Vilas, A., ed. Microbial Pathogens and Strategies for Combating Them: Science, Technology and Education – Vol. 1. Formatex Research Center, Badajoz, Spain, pp. 11-22. ISBN: 9788493984397

Nalco/Exxon Energy Chemicals, 1997. Part 9 – Microbio Control. In: Oilfield Chemicals Training Manual. Nalco/Exxon Energy Chemicals, Apr. 15, pp. 1-18.

Nelson, D.L., Cox, M.M., 2000. Lehninger Principles of Biochemistry. 3rd ed. Worth Publishers, New York, USA, pp. 21, G-4. ISBN: 1572591536

Newman, J., Thomas-Alyea, K.E., 2004. Electrochemical Systems. 3rd ed. John Wiley and Sons, Inc., Hoboken, USA. ISBN: 9780471477563

Nesic, S., Postlethwaite, J., Olsen, S. (1996), An electrochemical model for prediction of corrosion of mild steel in aqueous carbon dioxide solutions, Corrosion, 52, 280-294. ISSN: 00109312

Odom, J.M., Jessie, K., Knodel, E., Emptage, M., 1991. Immunological cross-reactivities of adenosine-5'-phosphosulfate reductases from sulfate-reducing and sulfide-oxidising bacteria. Applied and Environmental Microbiology 57, 727-733. ISBN: 00992240/91/03072707$02.00/0

Ollivier, B., Cayol, J-L., Fauque, G., 2007. Sulphate-reducing bacteria from oil field environments and deep-sea hydrothermal vents. In: Barton, L.L., Hamilton, W.A., ed. Sulphate-reducing Bacteria – Environmental and Engineered Systems. Cambridge University Press, New York, USA, pp. 305-328. ISBN: 978-0-521-85485-6

OREDA., 2015. Offshore and Onshore Reliability Database, OREDA 2015 Handbook, DNV.GL. http:/blogs.dnvgl.com/software/2015/06/new-edition-oreda-2015handbook/, last viewed 23 Mar, 2018, 16.00 h

Ozilgen, M., 1998. Food Process Modelling and Control: Chemical Engineering Applications. CRC Press, UK. ISBN: 9056991434

Pichtel, J., 2016. Oil and gas production wastewater: Soil contamination and pollution prevention. Applied and Environmental Soil Science 2016, 1-25. http://dx.doi.org/10.1155/2016/2707989

Picioreanu, C., van Loosdrecht, M.C.M., 2002. A mathematical model for initiation of microbiologically influenced corrosion by differential aeration. Journal of The Electrochemical Society 149, B211–B223. http://dx.doi.org/10.1149/1.1470657

Pope, D.H., Duquette, D., Wayner, P.C., Jr., Arland, H.J., 1989. Microbiologically Influenced Corrosion: A State-of-the-Art Review. 2nd ed. Materials Technology Institute of the Chemical Process Industries, St. Louis, USA. ISBN: 1877914096

Pots, B.F.M., John, R.C., Rippon, I.J., Thomas, M.J.J.S., Kapusta, S.D., Girgis, M.M., Whitman, T., 2002. Improvements on DeWaard-Milliams corrosion prediction and applications to corrosion management. In: CORROSION 2002, Apr. 7-11, Denver, USA, paper 02235. ISSN: 03614409

Rajasekar, A., Babu, T. G., Pandian, S. T. K., Maruthamuthu, S., Palaniswamy, N., Rajendran, A., 2007. Role of *Serratia marcescens* ACE2 on diesel degradation and its influence on corrosion. Journal of Industrial Microbiology & Biotechnology 34, 589-598. http://dx.doi.org/10.1007/s10295-007-0225-5

Rawat, J., Sharma, N., Khandelwal, A., 2014. Microbiological causes of corrosion. Digital Refining. http://www.digitalrefining.com/article/1000999,Microbiological_causes_of_corrosion.html#.Wfauu2hL9PY, viewed 30 Oct, 2017, 15:47 h.

Richardson, B.C., Joscelyn, K.B., Saalberg, J.H., 1979. Limitations on the Use of Mathematical Models in Transportation Policy Analysis. UMI Research Press, Ann Arbor, USA, pp. 1-15. ISBN: 0835710858, 9780835710855

Roberge, P.R., 2000. Handbook of Corrosion Engineering. McGraw-Hill, New York, USA, pp. 35-54, 187-220, 335-336, 1047-1059. ISBN: 0070765162

Sinnott, R.K., 2005. Chemical Engineering Design. 4th ed. Butterworth-Heinemann, Jordan Hill, GBR, pp. 756–764. ISBN: 9780080492551

Skovhus, T.L., Holmkvist, L., Andersen, K., Larsen, J., Pedersen, H., 2012. MIC Risk Assessment of the Halfdan Oil Export Spool. In: The SPE International Conference and Workshop on Oilfield Corrosion, May 28-29, Aberdeen, UK, document ID SPE-155080-MS. https://doi.org/10.2118/155080-MS

Skovhus, T.L., Andersen, E.S., Hillier, E., 2017. Management of microbiologically influenced corrosion in Risk-Based Inspection analysis. In: The Society of Petroleum Engineers International Oilfield Corrosion Conference and Exhibition, May 9-10, Aberdeen, Scotland, paper 179930. ISSN: 19301855

Smith, P., Roy, S., Swailes, D., Maxwell, S., Page, D., Lawson, J., 2008. A predictive model for microbial induced corrosion (MIC) in sub-sea production pipelines: Part 1 - Abiotic corrosion model. In: The SPE International Oilfield Corrosion Conference, May 27, Aberdeen, Scotland, paper 114135. https://doi.org/10.2118/114135-MS

Smith, P., Roy, S., Swailes, D., Maxwell, S., Page, D., Lawson, J., 2011. A model for the corrosion of steel subjected to synthetic produced water containing sulfate, chloride and hydrogen sulphide. Chemical Engineering Science 66, 5775-5790. http://dx.doi.org/10.1016/j.ces.2011.07.033

Sooknah, R., Papavinasam, S., Revie, R.W., 2007. Modelling the occurrence of microbiologically influenced corrosion. In: CORROSION 2007, Mar. 11-15, Nashville, USA, paper 07515. ISBN: 075152007CP

Sooknah, R., Papavinasam, S., Revie, R.W., 2008. Validation of a predictive model for microbiologically influenced corrosion. In: CORROSION 2008, Mar. 16-20, New Orleans, USA, paper 08503. ISBN: 085032008CP

Sorensen, K.B., Thomsen, U.S., Juhler, S., Larsen, J., 2012. Cost efficient MIC management system based on molecular microbiological methods. In: CORROSION 2012, Mar. 11-15, Salt Lake City, USA, paper C2012-0001111. Document ID: NACE-2012-1111

Suddath, C., 2009. A brief history of Friday the 13th. Time. http://www.time.com/time/nation/article/0,8599,1879288,00.html, viewed 23 Mar, 2017, 14:30 h.

Sullivan, M., 2004. Statistics – Informed Decision Making Using Data. Pearson Education, New Jersey, USA. ISBN: 0130618640

Szklarska-Smialowska, Z., 1986. Pitting Corrosion of Metals. NACE International, Houston, USA. ISBN: 9780915567195

Valencia-Cantero, E., Peña-Cabriales, J.J., Martínez-Romeros, E., 2003. The corrosion effects of sulfate- and ferric-reducing bacterial consortia on steel. Geomicrobiology Journal 20, 157-69. http://dx.doi.org/10.1080/01490450303885

Vance, I., Trasher, D.R., 2005. Reservoir souring: mechanisms and prevention. In: Ollivier, B., Magot, M., ed. Petroleum Microbiology. ASM Press, Washington, D.C., USA, pp. 123-42. http://dx.doi.org/10.1128/9781555817589

Videla, H.A., 2002. Prevention and control of biocorrosion. International Biodeterioration and Biodegradation 49, 259-270. http://dx.doi.org/10.1016/S0964-8305(02)00053-7

Videla, H.A., Herrera, L.K., 2005. Microbiologically influenced corrosion: looking to the future. International Microbiology 8, 169-180. ISSN: 11396709

Von Wolzogen Kuhr, C.A.H., van der Flugt, L.S.,1934. De grafiteering van gietijzer als electrobiochemisch proces in anaerobe gronden. Water (den Haad) 18, 147-165. (English translation published in 1961: Corrosion 17, 293-299. ISSN: 00109312).

Voordouw, G., Telang, A.J., Jack, T.R., Foght, J., Fedorak, P.M., Westlake, D.W.S., 1995. Identification of Sulfate-Reducing Bacteria by Hydrogenase Gene Probes and Reverse Sample Genome Probing. In: Minear, R.A., Ford, A.M., Needham, L.L. Karch, N.J., ed. Applications of Molecular Biology in Environmental Chemistry. CRC Press, Boca Raton, USA, pp. 81-97. ISBN: 0873719514, 9780873719513

Vose, D., 2008. Risk Analysis - A Quantitative Guide. 3rd ed. John Wiley and Sons, Chichester, UK, pp. 45-62. ISBN: 0470512849

Whitman, W.B., Bowen, T.L., Boone, D.R., 2006. The Methanogenic Bacteria. In: Dworkin, M., Falkow, S., Rosenberg, E., Schleifer, K-H., Stackebrandt, E., ed. The Prokaryotes. Springer New York, New York, USA, pp. 165. ISBN: 9780387307435

Xu, D., Li, Y., Gu, T., 2016. Mechanistic modeling of biocorrosion caused by biofilms of sulfate reducing bacteria and acid producing bacteria. Bioelectrochemistry 110, 52-58. http://dx.doi.org/10.1016/j.bioelechem.2016.03.003

Zhao, K., 2008. Investigation of microbiologically influenced corrosion (MIC) and biocide treatment in anaerobic salt water and development of a mechanistic MIC model. PhD Research thesis, The Russ College of Engineering and Technology of Ohio University.

Zou, W., Davey, K.R., 2016. An integrated two-step Fr 13 synthesis - demonstrated with membrane fouling in combined ultrafiltration-osmotic distillation (UF-OD) for concentrated juice. Chemical Engineering Science 152, 213-226. http://dx.doi.org/10.1016/j.ces.2016.06.020